Regulation of cohesin cleavage by separase in *Saccharomyces cerevisiae*

Nadine Christina Diana Hornig

Thesis submitted towards the degree of Doctor of Philosophy

University of London

University College London
Department of Biology
London, WC1E 6BT

Cancer Research UK
Chromosome
Segregation Laboratory
44 Lincoln's Inn Fields
London, WC2A 3PX

ProQuest LLC
789 East Eisenhower Parkway
P.O. Box 1346
Ann Arbor, MI 48106-1346

Abstract

The final irreversible step in the duplication and dissemination of genomes to daughter cells takes place at the metaphase to anaphase transition. Sister chromatid pairs that are aligned in metaphase split and separate in anaphase. This splitting is triggered by a specific protease called "separase", conserved in all eukaryotes. Separase cleaves Scc1, the central subunit of the "cohesin" complex that is required for holding together the sister chromatids in metaphase.

In budding yeast, separase' proteolytic activity is regulated in two ways: by its binding partner securin and through modification of the substrate Scc1. This thesis shows that securin supports separase localisation in the nucleus and ensures that separase gains full proteolytic activity by acting like a chaperone. It also shows that securin is a direct inhibitor of separase' proteolytic activity. Securin prevents binding of separase to its substrates. It also hinders the separase N-terminus from interacting with and possibly inducing an activating conformational change at the protease active site at the proteins C-terminus.

During chromosome condensation in prophase, part of cohesin leaves chromatin and it is unclear how separase specifically finds and cleaves the fraction of the cohesin that is left on chromosomes in metaphase. An assay was established to compare the cleavage of chromatin-bound versus soluble cohesin. This revealed that Scc1 in chromatin-bound cohesin is significantly preferred by separase over Scc1 in soluble cohesin. This difference was not due to the chromatin environment and can be explained by preferential phosphorylation of chromatin-bound Scc1. Site directed mutagenesis of ten Polo kinase phosphorylation sites in Scc1 reduced the rate of cleavage of chromatin-bound cohesin, and hyperphosphorylation of soluble Scc1 by overexpression of Polo kinase accelerated its cleavage in vitro. Phosphorylation site mutant Scc1 slowed anaphase progression in vivo leading to an increase in chromosome loss.

This thesis is dedicated to my family

Acknowledgments

I would like to thank all the people that helped and supported me throughout my thesis.

Especially, I would like to thank my supervisor Dr Frank Uhlmann for his never-ending support and encouragement.

I would also like to thank all the members of the Chromosome Segregation laboratory for being interesting people to work with and the people of the fifth floor for being so much fun.

I would like to thank my parents for supporting me through every level of education and my whole family, especially my sisters, for being always there for me.

I would like to thank my new family, Ingram for helping me so much and little Greta for being such a joy.

Finally, I would like to thank all my friends outside the institute.

Table of contents

Abstract....2
Acknowledgments....4
Table of contents....5
List of figures and tables....7
Abbreviations....9
Chapter 1....11
Introduction....11
1.1 The mitotic cell cycle....11
1.2 Regulation of mitosis....13
1.2.1 Cyclin dependent kinases....13
1.2.2 The anaphase promoting complex (APC)....14
1.2.3 Regulation of late mitotic events....16
1.3 The key players of metaphase to anaphase transition: separase and securin....18
1.3.1 Securin....18
1.3.2 Separase....19
1.4 Separase targets....21
1.4.1 Scc1....21
1.4.2 Rec8....24
1.4.3 Slk19....25
1.4.4 Separase cleavage sites....25
1.5 Surveying the metaphase to anaphase transition....26
1.5.1 The spindle checkpoint....26
1.5.2 The DNA-damage checkpoint....27
1.6 Separase and the exit from mitosis....29
1.6.1 Polo-like kinase....29
1.6.2 The mitotic exit network (MEN)....29
1.6.3 The FEAR pathway (CDC Fourteen Early Anaphase Release)....31
1.7 Regulation of cohesin cleavage....31
1.7.1 Scc1 phosphorylation....31
1.7.2 Separase phosphorylation....32
1.7.3 Separase auto-cleavage....32
1.8 Regulation of cohesin cleavage....33
1.8.1 Centromeric versus arm cohesion....33
1.8.2 The prophase pathway....34
Chapter 2....35
The dual mechanism of separase regulation by securin....35
2.1 Securin is needed for a nuclear localisation as well as a full proteolytic activity of separase....35
2.1.1 Separase accumulates in the nucleus from G1 – to anaphase....35
2.1.2 The nuclear concentration of separase depends on securin....37
2.1.3 Securin promotes separase nuclear accumulation independent of the cell cycle....39
2.1.4 Securin might concentrate separase in the nucleus by preventing separases' nuclear export....42
2.1.5 Securin supports full proteolytic activity of separase....43
2.2 Mechanisms of separase inhibition through securin....45
2.2.1 Securin is a protease inhibitor of separase....45

2.2.2 Separases' peptide recognition site is not essential for substrate binding 48
2.2.3 Securin interacts with separase N-and C-termini 50
2.2.4 The separase N-terminus is required for protease activity 52
2.2.5 Separase N- and C-termini bind each other. 55
2.2.6 Securin disrupts the separase N/C-terminal interaction 56
2.2.7 Separase activation is intramolecular 58
Chapter 3 59
Differential cleavage of chromatin-bound and soluble cohesin 59
3.1 Separase preferentially cleaves chromatin-bound Scc1 in vitro 60
3.1.1 Chromatin-bound Scc1 is cleaved faster than soluble Scc1 60
3.1.2 Preferred cleavage of chromatin-bound Scc1 is maintained after its solubilisation 63
3.2 The preferential cleavage of chromatin-bound Scc1 depends on its phosphorylation status 66
3.2.1 Chromatin-bound Scc1 is hyperphosphorylated compared to soluble Scc1 66
3.2.2 The cleavage rate of chromatin-bound Scc1 is regulated by phosphorylation 69
3.2.3 Hyperphosphorylation of soluble Scc1 increases its cleavage 70
3.2.4 Scc1 phosphorylation enhances both recognition and cleavage by separase 72
3.3 Phosphorylation-dependent preferential cleavage of chromatin-bound Scc1 in vivo is important for chromosomal stability 74
3.3.1 In vivo chromatin-bound Scc1 is preferentially cleaved depending on its phosphorylation 74
3.3.2 Delayed cleavage of chromatin-bound cohesin slows anaphase progression and causes chromosomal instability 76
3.4 Polo kinase co-localises with Scc1 on chromatin 78
Chapter 4 81
Discussion 81
4.1 Separase regulation by securin in the yeast Saccharomyces cerevisiae 81
4.1.1 Securin is a positive regulator of separase 81
4.1.2 Securin is a direct inhibitor of separase 82
4.2 Regulation of cohesion cleavage 92
Chapter 5 95
Materials and methods 95
5.1 Solutions, buffers and media 95
5.2 Molecular Biological techniques 98
5.3 Protein Biochemistry 100
5.4 Microscopy 108
5.5 Antibodies used in Western blot, Immunoprecipitation (IP) analysis and Immunohistochemistry (in situ) 109
5.6 Yeast physiology 111
5.7 Budding yeast strains 113
5.8 Plasmids 119
Bibliography 125
Appendix 137

List of figures and tables

Chapter 1:
Figure 1.1: Mitosis in the plant *Tradescantia virginiana* 12
Table 1.1: CDKs and cyclins in yeast and men 14
Figure 1.2: The cell cycle in somatic cells 15
Figure 1.3: A model of the regulatory network controlling the APC in mitosis 16
Figure 1.4: Esp1 and the CD Clan of Cysteine Proteases 20
Figure 1.5: Chromosome segregation in mitotic cells 22
Figure 1.6: ATP Hydrolysis-Dependent DNA Transport into the Cohesin Ring 23
Figure 1.7: Separases´ cleavage targets 26
Figure 1.8: Spindle checkpoint induced metaphase arrest 28
Figure 1.9: DNA-damage induced metaphase arrest 28
Figure 1.10: Comparison of early and late anaphase control of Cdc14 release 30

Chapter 2:
Figure 2.1: Securin is required for separase nuclear accumulation 36
Figure 2.2: Confocal analysis of separase in wild-type cells and cells deleted for securin 38
Figure 2.3: Separase associates at low levels to chromatin in securin deleted cells 39
Figure 2.4: Separase accumulates in the nucleus independently of a completed replication cycle 40
Figure 2.5: Separase accumulates in the nucleus independently of mitotic cyclins 40
Figure 2.6: Securin is sufficient to cause nuclear accumulation of separase 41
Figure 2.7: Nuclear retention of separase does not depend on the nuclear export receptor Crm1/Xpo1 43
Figure 2.8: Securin helps separase to acquire its full proteolytic activity 44
Figure 2.9: Securin inhibits separase proteolytic activity 46
Figure 2.10: Securin inhibits binding of Scc1 to separase 47
Figure 2.11: Securin inhibits a reaction with a cleavage site peptide 48
Figure 1.12: Interaction of separase with Scc1 occurs independently of cleavage site recognition 50
Figure 2.13: Scheme of the separase N-terminal deletion mutants 51
Figure 2.14: Securin interacts with the N-terminus of separase 52
Figure 2.15: The separase N-terminus is required for catalytic activity 53
Figure 2.16: The separase N-terminus is required for binding of the cleavage site peptide 54
Figure 2.17: The N- and C-termini of separase interact with eachother 56
Figure 2.18: The interaction between the separase N- and C-termini is disrupted by securin 57
Figure 2.19: Separase activation is intramolecular 58

Chapter 3:
Figure 3.1: Experimental outline to compare the rates of Scc1 cleavage in chromatin-bound versus soluble cohesin 60
Figure 3.2: Scc1 in chromosomal cohesin is cleaved at faster rate than Scc1 in soluble cohesin 61

Figure 3.3: Quantification of remaining full-length Scc1 in the chromatin-bound (cb) and soluble (sol) fraction over time 62
Figure 3.4: Cleavage rates of HA and myc epitope-tagged Scc1 in direct comparison 63
Figure 3.5: Chromatin release of cohesin by DNase I digest 64
Figure 3.6: Scc1 in cohesin that was released from chromatin by DNase I treatment is cleaved at a similar rate to chromosomal Scc1 65
Figure 3.7: Summary of rate constants obtained in parallel reactions for cleavage of Scc1 in chromosomal, chromatin-released, and soluble cohesin 66
Figure 3.8: Schematic representation of the 10 known Polo phosphorylation sites in Scc1 67
Figure 3.9: Effect of mutations replacing polo phosphorylated serines to alanines 68
Figure 3.10: Scc1 in chromatin-bound cohesin is hyperphosphorylated compared to Scc1 in soluble cohesin 68
Figure 3.11: Response of the Scc1 cleavage rate to phospho-site mutations and to dephosphorylation by l-phosphatase 69
Figure 3.12: Phosphorylation of soluble Scc1 by overexpressed Polo makes its cleavage comparable to chromatin-bound Scc1 71
Figure 3.13: Fast cleavage of recombinant, phosphorylated Scc1 is not due to higher affinity for separase 73
Figure 3.14: Phosphorylation accelerates cleavage of chromosomal Scc1 *in vivo* 75
Figure 3.15: Separase distribution between soluble and chromatin-bound fractions 76
Figure 3.16: 10xS→A mutant Scc1 dissociates from chromatin later and delays elongation of the anaphase spindle 77
Figure 3.17: 10xS→A mutant Scc1 confers increased chromosome loss 78
Figure 3.18: Chromatin provides a Polo-rich environment 79

Chapter 4:
Figure 4.1: Model of separase and its inhibition by securin 84
Figure 4.2: The C-terminus of separase and the N-terminus of securin share a specific profile 85
Figure 4.3: Separase regulation at the metaphase to anaphase transition 87
Figure 4.4: Secondary structure alignment of Esp1 (*S.cerevisiae*), Cut1 (*S.pombe*) and the D12 subunit of the vaccinia virus mRNA capping enzyme 89
Figure 4.5: Regions of similarity between the N-terminus of Esp1 (*S.cerevisiae*) and the D12 subunit of the vaccinia virus capping enzyme 90
Figure 4.6: The D1 subunit of the vaccinia virus capping enzyme and the Cysteine Proteinase Gingipain (Porphyromonas gingivalis) show a similar tertiary structure 91

Abbreviations

amk	acyloxomethylketone
APC	Anaphase Promoting Complex
ATP	Adenosine triphosphate
BSA	Bovine Serum Albumin
Cdc	Cell Division Cycle
CDK	Cyclin Dependent Kinase
DAPI	4',6-diaminidino-2-phenylindole
DNA	Deoxyribonucleic acid
dNTPs	Deoxyriboucleotide triphosphates
DTT	dithiothreitol
Δ	deletion
FACS	Fluorescence Associated Cell Sorting
FEAR	CDC Fourteen Early Anaphase Release
g	gram
G1/2	Gap 1 or 2
GEF	GDP/GTP exchange factor
GFP	green fluorescent protein
GTP	guanosine triphosphate
GDP	guanosine monophosphate
HA	Hemagglutinin A
HU	Hydroxyurea
IP	Immunoprecipitation
M phase	mitotic phase
MEN	mitotic exit network
MPF	M-phase promoting factors
mg	milligram
ml	millilitre
mM	millimolar
ng	nanogram
noc	nocodazole
ORF	open reading frame

PCR	polymerase chain reaction
Polo	Polo like kinase
RNA	ribonucleic acid
RSC	remodels the structure of chromatin
S	sedimentation coefficient
S phase	Synthesis phase
SDS	sodium dodecyl sulphate
SPB	spindle pole pody
THR	Three Rows
µg	microgram
µl	microlitre
wt	wild type
YE	yeast extract

Chapter 1

Introduction

In order to divide a cell must double its mass and distribute its components equally between two daughter cells. Cell division can be triggered by different environmental signals. These signals are transmitted through signal cascades to the DNA and activate the transcription of cell division specific genes. The molecular processes of a cell division are subjected to a defined temporal order. Their coordinated regulation, also called cell cycle control, is essential for the survival of a healthy cell. Mistakes in the cell cycle control can lead to deregulated cell growth and chromosomal missegregation.

The molecular bases of the cell cycle regulation were discovered in the beginning of the seventies. Biochemical analysis performed on sea urchin and *Xenopus laevis* fertilised eggs led to important discoveries of cell cycle control mechanisms [1, 2]. These model organisms were albeit not suited for genetical analysis. The two fungi *Saccharomyces cerevisiae* and *Schizosaccharomyces pombe* are good organisms for genetic manipulation. Mutational analysis on these unicellular organisms led to the further identification and characterisation of genes involved in the control of the cell cycle [3, 4].

1.1 The mitotic cell cycle

The somatic cell cycle is defined as the period between two mitotic divisions. This period is subdivided into a G1-, S- and G2-phase. The two key control points in the cell cycle are in G1-phase and at the end of the G2-phase. During G1 a commitment is made to enter a replication cycle. This commitment is defined by the restriction point in animal cells, and the START in yeast cells. Once this decision has been taken, cells are committed to begin a replication- or S-phase. The end of G2 is marked by the decision to enter mitosis or M-phase. This in turn depends on a correctly completed S- and G2-phase.

Mitosis is divided into five subsequent phases: prophase, prometaphase, metaphase, anaphase and telophase (Fig.1.1).

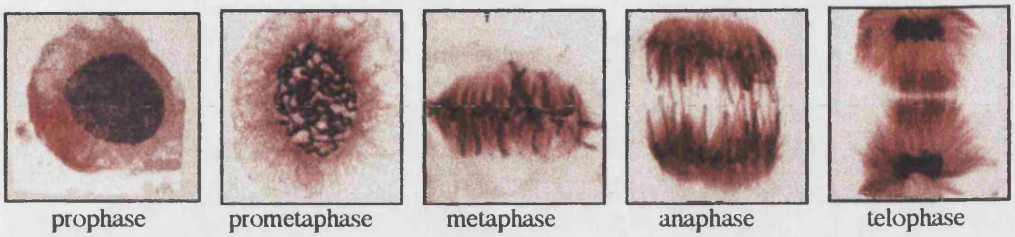

Figure 1.1: Mitosis in the plant *Tradescantia virginiana*
During prophase and prometaphase chromosomes start to condense and appear as individual chromosomes. In metaphase the chromosomes align at the cell equator known as metaphase plate. Microtubules emanating from opposite spindle poles attach to the centromeres of each sister chromatid. As anaphase commences, sister chromatids split and are pulled to opposite poles of the cell. In telophase the DNA starts to decondense and two new daughter cells form.

During prophase, the replicated chromosomes undergo extensive condensation and the mitotic spindle begins to emanate from both spindle poles, located at opposite ends of the cell. In prometaphase the microtubules of the mitotic spindle begin to interact with the chromosomes, and chromosomes start to assemble at the metaphase plate with their centromeres situated in the middle of the mitotic spindle. The kinetochore, a proteinaceous structure, assembled at the surface of the centromere, acts as the site of spindle microtubule binding. Each kinetochore of the replicated chromosome is pointed toward one side of the spindle. The congression of chromosomes and the alignment of the centromeres on the metaphase plate is an essential prerequisite for the orderly separation of the replicated genome into two equal parts. In metaphase the alignment of the replicated chromosomes at the metaphase spindle is completed and the chromosomes decrease their movement significantly. Anaphase commences with the initial splitting of sister chromatids. The splitting depends on the targeted destruction of a protein complex that holds the chromatids together. The major mechanism for chromosome movement in anaphase is motor-powered kinetochore movement coupled to microtubule disassembly at the kinetochore. Each kinetochore is pulled towards the spindle pole by microtubule depolymerisation. Consequently,

sister chromatids separate from each other, each moving away from the metaphase plate and toward one of the two spindle poles. In telophase, the chromosomes have moved close to the spindle pole regions, and the spindle midzone begins to clear.

1.2 Regulation of mitosis

1.2.1 Cyclin dependent kinases

A unifying feature in the cell cycles of yeast and animals is the existence of a cyclin dependent kinase (CDK) and a mitotic cyclin of either the A or the B class. The activity of CDK is controlled by the phosphorylation state of the catalytic subunit of the serine/threonine kinase and by the degradation of the cyclin component. By phosphorylating appropriate substrates, the kinase provides MPF (M-phase promoting factors) activity, which stimulates mitosis. A prominent substrate is histone H1 whose phosphorylation coincides with chromatin condensation, a prerequisite for proper chromosome segregation.
Cdc28, the CDK of *S.cerevisiae*, associates with different sets of cyclins to control the cell cycle [5]. The START is triggered by the association of the kinase with G1 or A cyclins, whereas mitosis coincides with its association with B cyclins (Table 1.1). This mitotic CDK activity is responsible for sister chromatid separation during anaphase.

Entry into mitosis requires activation of Cdc28. For this to occur, inhibitory phosphates on Cdc28 must be removed by the phosphatase Mih1 (Cdc25 in fission yeast). Proper timing is assured by the opposing effect of the kinase Swe1 (Wee1 in fission yeast) building a switch-like mechanism for Cdc28 activation [6, 7]. Various regulatory mechanisms converge on this kinase/phosphatase switch, shifting the balance towards Mih1 for mitotic entry or towards Swe1 to keep the cell in G2. The morphogenetic pathway, which ensures proper bud shaping shortly after bud emergence, as well as the correct positioning of the pre-mitotic spindle, is one of the key regulators of that switch.

In *S.cerevisiae* cell cycle control is exerted through the interaction of different cyclins (A-type *CLN1-2*, B-type *CLB1-6*) with a single CDK, the Cdc28 kinase (Cdc2 in *S.pombe*).

Cyclin	**Protein kinase**	**process regulated**
Cln1,Cln2,Cln3	Cdc28	Start (G1 to S)
Clb5,Clb6	Cdc28	S-phase
Clb3, Clb4	Cdc28	M-phase entry
Clb1, Clb2	Cdc28	M-phase progression

In humans:

Cyclin	**Protein kinase**	**process regulated**
Cyclin D1-3	Cdk4,6	G1-phase progression
Cyclin E	Cdk2	G1 to S-phase
Cyclin A	Cdk2	S-phase progression
Cyclin A	Cdk1	S through G2
Cyclin B	Cdk1	M-phase

Table 1.1: CDKs and cyclins in yeast and men

1.2.2 The anaphase promoting complex (APC)

The initiation and coordination of mitotic events are governed by ubiquitin-dependent proteolysis of key regulatory proteins, including mitotic cyclins [8-11]. A major step in this targeted protein destruction is catalysed by a multimeric ubiquitin ligase known as the anaphase-promoting complex (APC) or cyclosome. APC activity rises abruptly at metaphase, resulting in the destruction of proteins that inhibit sister-chromatid separation. APC-dependent destruction of B-cyclins initiates spindle disassembly, cytokinesis and the resetting of replication origins for the next cell cycle (Fig.1.2)

The APC is an ubiquitin ligase, which collaborates with an ubiquitin-activating enzyme and an ubiquitin-conjugating enzyme to catalyse the transfer of ubiquitin molecules to lysine side chains on target proteins [12]. Target proteins are recognised by the APC through a destruction-box (D-box or KEN-box) [13]. The ubiquitylated proteins are subsequently degraded by the 26S proteasome.

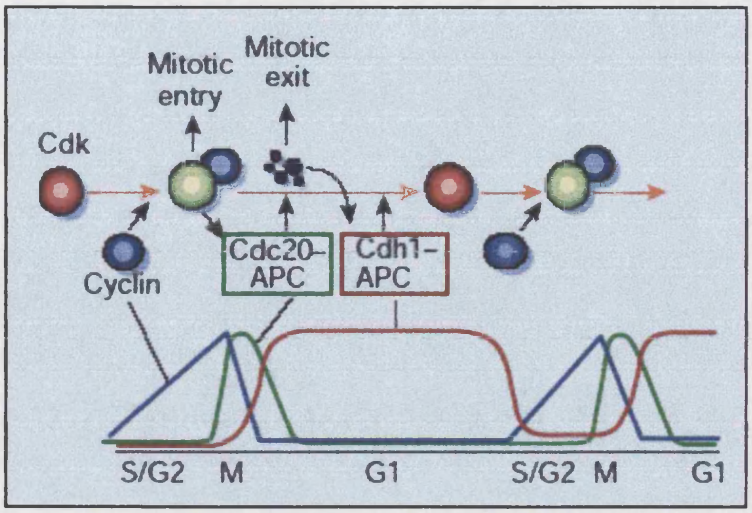

Figure 1.2: The cell cycle in somatic cells
Cyclin-dependent activation of Cdk not only leads to mitotic entry but also promotes activation of Cdc20–APC, which then triggers cyclin destruction and mitotic exit. Cdk inactivation in late mitosis results in the activation of Cdh1–APC, which maintains cyclin destruction (and so Cdk inactivity) throughout G1. The loss of Cdk activity causes Cdc20–APC inactivation, and cyclin can accumulate again. Phases of the cell cycle are S ('synthesis', in which DNA replication occurs) and M (nuclear division, or mitosis, followed by cell division, or cytokinesis). G1 is a 'gap' phase in which growth takes place. (D.Morgan and J.Roberts, Nature, Volume 418, 1.8.2002)

The APC needs to be activated, in order to be able to ubiquitylate proteins. This activation is cell cycle regulated and depends on two proteins, Cdc20 and Hct1/Cdh1 [14, 15]. Cdc20 and Hct1/Cdh1 are thought to be substrate specific APC activators, such that Cdc20 stimulates the destruction of the anaphase inhibitor Pds1/securin, whereas Hct1/Cdh1 targets the major mitotic cyclin Clb2 for destruction, a prerequisite for cells to exit mitosis [14-17] (Fig.1.2). The most striking difference between Cdc20 and Hct1/Cdh1 lays not so much in their substrate specificity but in their regulation. Whereas the Cdc20-APC appears to be stimulated by mitotic CDK activity, the Hct1/Cdh1-APC is inhibited by this activity. Cdc20 and several APC subunits undergo CDK-dependent mitotic phosphorylation, although biochemical evidence that this phosphorylation directly influences the activity of Cdc20 or the APC is still missing. In budding yeast, phosphorylation of Hct1/Cdh1 by Cdc28 blocks the ability of Hct1/Cdh1 to activate the APC [18]. Cdc28 thus blocks its own

inactivation by the Hct1/Cdh1-APC, explaining the inverse correlation between the activities of Cdc28 and Hct1/Cdh1-APC during the cell cycle. (Fig.1.3)

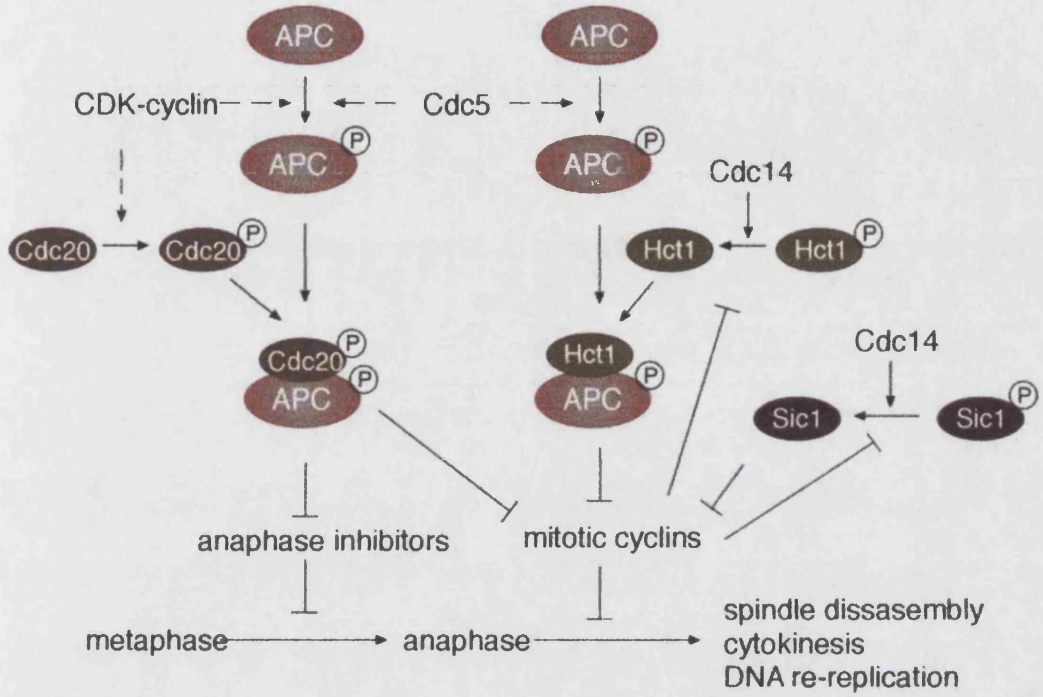

Figure 1.3: A model of the regulatory network controlling the APC in mitosis
In somatic cells, the Cdc20–APC is stimulated by mitotic CDK activity and is responsible for the destruction of anaphase inhibitors and cyclins. The dashed arrows indicate that the ability of CDK activity and Polo-like kinase (Cdc5) to stimulate the Cdc20–APC is poorly understood and perhaps indirect. Hct1-APC is inhibited by CDK activity, but late mitotic gene products like Cdc14 activate the Hct1-APC. This allows stable APC activation in G1. In budding yeast, Cdc20–APC may target some cyclins for destruction, but at least one cyclin type (Clb2) is targeted primarily by the Hct1–APC.

1.2.3 Regulation of late mitotic events

The switch-like features of CDK inactivation are enhanced by a similar antagonistic relationship between Cdc28 and Sic1, a protein that binds and inhibits Cdc28-cyclin complexes in late mitosis and G1. Phosphorylation of Sic1 by Cdc28 destabilises Sic1, and phosphorylation of the transcription factor Swi5 reduces *SIC1* expression. Swi5 promotes exit from mitosis by inducing *SIC1* expression in telophase [19-21]. Because of these relationships, Sic1 levels are

low from S phase to early mitosis but rise abruptly as CDK activity declines in late mitosis. Favourable growth conditions then stimulate the production of G1 cyclins, which are not Sic1 targets and therefore are able to turn off Cdh1 induced APC-resistant CDK activity.

The phosphatase Cdc14 has been implicated in the direct control of cyclin destruction. Cdc14 catalyses dephosphorylation of Hct1 at the inhibitory CDK sites, contributing to Hct1–APC activation [18]. Cdc14 also removes CDK-dependent phosphates from Sic1 and Swi5, leading to Sic1 accumulation [22]. Cdc14 is thus positioned to be a key regulator of CDK inactivation in late mitosis. Cdc5 is a member of the highly conserved family of Polo-related protein kinases, which have been implicated in the control of mitosis in a wide range of eukaryotes [23]. Polo-like kinases in many species are required for mitotic exit. Like Cdc5 in budding yeast, the Polo-like kinases of fission yeast and *Drosophila* are required for cytokinesis but not for anaphase onset [24, 25].

The ordering of Cdc20 and Hct1/Cdh1 activation seems to be based on the ability of Cdc20 to promote the destruction of proteins that inhibit Hct1/Cdh1 activation. In fact, the best-known Cdc20 target, the anaphase inhibitor Pds1/securin, may also be an inhibitor of cyclin destruction: over-expression of a non-degradable mutant form of Pds1 blocks not only sister chromatids separation but also prevents cyclin destruction and cytokinesis [26, 27]. Cells carrying mutations in *CDC20*, arrest in metaphase with undegraded Pds1, whereas *pds1* cells with mutations in *CDC20* arrest after anaphase with stable Clb2 [16, 28]. Thus, Cdc20 is required for cyclin destruction even in the absence of Pds1, suggesting that Cdc20 must promote the destruction of some other inhibitor of Hct1/Cdh1-APC activation. As Hct1/Cdh1 is required for destruction of Clb2, Cdc20 may target other mitotic cyclins such as Clb3 and Clb5. The destruction of other cyclins by Cdc20 would partially lower CDK activity (despite Clb2 stability), causing partial dephosphorylation of Hct1/Cdh1 and Sic1, and thereby triggering the switch that activates the Hct1/Cdh1-APC and causes Sic1 accumulation. (Fig.1.3)

1.3 The key players of metaphase to anaphase transition: separase and securin

1.3.1 Securin

A key event in the completion of the mitotic decision, and therefore subject to tight regulation, represents the separation of sister chromatids at the onset of anaphase. The metaphase to anaphase transition coincides with the proteolytic degradation of securin. The initial characterisation of securin, Pds1 in budding yeast, uncovered two complementary roles. Although not essential, securin is required for efficient chromosome segregation in anaphase. At the same time securin is needed to prevent anaphase in response to spindle and DNA damage [28-31]. It became clear that securin is an inhibitor of sister chromatid separation that has to be degraded via ubiquitylation by the APC [26, 32, 33]. While present in cells securin is bound to the cysteine protease Esp1/separase [31, 34]. Separase itself is necessary and sufficient for sister chromatid separation in anaphase [35, 36]. In crude in vitro systems securin prevents separase from cleaving Scc1 [37, 38].

In fission yeast, as well as in budding yeast, the C-terminus of securin is thought to interact with N-terminal regions of separase [30, 34]. A similar interaction has also been shown in *Drosophila* and humans [37, 39].

Securins are found in most organisms studied. Although they share very little primary sequence similarity, they all contain D-or KEN-boxes at their N-termini, which is the recognition sequence for ubiquitylation by the APC. Upon activation of the APC by Cdc20 in metaphase, securin is ubiquitylated and subsequently degraded. As a consequence separase is free to separate sister chromatids.

Several lines of evidence suggested that securin might have not only an inhibitory role on separase function but might also be needed to activate separase at the metaphase to anaphase transition. The fission yeast Cut1/securin is essential and thought to help localising separase to the mitotic spindle [40]. Studies in yeast that are discussed in this thesis in parallel with studies conducted in other laboratories showed that Pds1/securin is needed for

the nuclear localisation as well as for proper spindle association of Esp1/separase [34, 41]. Furthermore phosphorylation of securin by Cdc28 is required for efficient nuclear localisation of separase [42].

1.3.2 Separase

Separases have been first identified as Esp1 in budding yeast and Cut1 in fission yeast [43-45]. Mutational defects in Esp1 have initially been shown to lead to a lethal state characterised by the accumulation of Extra Spindle Pole bodies (ESP) [45]. The lethality of esp1 mutants was then described to be a consequence of an aberrant behavior of the mitotic spindle, leading to a failure of a correct nuclear division and massive chromosome nondisjunction, with one daughter cell generally acquiring most of the DNA and both spindle poles. This cell then frequently proceeded to initiate a new cell cycle, leading to increases in both DNA content and the number of Spindle Pole Bodies (SPBs) [43]. Later studies showed that esp1 mutants failed to separate sister chromatids when shifted to non-permissive temperatures. It became clear that Esp1 was responsible for the sudden disappearance of cohesion between sister chromatids at the metaphase to anaphase transition [31]. Concomitantly, it turned out that sister chromatid separation at the anaphase onset is promoted by cleavage of the Scc1 subunit of the cohesin complex holding sister chromatids together [38] and that Esp1 was the protease responsible for this cleavage [35].

Separases are large (180 to 250kD) proteins with a highly conserved C-terminal domain. This domain contains the catalytic dyad of the protease common to caspases (CD-clan of proteins), which is composed of five parallel β-strands linked by helices. At the end of the two central strands lie the conserved histidine and cysteine residues that form the catalytic dyad [35] (Fig1.4).

A

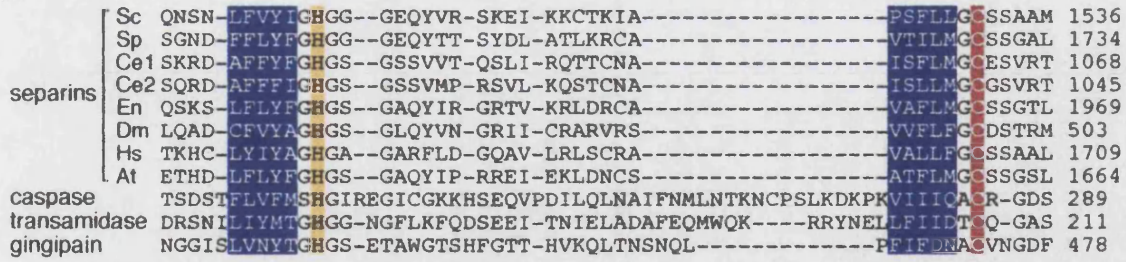

B

Figure 1.4: Esp1 and the CD Clan of Cysteine Proteases
(A) Sequence conservation between separases in the region of the proposed proteolytic catalytic site. Sequence alignment in the region of the strictly conserved His and Cys residues is shown together with the sequences of human caspase 1, the transamidase Gpi8, and gingipain. Key to sequences: separins from S. cerevisae Esp1 (AAB03897), S. pombe Cut1 (A35694), two proteins from C. elegans (AAA83576 and the WormPep-Entry CE22098), E. nidulans BimB (P33144), D. melanogaster (conceptual translation of AC0114811), H. sapiens (BAA11482), A. thaliana (CAA19812), human caspase 1 (P29466), human Gpi8 (CAA68871), and P. gingivalis gingipain (P95493). (B) The catalytic site of gingipain is shown as a model for that of separase. The histidine and cysteine catalytic residues are colored in yellow and red respectively, whereas hydrophobic parallel β-strands on the N-terminal side of these catalytic residues are shown in blue. The polypeptide chain between the two strands is in green. Residues within separases that are proposed to correspond to these structural motifs are marked with the same color scheme in the alignment in A. The figure was drawn with MOLSCRIPT. (F.Uhlmann et al., Cell, Vol 103, 27.10.2000)

Separase's large N-terminal domain is unconserved on the primary sequence level. Nevertheless it is present in all eukaryotes studied, indicating an important role for this large N-terminal part. In fission yeast, N-terminal sequences are required for the function of separase and have been implicated in its nuclear localisation, and more central sequences in the possible cytoplasmic retention of the protein [40].

Tertiary structure predictions in dipteria revealed alpha-alpha superhelical folds in the N-terminal domains of separase. The compatibility of

these folds with a wide range of primary sequences could explain the rapid divergence of N-terminal separase sequences as well as securins, which contact this region [46].

Like caspases, separases in vertebrate cells undergo auto cleavage upon their activation, following APC-mediated securin destruction. In flies, where separase appears to have split into two proteins - SSE containing the protease domain and Three Rows (THR) as the N-terminal part - the latter also undergoes cleavage upon activation of the protease. Cleavage of THR does not appear to be necessary for separase activity but instead may contribute to its inactivation during telophase [47]. Auto cleavage of separase in vertebrate cells may have a similar role.

1.4 Separase targets

1.4.1 Scc1

The main proteolytic target of separase is a protein complex, called cohesin complex, which mediates cohesion between sister chromatids after their replication in S-phase. The yeast cohesin complex contains an SMC heterodimer formed by the interaction between two different Smc proteins, called Smc1 and Smc3 [48]. These are bound to a third protein, Scc1, whose cleavage by separase triggers the pole ward movement of sisters at the metaphase-to-anaphase transition [38, 49] (Fig1.5). Separase and Scc1 represent crucial players in the process of sister chromatid separation. This mechanism to initiate anaphase is indeed conserved in eukaryotes from budding yeast to human.

Scc1 binds a fourth cohesin subunit, Scc3, whose function is still unclear. Recent findings showed that the N- and C-terminal domains of Scc1 bind, respectively, to the Smc3 and Smc1 heads of the Smc1/3 heterodimer [48]. (Fig1.6) This suggested that cohesin forms a large proteinaceous ring within which the DNA strands could be trapped. The hypothesis that sister chromatids are connected via a topological rather than a chemical bound would fit with the

observation that cohesin does not bind very strongly to DNA [50, 51] and could explain how it can very quickly be released from chromosomes after cleavage of its Scc1 subunit [38].

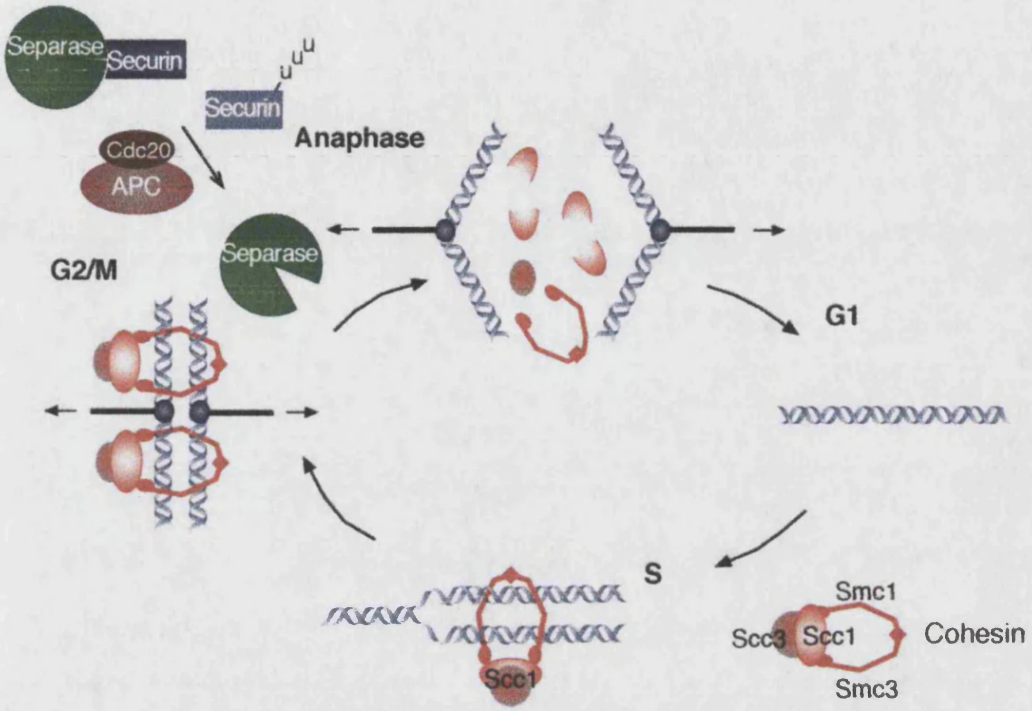

Figure 1.5: Chromosome segregation in mitotic cells
In late G1 phase, the cohesin complex is loaded on chromosomes and holds sister chromatids together after the DNA has been replicated. At the beginning of mitosis, microtubules attaching to the centromeric region of each sister chromatid exert a pulling force towards opposite spindle poles. This force is counteracted by the cohesin complex that is released from chromosomes in anaphase through the proteolytic cleavage of Scc1 by separase.

One of the still unsolved questions is how cohesin is loaded onto DNA before replication and how sister chromatid cohesion is established after replication. Studies in budding yeast suggest that cohesin binding to chromatin is accomplished by an ATP hydrolysis-dependent transport of DNA into the cohesin ring [52]. These studies also present evidence that the two Smc subunits of cohesin by themselves form a ring, closed at interacting ATPase head domains. In addition to an intact cohesin ring structure, functional ATPase heads are indispensable for DNA binding, suggesting that ATP hydrolysis may be coupled to DNA transport into the cohesin ring. Parallel studies suggest that

ATP hydrolysis drives the temporary disconnection of Scc1 from Smc heads that are needed for DNA entrapment and that this process is promoted by Scc2/4 [53]. Scc2 and Scc4 are required to load cohesin on chromosomes. DNA is released in anaphase when separase cleaves cohesin's Scc1 subunit. A cleavage fragment of Scc1 could disrupt the interaction between the two Smc heads, thereby opening the ring (Fig.1.6) [52].

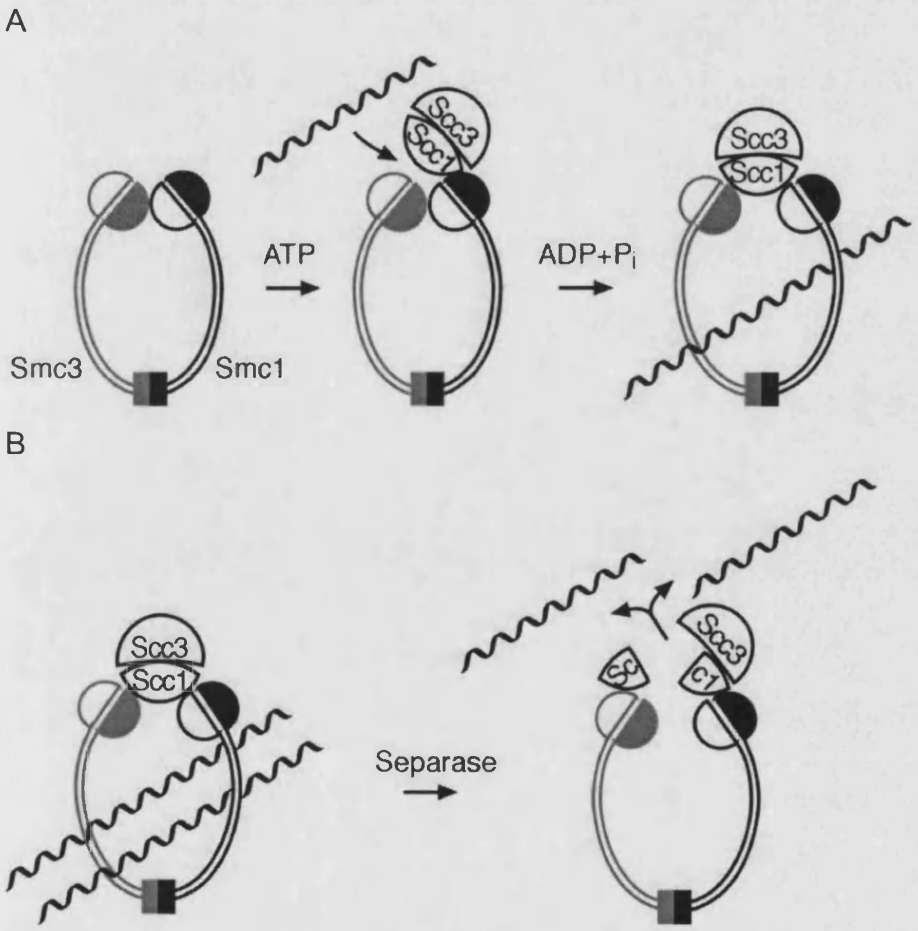

Figure 1.6: ATP Hydrolysis-Dependent DNA Transport into the Cohesin Ring
(A) The cohesin Smc dimer forms a ring. ATP binding by Smc1 is required for association of Scc1 when it is synthesized at the G1/S transition. DNA might then induce ATP hydrolysis and its own active transport into the ring. During this process Smc heads separate but remain connected by Scc1. (B) During DNA replication two sister strands become entrapped in the cohesin ring. At anaphase onset Scc1 is cleaved by separase. The C-terminal cleavage product, bound to Smc1, prevents the Smc heads from interacting, allowing release of sister strands from the open ring. (S.Weitzer et al., Current Biology, Volume 13, 11.11.2003)

1.4.2 Rec8

During meiosis I, cohesion between sister chromatid arms is essential for holding homologs together after their recombination to produce chiasmata. In yeast, this cohesion is destroyed by separase-mediated cleavage of a meiosis specific variant of Scc1 called Rec8 [54]. Cleavage of Rec8 along chromosome arms occurs at the onset of anaphase I, but Rec8 in the vicinity of centromeres is cleaved only at the onset of anaphase II. The persistence of centromeric cohesion during meiosis I is essential for chromatid segregation during meiosis II.

In *Drosophila*, the protein Mei-S332 has been implicated in the retention of centromeric cohesion until onset of meiosis II. Mei-S332 is concentrated at pericentric chromosome regions from metaphase I to metaphase II in meiotic cells as well as during metaphase of mitotic cells [55, 56]. In flies carrying *mei-S332* mutations, a high frequency of sister centromeres are separated already by late anaphase I [57], and this phenomenon is associated with a high frequency of nondisjunction, lagging chromosomes, and chromosome loss during meiosis II [58].

A protein with analogous function and distantly related structure to Mei-S332 in *Drosophila* has been discovered in fission yeast. Recent studies in fission yeast revealed that the pericentric protein Sgo1 protects centromeric Rec8 from cleavage during meiosis I, probably by shielding Rec8 from separase action [59, 60]. A genome-wide screen in *S.cerevisiae* identified three mutants, *iml3*, *chl4*, and *sgo1*, whose chromosome segregation pattern predicts an involvement in the maintenance of centromeric cohesion during meiosis I [61]. All three proteins are, to different extents, required to retain cohesin around centromeres during anaphase I and localise to centromeric regions. The finding that Sgo1, like Mei-S332, is a coiled-coil protein and dissociates from centromeric regions at the onset of anaphase during mitosis and the onset of anaphase II during meiosis [55, 62, 63] further raises the possibility that *SGO1* is the functional homolog of *MEI-S332* in *S. cerevisiae*.

1.4.3 Slk19

The third known proteolytic separase target, besides Scc1 and Rec8, is Slk19 [64]. The kinetochore and spindle-associated protein Slk19 is cleaved by separase during anaphase. Unlike Scc1, whose C-terminal cleavage product is rapidly degraded via the N-end rule, the Slk19 cleavage product is stable [65-67]. According to the N-end rule pathway, a set of molecular components recognise and degrade proteins bearing N-degrons, a destabilising N-terminal residue of a protein [65]. The escape of the Slk19 cleavage product from degradation is important to allow cleaved Slk19 to stabilise the anaphase spindle. Accumulation of uncleaved Slk19 is incompatible with high-fidelity chromosome segregation. This demonstrates that separase cleavage can, not only destroy proteins, like the cohesins, but that cleavage can also generate new protein species with altered properties.

Furthermore, and independently of its cleavage, the localisation of Slk19 to the spindle midzone in anaphase depends on separase. Another protein at the spindle midzone, Ase1, is also mislocalised in the absence of separase. The spindle midzone is thought to be the region where microtubule plus ends from opposite spindle pole bodies overlap [68], and Slk19 and Ase1 might be involved in protecting the plus ends from shrinkage, thereby stabilising the anaphase spindle. A normal spindle midzone fails to form during anaphase in the absence of separase [35], showing that separase and Slk19 might act in the same pathway to stabilise the spindle [64].

1.4.4 Separase cleavage sites

All three known budding yeast separase substrates, Scc1, Rec8 and Slk19, are cleaved at one or two conserved peptide motifs, about eight amino acid in length (Fig1.7) [38, 54, 64], and related motifs are found at separase cleavage sites in other organisms [36, 47, 69-71].

```
                    ↓
Scc1 173  DTSLEVGRRFSPDE 186
     261  DNSVEQGRRLGESI 274
Rec8 424  FSSVERGRKRAHSL 437
     446  TRSHEYGRKSFRNN 459
          .pSh-.GRp...s.
Slk19 70  DRSIDYGRSSALNN  83
```

Figure 1.7: Separases' cleavage targets
Sequence alignment of the known separase cleavage sites in Scc1 and Rec8 (p, polar (CDEHKNQRST); h, hydrophobic (ACFGHILMVWY); minus, negatively charged (DE); s, small (ADGNPSTV)). The consensus was used to screen the *Saccharomyces cerevisiae* proteome with the ISREC pattern finder (www.isrec.isb-sib.ch/software/PATFND_form.html). (M.Sullivan et al, Nature Cell Biology, Volume 3, 9.2001)

Separase always cleaves downstream of a conserved arginine residue. Mutation of the arginine to a negatively charged amino acid largely abolishes cleavage. The exact sequence requirements for recognition of the cleavage site motif have been characterised. A systematic mutational analysis of the major separase cleavage site in Scc1 showed that a core {DE}XXR element within the cleavage site motif bears most weight for recognition by separase in *Saccharomyces cerevisiae* [72]. In higher eukaryotes, an EXXR motif appears to be the main conserved feature at separase cleavage sites [36, 47, 69, 70]. This suggests that cleavage site recognition by separase follows a fundamentally similar principle in all organisms.

1.5 Surveying the metaphase to anaphase transition

1.5.1 The spindle checkpoint

All eukaryotic cells possess elaborate mechanisms that regulate the timing of separase activation and prevent it from occurring in the presence of incomplete DNA replication and of chromatid pairs that have not yet bi-oriented. At metaphase of mitosis, sister kinetochores must be bi-oriented and attached to microtubules emanating from opposite spindle poles. This 'amphitelic' attachment is dependent on cohesion between sister chromatids which

counteracts the pulling force exerted by the microtubules, and is promoted by the Ipl1/Aurora B kinase [73, 74]. In budding yeast, most chromosomes start off after replication with both sister kinetochores attached to the same spindle pole. Aurora B kinase is required to correct this monopolar or syntelic attachment into the requisite bipolar or amphitelic attachment at metaphase [73]. This implies that aurora B dissolves non-productive kinetochore-microtubule interactions until bipolar tension is reached. Consistent with this idea, interference with aurora B kinase activity in tissue culture cells leads to chromosome alignment defects [75-77]. Once bipolar tension at kinetochores has been established, aurora B must stop dissolving attachments.

A surveillance mechanism, known as the spindle checkpoint, detects unattached chromosomes, syntelically attached chromosomes and possibly also chromosomes that have attached to only one pole, known as monotelic attached chromosomes. Unattached or misattached chromosomes or treatment with spindle depolymerising drugs like nocodazole trigger the production of a complex containing the Mad1/Mad2, BubR1 (Mad3), and Bub3 proteins. This complex binds to the APC's activator protein Cdc20, preventing its interaction with the APC, [78] and thereby blocks ubiquitylation of both securin and cyclin B [79] (Fig.1.8). The persistence of cyclin B keeps Cdc28 active, which maintains cells in a mitotic state in which chromosomes remain condensed, whereas the persistence of securin prevents cleavage of Scc1 through separase.

1.5.2 The DNA-damage checkpoint

Another surveillance mechanism that regulates the timing of separase activation is the DNA-damage checkpoint. In response to DNA damage, cells are arrested in metaphase through the activation of Rad53 and Chk1. The role of Rad53 in the DNA damage checkpoint is to maintain CDK activity high [80, 81]. Chk1 targets the anaphase inhibitor securin [81, 82], which is phosphorylated and stabilised during the DNA-damage arrest in a Chk1-dependent manner [26, 28, 81] (Fig.1.9). The fact that cells lacking Chk1 or Pds1 exhibit a partial DNA-damage induced metaphase arrest, whereas cells lacking both Chk1 and Rad53, Pds1 and Rad53 show no metaphase arrest,

suggests that there is a Rad53 target in addition to securin regulating establishment of the arrest [81-83].

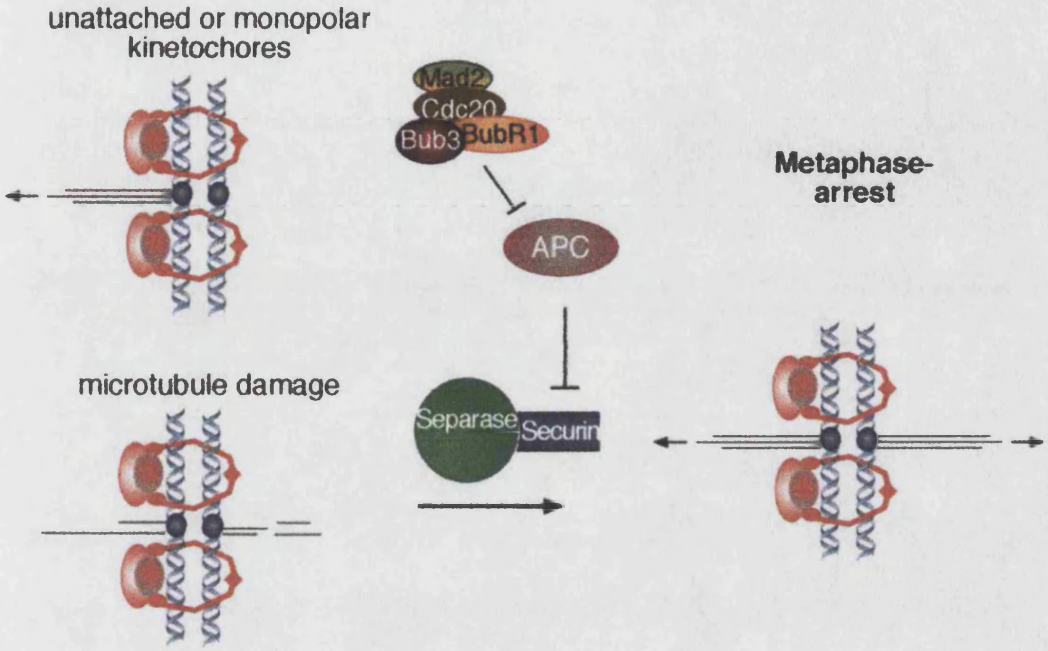

Figure 1.8: Spindle checkpoint induced metaphase arrest
Unattached or misattached chromosomes as well as microtubule damage cause the production of a Mad/Bub complex that sequesters the APC activator Cdc20. This prevents the proteolysis of securin by inhibiting APC activity.

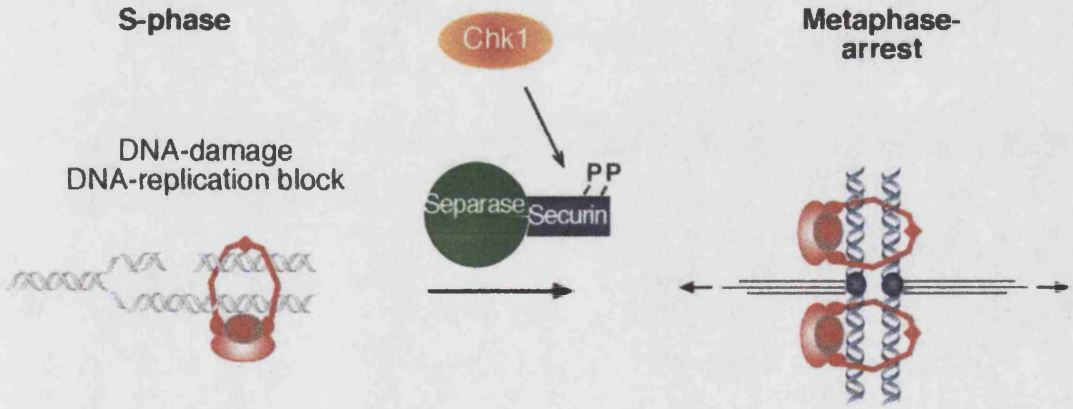

Figure 1.9: DNA-damage induced metaphase arrest
DNA-damage causes a metaphase arrest through the phosphorylation of securin by Chk1.

1.6 Separase and the exit from mitosis

In addition to its role in controlling sister chromatid separation, separase is also involved in the exit from mitosis and interestingly this function is independent of its protease activity. In budding yeast, exit from mitosis depends at least in part on the movement of one spindle pole body into the bud [84, 85]. The cell monitors the position and successful segregation of the inherited spindle pole through the GTP binding protein, Tem1. Tem1 binds GDP while in the mother cell, but binds GTP when brought into contact with its GDP/GTP exchange factor (GEF) Lte1, which is confined to the daughter cell [84, 86]. Lte1 is itself activated through phosphorylation by the Polo kinase Cdc5 [87].

1.6.1 Polo-like kinase

As in other eukaryotes, the budding yeast polo kinase homologue, Cdc5, plays multiple key roles in the coordination of mitosis, including the G2/M transition, chromosome separation and cytokinesis. Cdc5 accumulates in the nuclei of G2 and early M-phase cells and disappears from cells as they complete mitosis [88]. Cdc5 is required to activate Hct1/Cdh1-dependent ubiquitylation of late mitotic substrates such as Clb2, whose degradation is important for exit from mitosis. Cdc5 is like Cdc20 itself a substrate of the APC and is degraded in G1 by an Hct1/Cdh1-APC dependent mechanism [17, 80]. Degradation of Cdc5 in G1 might provide a feedback mechanism by which the APC destroys its activator at the onset of the next cell cycle.

Cdc5 localises to centrosomes early in mitosis, then accumulates on the central region of the spindle and persist at the midbody through cytokinesis, in addition to locating at kinetochores [89-91].

1.6.2 The mitotic exit network (MEN)

Besides Cdc5 and Tem1, the protein kinases Cdc15 and Dbf2, Dbf20, the Mob1 protein, in complex with Dbf2, and the Cdc14 protein phosphatase are

needed for cells to exit mitosis. These proteins contribute to the so called 'mitotic exit network' (MEN) (Fig.1.10). All the components of the network are essential for the B cyclin removal by the Hct1/Cdh1–APC and for Sic1-dependent CDK inactivation after anaphase [85, 92, 93]. The MEN is thought to work in the following order: GTP-bound Tem1 binds to the kinase Cdc15 [94], which in turn activates through phosphorylation the Dbf2 kinase. Dbf2 must be complexed with Mob1 to undergo proper activation by Cdc15 [95]. The activated Dbf2/Mob1 complex and Cdc5 then trigger the release of the Cdc14 phosphatase from the nucleolus by dissociation from its sequestering factor Net1 [87, 95-98]. As a consequence, Cdc14 is free to dephosphorylate its targets and promote mitotic exit.

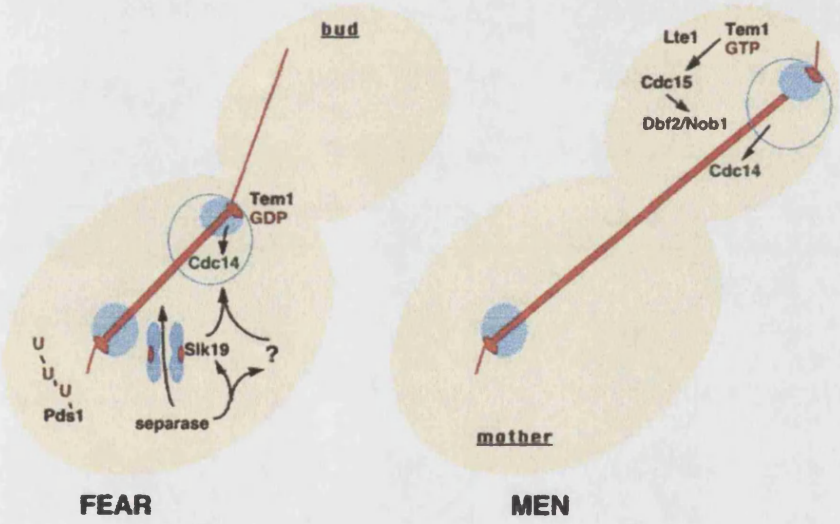

Figure 1.10: Comparison of early and late anaphase control of Cdc14 release
Separase has been shown to play a role in Cdc14 release from the nucleolus, in addition to its previously characterised role in chromatid separation. At least one of the separase targets is the kinetochore protein Slk19, but other targets (signified by "?") are suggested, based on the *esp1* mitotic exit phenotype. Together with Cdc5, these proteins make up the FEAR network. The early anaphase release of Cdc14 may be confined to the nucleus. In contrast, the MEN functions to maintain Cdc14 release at later stages of spindle elongation. This pathway works through previously characterised components, many functioning at the spindle poles, and may promote Cdc14 release to the cytoplasm (W.S.Saunders, Molecular Cell, Volume 9, 2.2002)

1.6.3 The FEAR pathway (CDC Fourteen Early Anaphase Release)

Although the total and maintained release of Cdc14 in late anaphase, crucial for mitotic exit, depends on the MEN pathway, a partial release of Cdc14 from the nucleolus happens already in early anaphase [99, 100]. Such early release of Cdc14 depends on the FEAR network. So far the proteins separase/Esp1, Slk19, Spo12, and Cdc5 constitute the first members of the FEAR network (Fig.1.10). Unlike Spo12 mutants, that were blocked primarily in the early release of Cdc14, Cdc5 mutants were blocked both in the early and late Cdc14 release. Separase mutants show a delay in the early anaphase release of Cdc14 [100] and separase activation at the onset of anaphase is sufficient to promote release from the nucleolus and activation of Cdc14 [101]. At least one of the separase targets, the kinetochore protein Slk19, acts downstream of separase in the FEAR pathway, as the early release of Cdc14 is significantly reduced when Slk19 is deleted [100] and mitotic exit is delayed. Interestingly, the ability of separase to activate Cdc14 is independent of its protease function but may involve promoting phosphorylation of the Cdc14 inhibitor Net1 [101]. This non-proteolytic separase function is co-regulated with its proteolytic activity by the separase inhibitor securin. This could explain the coupling of anaphase and mitotic exit - after securin degradation at anaphase onset, separase cleaves cohesin to trigger chromosome segregation and concurrently uses a non-proteolytic mechanism to initiate mitotic exit [101].

1.7 Regulation of cohesin cleavage

1.7.1 Scc1 phosphorylation

Securin destruction by the APC is essential for anaphase onset and stabilisation of securin in response to spindle or DNA damage is an efficient way to prevent anaphase [26, 32, 33]. Mutant cells that lack securin still block cyclin B destruction in the presence of spindle poisons, but fail to block cleavage of Scc1 by separase, which results in loss of sister chromatid

cohesion [27, 28]. However, yeast securin mutants are viable at low temperatures (23°C) and Scc1 cleavage continues to be cell cycle regulated in these mutants. This suggested another, securin independent control mechanism of separase activation at the metaphase to anaphase transition. Phosphorylation of Scc1 by Polo-like kinase is required for Scc1 cleavage in vitro and mutation of two key phosphorylation sites in Scc1 are synthetically lethal in the absence of securin [102]. Polo could therefore be a securin independent regulator of cohesin cleavage.

1.7.2 Separase phosphorylation

The securin gene can also be deleted in human tissue culture cells [103] and even in mouse embryos without causing lethality [104, 105]. In contrast to yeast cells, mammalian cells that lack securin are still capable of blocking the loss of sister chromatid cohesion when treated with spindle poisons. This could be due to the existence of several securin genes in mammalian cells or these cells could block separase activation by a securin-independent mechanism. In accordance with the latter, high levels of cyclin B/CDK levels in *Xenopus* extracts can prevent separase activation despite securin destruction [37]. It turned out that in human cells phosphorylation of separase at Ser1126 is necessary for separase inactivation. When this residue was mutated to alanine, separase failed to be inactivated by high levels of CDK activity but could nevertheless be inhibited by securin. Ser1126 is quantitatively phosphorylated during metaphase and becomes at least partly dephosphorylated upon anaphase onset [37].

1.7.3 Separase auto-cleavage

Yet another level of separase regulation has been revealed in human cells and *Drosophila* embryos. After its activation at anaphase onset, separase cleaves itself [37, 47, 106]. The large human separase protein is thus split into two halves. These fragments stay associated with each other, and separase

activity initially does not seem to be diminished by this cleavage [69, 70]. The carboxy-terminal half of the protein becomes unstable, however, and disappears during the following G1 phase [106]. As this part of separase contains the protease active site, this ultimately leads to a downregulation of separase activity. In *Drosophila*, separase is composed of two smaller polypeptides, called Three Rows and separase [39], which may be the result of a primordial separase gene having split on the evolutionary lineage leading to *Drosophila*. The Three Rows polypeptide is cleaved in anaphase, and its carboxy-terminal fragment is destabilised and disappears from cells. Even though this fragment does not contain the protease active site, a separase complex without it is inactive [47]. Three Rows cleavage thus causes inactivation of separase after anaphase onset.

1.8 Regulation of cohesin cleavage

1.8.1 Centromeric versus arm cohesion

Cohesin establishes sister chromatid connections during replication at both centromeres and discrete sites along chromosome arms, but appears to be enriched in the vicinity of centromeres [107-111]. Studies in *S. pombe* indicate that the enrichment of cohesin at centromeres results from the intrinsic ability of centromeric heterochromatin to recruit high levels of cohesin. The heterochromatin protein 1 (HP-1), Swi6, is specifically required for cohesion between sister centromeres but not along chromosome arms [49, 112].
Recent findings in *S.cerevisiae* report that the RSC (remodels the structure of chromatin), an ATP-dependent chromatin remodeler [113, 114], instead is necessary for cohesin's association with chromosomal arms but not with centromeric binding sites [115]. RSC's association with chromosomal arms precedes the arrival of the core cohesin subunit Scc1 in late G1/S phase about 15 min suggesting a role for RSC in the early stages of the multistep process of sister chromatid cohesion, including cohesion loading on chromosomes. Indeed, Scc1 fails to associate specifically with cohesin binding sites on

chromosomal arms, but remains associated with centromeres in *rsc* mutants. Thus, unlike the Scc2/Scc4 loading factors, required for cohesin loading on both chromosomal arms and centromeres [50], or the heterochromatin proteins HP-1/Swi6, which recruits cohesin at centromeres but not arms [116, 117], RSC might be specifically needed for cohesin loading at chromosomal arms.

1.8.2 The prophase pathway

In higher eukaryotes, the bulk of cohesin dissociates from chromosomes during prophase, when chromosomes start to condense, and prometaphase, when they bi-orient on the mitotic spindle. This dissociation occurs at the chromosome arms and is thought to be independent of separase [51, 118] as it happens before separase activation, but appears to depend on the mitotic kinase Polo. Phosphorylation of arm cohesin by Polo facilitates its removal from chromosomes [119]. At the same time, a related complex, called condensin, binds to the axes of both chromatids and contributes to the mitosis specific chromosome compaction [49]. The fraction of cohesin that persists mainly on the centromeres of chromosomes until metaphase [106, 120] is responsible for holding sisters together while they bi-orient during prometaphase. This fraction is then targeted by separase whose cleavage of the cohesin complex triggers anaphase [35, 36].

Chapter 2

The dual mechanism of separase regulation by securin

2.1 Securin is needed for a nuclear localisation as well as a full proteolytic activity of separase

Securin was initially characterised as a separase inhibitor that has to be degraded by the anaphase promoting complex to allow sister chromatids to separate in anaphase [26, 32, 33]. The inhibition of separase by securin could suggest that in cells lacking securin, separase is overly active, but this is not the case. Budding yeast and human cells lacking securin show compromised separase function [31, 103], and in fission yeast and *Drosophila* securin is essential for sister chromatid separation and therefore apparently for separase activity. The supportive role of securin for separase activity could be explained in two ways. Securin might be required in a chaperone-like function to ensure that separase adopts proteolytic activity [103]. Securin might also be required for a correct subcellular localisation of separase [34, 40].

2.1.1 Separase accumulates in the nucleus from G1 – to anaphase

To study the subcellular distribution of separase during the cell cycle in *S.cerevisiae*, I synchronised cells in G1 using alpha-factor and released cells synchronously in one cell cycle. Separase that has been endogenously tagged with the myc epitope tag showed a nuclear concentration in 50% of the cells in G1 (Fig.2.1). As soon as cells were released into S-phase the amount of cells with a positive nuclear separase signal increased to 80%. Approximately 60 minutes after the release, cells had reached metaphase and had a nuclear concentration of separase in nearly 90% of the cells.

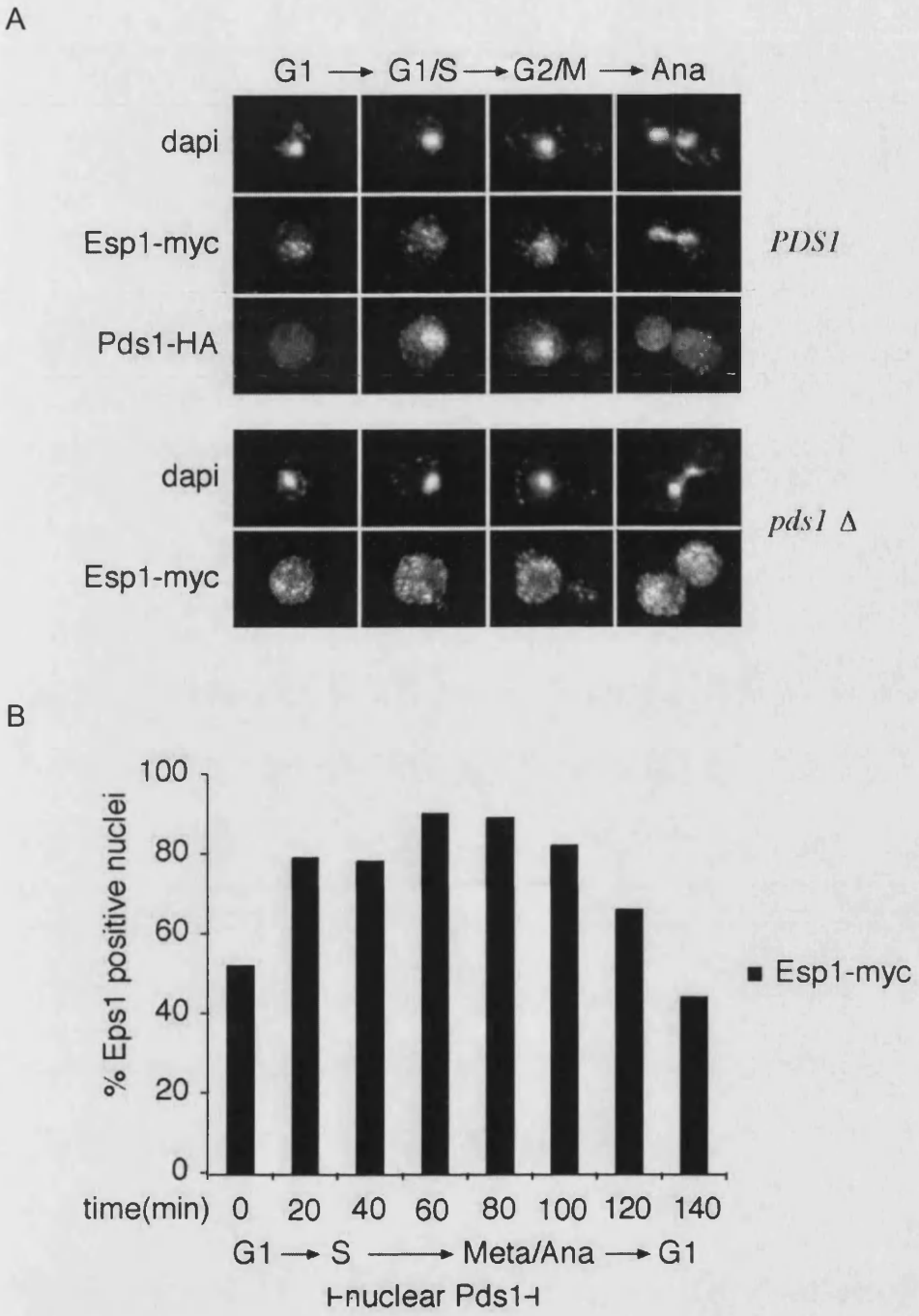

Figure 2.1: Securin is required for separase nuclear accumulation
(A) Wild-type cells, Y455 (*MATa, ESP1-myc18, PDS1-HA3, TetOs::URA3, TetR-GFP*), and cells deleted for securin, Y291 (*MATa, pds1Δ, ESP1-myc18, TetOs::URA3, TetR-GFP*), were arrested in G1 by mating pheromone α-factor and released into a synchronous cycle. Cells were fixed and processed for in situ immunofluorescense against the myc epitope on separase using monoclonal antibody 9E10 and against the HA epitope on securin using monoclonal antibody 16B12 (Babco). DNA was visualised by staining with 4',6-diamidino-2-phenylindole (dapi). Cells at characteristic cell cycle stages are shown. (B) Quantification of the nuclear separase signal shown in A.

The nuclear separase signal was strongest in metaphase and anaphase. Nuclear separase concentrations remained high until anaphase and slowly dropped when cells exited mitosis and went into the next cell cycle. Although a dotlike signal of separase was also visible in the cytoplasm throughout the cell cycle there is a clear nuclear concentration of separase that increased gradually from G1/S- to anaphase. This makes sense as separase is needed in anaphase to cleave the Scc1 subunit of the cohesin complex to release sister chromatids, allowing the cells to go into the next cell cycle.

2.1.2 The nuclear concentration of separase depends on securin

Securin inhibits the cleavage of the Scc1 subunit of the cohesin complex until anaphase onset where it is targeted for degradation by the APC. Interestingly, the promoter regions of securin and Scc1 are under the same control so that there is no substrate Scc1 produced without the appearance of the inhibitor securin. Securin is entirely nuclear right after its synthesis in S-phase until its destruction in metaphase. Hence there is no cell cycle accumulation like in the case of separase albeit high nuclear securin levels coincide with high nuclear separase levels.

To investigate if one possible positive function of securin on separase activity is to help separase to localise to its site of action, I followed the subcellular distribution of separase in cells that have been deleted for securin. Interestingly, these cells never showed a nuclear concentration of separase throughout the cell cycle. Instead the cytoplasm now appeared brighter, indicating a higher concentration of separase in this compartment (Fig.2.1-A). Securin deleted cells appear bigger and sometimes misshaped compared to wild-type cells and they take approximately 20 minutes longer to go through one cell cycle. In order to have a better resolution of the nuclear region in cells deleted for securin, I performed a confocal microscopy analysis on wild-type cells and cells that have been deleted for securin. This confirmed a broad exclusion of separase from the nucleus (Fig.2.2) in securin deleted cells.

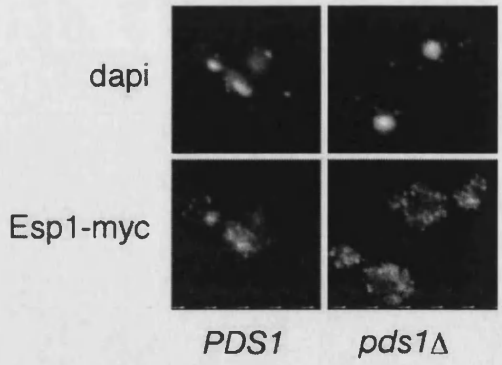

Figure 2.2: Confocal analysis of separase in wild-type cells and cells deleted for securin
Wild-type cells, Y292 (*MATa, ESP1-myc18, TetOs::URA3, TetR-GFP*), and cells deleted for securin, Y291 (*MATa, pds1Δ, ESP1-myc18, TetOs::URA3, TetR-GFP*) were treated as described in Figure 1. Confocal microscopy was performed on a laser scanning confocal microscope LSM510 (Zeiss Co.)

These results strongly suggest that securin is indeed needed for the nuclear concentration of separase during the cell cycle. Although securin disappeared in anaphase and is absent in wild-type G1 cells, separase is still concentrated in the nuclei of some of these cells. It could be that separase leaves the nucleus rather slowly after securin is destroyed. In fact separase is active cleaving the cohesin complex from anaphase until next G1.

The cohesin subunit Scc1 is cleaved on time in budding yeast cells lacking securin [102], suggesting that a certain level of separase, sufficient to cleave Scc1, can reach the nucleus even in the absence of securin. To address this directly, I observed separase on chromatin spreads in which cytoplasmatic components of the cell are washed away [121, 122]. Separase was seen associated with metaphase chromatin in wild-type cells, and to a lesser but still significant extent, it was seen on spreads from metaphase cells lacking securin (Fig.2.3). Separase was no longer chromatin associated in anaphase. Instead, and as reported previously [31, 34], separase was visible at spindle poles and, in wild-type cells, also at the anaphase spindle. The association of a low level of separase with chromatin in the absence of securin indicates that separase can indeed enter the nucleus independently of securin.

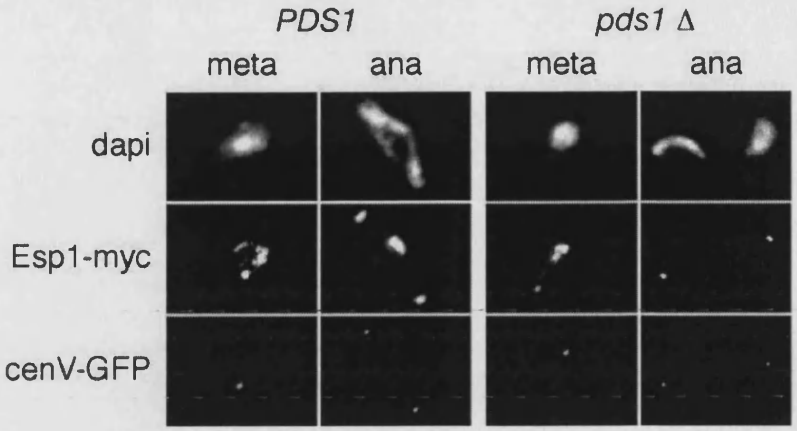

Figure 2.3: Separase associates at low levels to chromatin in securin deleted cells
Chromosome spreads of wild-type cells, Y292 (*MATa, ESP1-myc18, TetOs::URA3, TetR-GFP*), and cells deleted for securin, Y291 (*MATa, pds1Δ, ESP1-myc18, TetOs::URA3, TetR-GFP*), in metaphase and anaphase from a cell cycle experiment. Cells were arrested in G1 by mating pheromone α-factor and released into a synchronous cycle. Cells were fixed and processed for in situ immunofluorescense against the myc epitope on separase using monoclonal antibody 9E10. The cell cycle stage of individual chromosome spreads was confirmed by visualising sister chromatids close to centromere V by GFP.

2.1.3 Securin promotes separase nuclear accumulation independent of the cell cycle

Securin binds and inactivates separase at the end of G1-phase, but separase gradually accumulates in nuclei throughout G2, reaching maximum levels only in mitosis. This could mean that cell cycle-dependent events other than the presence of securin contribute to the nuclear accumulation of separase. To see if the replication phase was mandatory for separases' nuclear accumulation, cells were arrested in S-phase using the replication inhibitor hydroxyurea. However, the nuclear concentration of separase was unchanged when DNA replication was blocked, compared to cells that had reached metaphase (Fig.2.4).

To investigate if high mitotic cyclin levels are needed for a proper nuclear concentration of separase, I used cells that are temperature sensitive for the mitotic cylins clb1-4 (clb1,3,4del, clb2ts) [123], arrested them in metaphase using the spindle depolymerising drug nocodazole and shifted them to 37°C to inactivate the cyclins. Separase nuclear accumulation was not altered after

inactivating the mitotic cyclins compared to wild-type cells treated in the same way (Fig.2.5). Therefore cell cycle stages do not seem to have a major influence in the nuclear accumulation of separase.

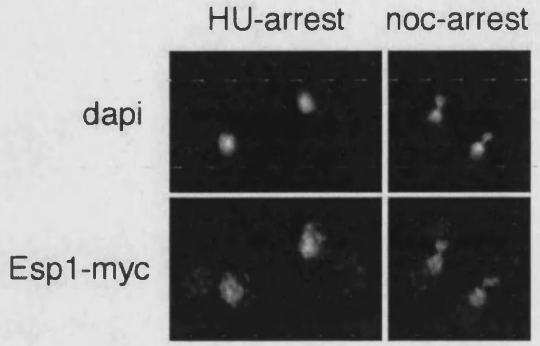

Figure 2.4: Separase accumulates in the nucleus independently of a completed replication cycle
Wild-type cells, Y292 (*MATa, ESP1-myc18, TetOs::URA3, TetR-GFP*), and cells deleted for securin, Y291 (*MATa, pds1Δ, ESP1-myc18, TetOs::URA3, TetR-GFP*), were arrested in S-phase using the replication inhibitor hydroxyurea and in M-phase using the microtubule depolymerising drug nocodazole. Cells were fixed and processed for in situ immunofluorescense against the myc epitope on separase using monoclonal antibody 9E10. DNA was visualised by staining with 4',6-diamidino-2-phenylindole (dapi). S- and M-phase arrested cells are shown.

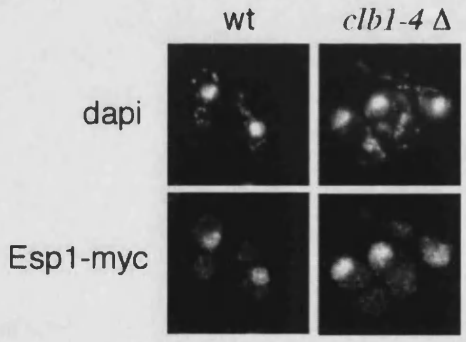

Figure 2.5: Separase accumulates in the nucleus independently of mitotic cyclins
Wild-type cells, Y292 (*MATa, ESP1-myc18, TetOs::URA3, TetR-GFP*) and cells that are temperature sensitive for the mitotic cyclins clb1-4, Y456 (*MATa, ESP1-myc18, clb1Δ, clb3Δ, clb4Δ, clb2*-ts) were arrested in metaphase using the spindle depolymerising drug nocodazole, then shifted to 37°C. Cells were fixed and processed for in situ immunofluorescense against the myc epitope on separase using monoclonal antibody 9E10. DNA was visualised by staining with 4',6-diamidino-2-phenylindole (dapi).

Alternatively, the presence of securin might be sufficient to cause nuclear accumulation of separase, but it might be a relatively slow process or require an excess of securin over separase. In this case, even G1 cells should accumulate nuclear separase if securin is ectopically expressed. To test this, I arrested cells lacking securin stably in G1 by pheromone treatment and then induced expression of securin from the galactose-inducible *GAL1* promoter (Fig.2.6) [26].

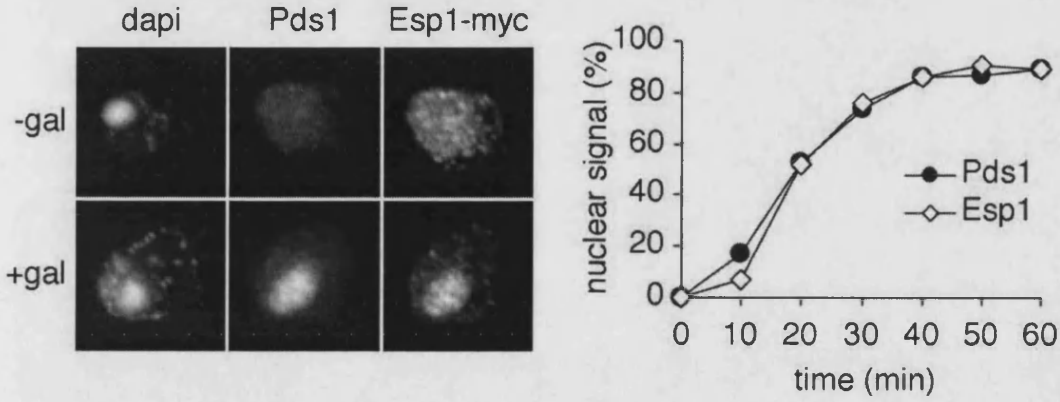

Figure 2.6: Securin is sufficient to cause nuclear accumulation of separase
Cells deleted for securin, Y576 (*MATa, pds1Δ, ESP1-myc18, GAL1-PDS1mdb*), were arrested in G1 using α-factor and expression of securin from the *GAL1* promoter was induced by addition of 2% galactose to the culture. Complete arrest in G1 before and throughout the experiment was confirmed by FACS analysis. Securin was detected using antibody sc-9076 (Santa Cruz Biotech). Examples of cells before and 30 min after galactose addition are shown.

As soon as securin appeared in the nucleus, separase had redistributed and was also concentrated in the nucleus, reminiscent of cells in mitosis. This demonstrates that expression of securin in G1 is sufficient to cause nuclear accumulation of separase. Because levels of securin after expression from the *GAL1* promoter were about 10-fold higher than endogenous levels in metaphase, an excess of securin might be sufficient to promote fast nuclear separase accumulation.

2.1.4 Securin might concentrate separase in the nucleus by preventing separases' nuclear export

Together, this suggests that separase can enter the nucleus independently of securin, but that the presence of securin is required and sufficient to cause nuclear concentration of separase.

One possible mechanism to explain this observation is that separase is in equilibrium of import and export from the nucleus. Securin, once present in the nucleus, could act to prevent nuclear export of separase thereby concentrating the protease in the nucleus. A search in the amino acid sequence of separase revealed a putative bipartite nuclear localisation sequence (NLS) RKAQNLALSLLKKKNK at amino acids 798-813 as well as several possible nuclear export sequences, Lx1-3Lx2-3LxL, for the major nuclear export receptor Crm1/Xpo1. The NLS was mutated at the lysins K809N, K810N and K811N to destroy the nuclear localisation signal. Separase mutated in these three lysins was still functional as it was able to cleave its substrate Scc1. The proteolytic activity of this separase mutant was measured incubating extract containing overexpressed mutant separase with chromatin-bound Scc1 [38].

NLS-mutated and wild-type separase were expressed from the inducible *GAL1* promoter in wild-type cells for 20 minutes and the nuclear separase signal was scored. No significant decrease in the nuclear concentration of the NLS mutated separase compared to wild-type separase was observed, indicating that the mutation of the putative NLS did not interfere with nuclear localisation of separase.

To investigate if securin achieves nuclear concentration of separase by blocking separases' nuclear export through the Crm1/Xpo1 receptor, wild-type cells and cells deleted for securin were treated with leptomycin B, a drug that efficiently blocks nuclear export through the Crm1/Xpo1-receptor [124]. Cells deleted for securin did not show any nuclear concentration of separase after leptomycin B treatment (Fig.2.7).

I then used a temperature sensitive mutation of the Crm1/Xpo1-receptor [124] and compared separases' nuclear concentration in G1 arrested cells at the permissive (25°C) and the restrictive temperature (37°C). Inactivation of the Crm1/Xpo1-receptor at 37°C, however, did not show any increase in the nuclear

localisation of separase (data not shown). Therefore, securin causes nuclear concentration of separase by a mechanism different from preventing Crm1/Xpo1-mediated nuclear export.

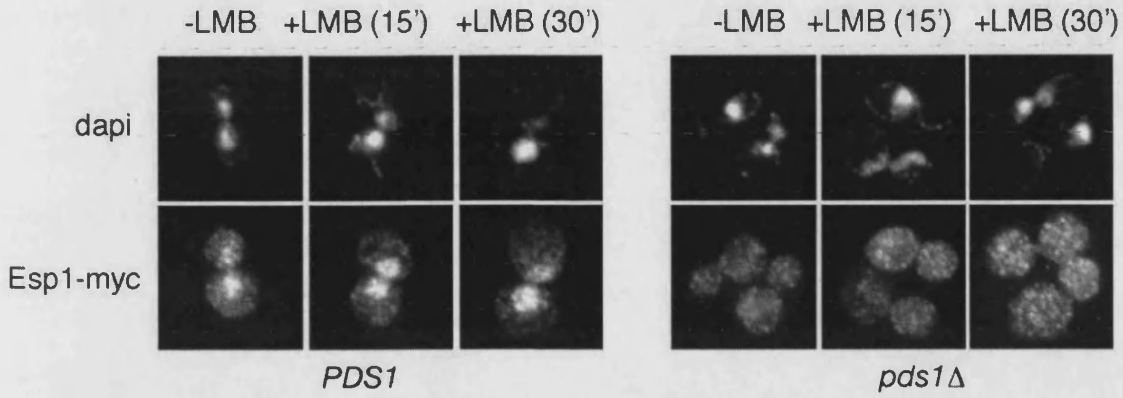

Figure 2.7: Nuclear retention of separase does not depend on the nuclear export receptor Crm1/Xpo1
Wild-type cells, Y292 (*MATa, ESP1-myc18, TetOs::URA3, TetR-GFP*), and cells deleted for securin, Y291 (*MATa, pds1Δ, ESP1-myc18, TetOs::URA3, TetR-GFP*), were treated with leptomycin B for 15 min and 30 min. Cells were fixed and processed for in situ immunofluorescense against the myc epitope on separase using monoclonal antibody 9E10. DNA was visualised by staining with 4',6-diamidino-2-phenylindole (dapi).

2.1.5 Securin supports full proteolytic activity of separase

In addition to its role in separase localisation securin might act in a chaperone-like function, possibly facilitating proper folding of the large separase polypeptide. This has been suggested for separase isolated from human cells lacking securin [103]. To address this directly in budding yeast, I measured the proteolytic activity of separase in wild-type and securin deleted cells that were both arrested in G1 by alpha factor treatment (Fig.2.8).

At this stage securin is absent from both cell types as it is degraded in anaphase and does not re-accumulate before the next S-phase. In contrast to securin deleted cells, separase in wild-type cells was previously bound to securin. I prepared extracts from both cells that contained comparable levels of separase. I then measured the protease activity of separase in both extracts by incubating them with saturating levels of Scc1 on a metaphase chromatin

preparation [35]. Separase in wild-type cell extracts was at least two-fold more active in cleaving Scc1 as compared to separase from securin deleted cells.

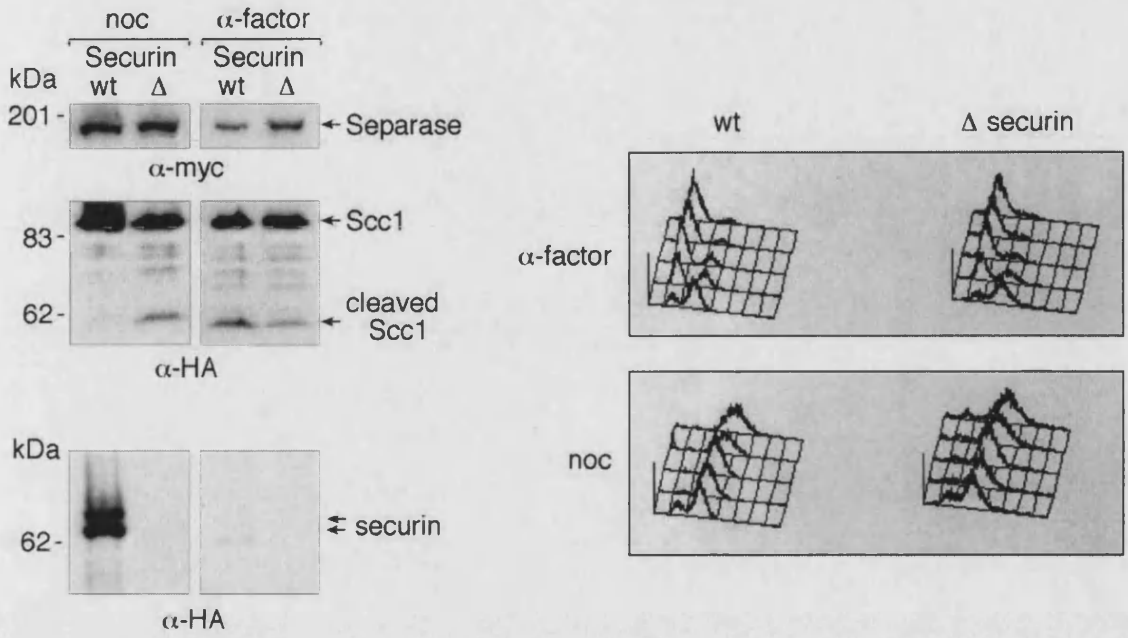

Figure 2.8: Securin helps separase to acquire its full proteolytic activity
Separase activity in wild-type, Y189 (*MATa, ESP1-myc18*), and securin deleted, Y543 (*MATa, pds1Δ, ESP1-myc18*), cells was measured. Cells were arrested in metaphase (noc) or G1 (α-factor), extracts were prepared, and Scc1 cleavage activity was measured using chromatin from metaphase cells as a substrate.

This suggests that the initial binding to securin helps separase to acquire activity after securin is destroyed. The two-fold difference in separase activity is likely an underestimate. Western blotting revealed residual low levels of securin in the wild-type cell extract that may have partly inhibited separase and that might stem from minor impurities of non-G1 cells in the preparation.

2.2 Mechanisms of separase inhibition through securin

While present in cells, securin is bound to separase [31, 34] and in crude *in vitro* systems this prevents separase from cleaving Scc1 [37, 38]. Whether securin is itself sufficient to inhibit separase, and by which mechanism securin prevents separase from attacking Scc1, was unknown. In particular, it was unclear how binding of securin to the separase N-terminus could influence the activity of the protease domain that is located at the protein's very C-terminus.

2.2.1 Securin is a protease inhibitor of separase

I therefore addressed the mechanism by which securin, while bound to separase, inhibits it from cleaving Scc1. Securin could directly inhibit the protease activity of separase, or other proteins might cooperate with securin in rendering or maintaining separase inactive. The laboratory had previously established the use of virtually pure separase and Scc1 for an in vitro assay to measure separases' proteolytic activity [38]. Separase was overexpressed in yeast and purified via a chitin binding domain on chitin beads. Scc1 was purified form baculovirus infected insect cells as well via a chitin binding domain on chitin beads. To see whether securin was sufficient to inhibit separase, I added purified securin to this reaction. The C-terminal half of securin is expected to bind to separase [30], so a fragment was designed spanning a C-terminal domain (amino acids 256-359) of securin/Pds1 fused to GST. This fragment was expressed in bacteria and purified by P.Knowles in collaboration with N.McDonald in the structural biology laboratory at Cancer Research UK (Fig.2.9-A). When this recombinant securin fragment was added to the separase assay, Scc1 cleavage was efficiently inhibited (Fig.2.9-B). In a control reaction GST alone did not inhibit separase (data not shown). This demonstrates that securin is indeed a protease inhibitor for separase.

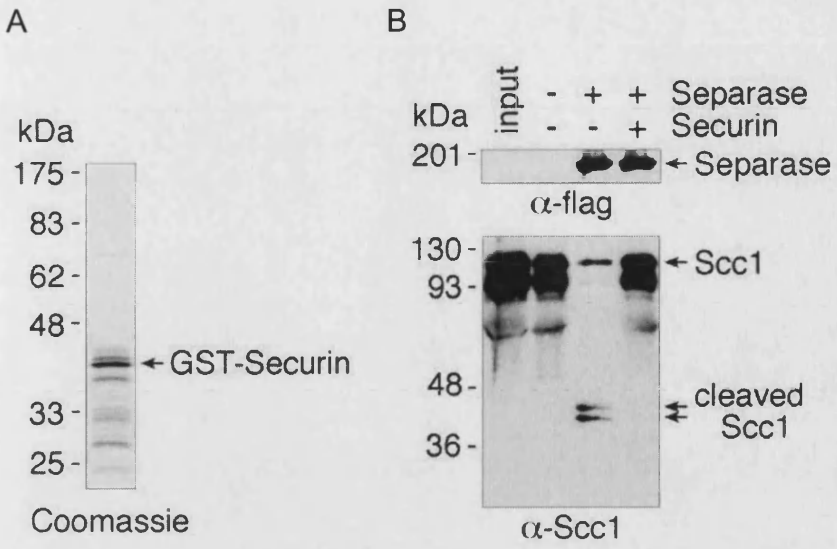

Figure 2.9: Securin inhibits separase proteolytic activity
(A) Preparation of the securin fragment (amino acids 256-359) used for the experiment. The fragment, fused to GST, was purified on glutathione sepharose. Numerous breakdown products of the fragment are present in the preparation. (B) Inhibition of separase cleavage of Scc1. For the cleavage assay separase was purified on chitin beads, and recombinant Scc1 was added as described [35]. This reaction was performed with or without addition of the securin fragment.

Securin is thought to bind to the N-terminus of separase [30, 34] while the protease active site is situated close to its C-terminus [35]. Securin might therefore cause an allosteric change within separase that inactivates the protease active site or it might prevent substrates from binding to separase. To test the latter, I measured the binding of recombinant Scc1 to separase that was immobilised via a chitin binding domain-tag on chitin beads. I used a separase variant carrying an active site point mutation (H1531A, [35]) to prevent Scc1 from being cleaved after binding. Figure 2.10 shows that Scc1 binding to separase was readily detected in this assay. When the inactivating securin fragment was incubated with the separase beads before adding Scc1, securin bound to separase and the binding of Scc1 was prevented. When separase was incubated with Scc1 first to allow binding, and then securin was added, Scc1 was displaced by securin from separase (Fig.2.10). This indicates that securin binding to separase prevents the interaction of separase with its substrate, and that the interaction of securin with separase is likely to be stronger, or more stable than, the interaction with Scc1.

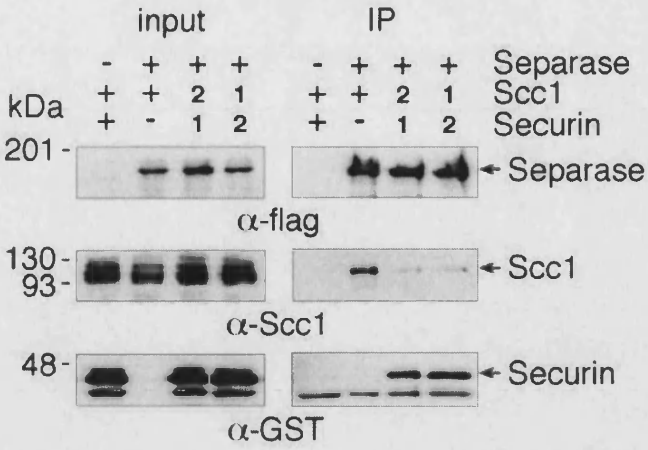

Figure 2.10: Securin inhibits binding of Scc1 to separase
The catalytically inactive separase variant, H1505A, was purified from strain Y364 (*MATa, pep4Δ, GAL1-flag-ESP1(H1505A)-CBD*) on chitin beads and binding of recombinant Scc1 was analysed. Securin was added either before (1), or after (2), the incubation with Scc1.

I then analysed if securin had any effect on the binding of the protease inhibitor Bio-SVEQGR-amk to separase [35]. This inhibitor is a short biotinylated peptide spanning an Scc1-derived cleavage site motif linked to a reactive acyloxomethylketone (amk) group that covalently binds to and inhibits the separase active site cysteine residue. If securin prevents Scc1 binding to separase by occupying a substrate binding site at the separase N-terminus, the small peptide inhibitor might still gain access to the active site at the C-terminus. Separase was purified again on chitin beads, incubated with or without securin, and Bio-SVEQGR-amk was added (Fig.2.11-A). The inhibitor bound to separase, as detected by Western blotting against its biotin moiety, but binding was prevented by preincubation of separase with securin.

This indicates that securin does not only hinder access of the substrate protein Scc1, but also of a reactive cleavage site peptide. Peptide binding could be blocked if securin binds tightly into the separase active site groove. However, when the protease active site was occupied by Bio-SVEQGR-amk this did not perturb the subsequent interaction of securin with separase (Fig. 2.11-B). Indeed securin makes only a weak contact with the separase C-terminus (see below). Therefore securin might prevent binding of the cleavage site peptide to separase by an alternative mechanism, maybe by causing an allosteric change that distorts the active site.

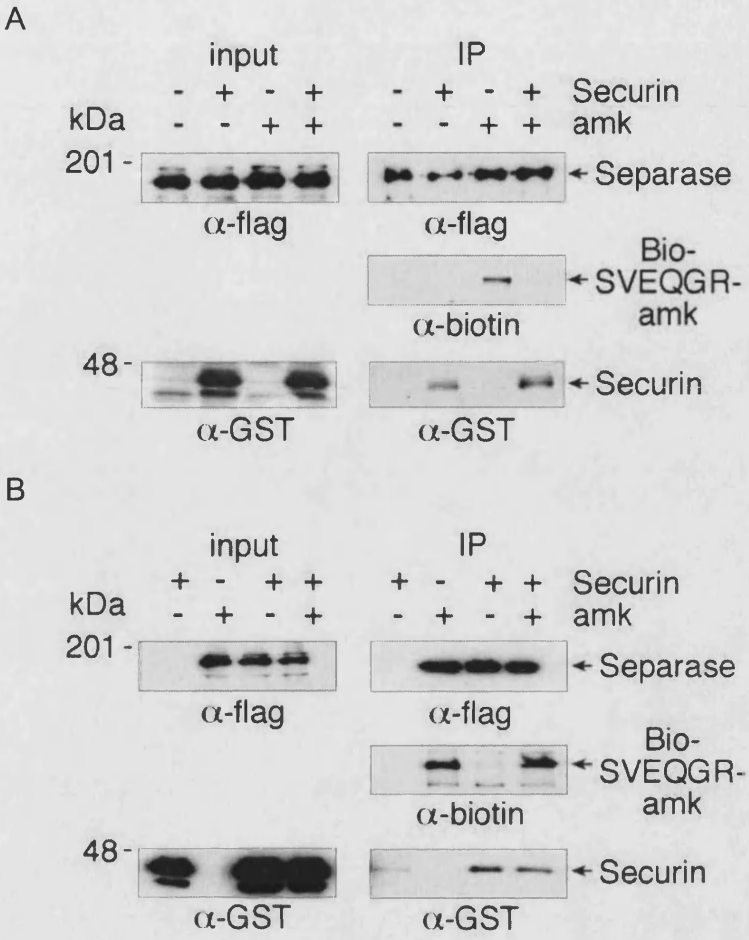

Figure 2.11: Securin inhibits the reaction of separase with a cleavage site binding peptide
(A) Separase was purified from strain Y334 (*MATa, GAL1-flag-ESP1-CBD*), and the binding of the peptide inhibitor Bio-SVEQGR-amk (amk) was measured with or without addition of securin. (B) Same as (A), but the binding of securin was measured after the addition of the peptide inhibitor Bio-SVEQGR-amk (amk).

2.2.2 Separases' peptide recognition site is not essential for substrate binding

To better understand how separase recognises its cleavage substrates, I investigated whether the cleavage site motif is the only determinant that mediates interaction with separase. I made again use of the Bio-SVEQGR-amk peptide inhibitor of separase and asked whether separase in which the cleavage peptide recognition pocket was occupied with Bio-SVEQGR-amk was still able to interact with Scc1. As a comparison, the interaction of free separase with Scc1 was analysed. To prevent cleavage of Scc1 during binding to free

separase, a catalytic inactive separase (C1531A, [35]), in which the active site cysteine was mutated to alanine, was used (Fig.1.12).

Both wild-type and C1531A separase were isolated after overexpression in yeast by chitin affinity purification. Wild-type separase was incubated with Bio-SVEQGR-amk, then recombinant Scc1 was added to test binding to the two different separase preparations. Proteolytically inactive C1531A separase without peptide inhibitor interacted with Scc1, as has been seen before [35]. Wild-type separase that had been incubated with the cleavage site peptide inhibitor bound Scc1 with indistinguishable efficiency. This suggests that separase makes contact with Scc1 that are independent of cleavage site peptide recognition. I confirmed that the peptide inhibitor was indeed bound to separase by Western blotting against the biotin moiety attached to the inhibitor N-terminus. No Scc1 cleavage was detectable after the incubation, which further confirmed that all wild-type separase was bound and inhibited by the peptide. I also added Scc1 to wild-type separase that had not been treated with the peptide inhibitor. As expected Scc1 was cleaved in this reaction, but now the C-terminal cleavage fragment interacted with separase. Since this fragment does not contain a cleavage site motif, this provides further evidence that contacts between separase and Scc1 exist that lie outside the cleavage site motif (Fig.2.12).

Together these results indicate that the catalytic dyad of separase, although essential for Scc1 cleavage, is not necessary for binding of the substrate to the protease.

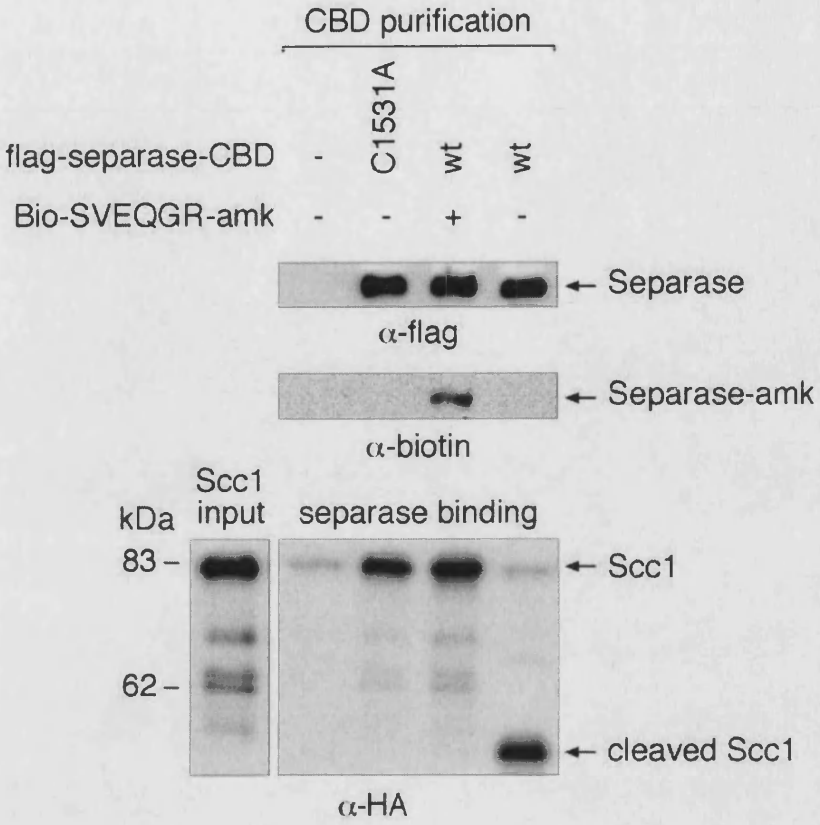

Figure 2.12: Interaction of separase with Scc1 occurs independently of cleavage site recognition
Wild-type or catalytically inactive (C1531A) separase, fused to a flag epitope and chitin binding domain (CBD), were purified after overexpression under the inducible *GAL*-promoter. Wild-type separase was incubated with or without the peptide inhibitor Bio-SVEQGR-amk. After the incubation, binding of recombinant Scc1, marked with an HA epitope tag, to the different separase preparations was analysed. A control binding reaction of Scc1 to beads after a mock purification is included. Scc1 bound to free catalytically inactive separase and to peptide-inhibited wild-type separase with comparable efficiency. A C-terminal cleavage product of Scc1, produced after incubation with uninhibited wild-type separase, also associated with separase.

2.2.3 Securin interacts with separase N-and C-termini

Because the protease active site is located at the separase C-terminus, I wanted to see which parts of separase directly interact with securin and thereby confer the inhibition. I constructed different N-terminal deletion mutants of separase that were overexpressed in yeast and purified on chitin beads as above (Fig.2.13). One of the constructs lacked only the first 155 amino acids from the N-terminus (156C), another construct comprised the conserved separase domain (1196C), a third construct only included the C-terminal half of

the separase domain that is predicted to fold into the protease domain (1390C). When the inhibiting GST-securin fragment was added, it bound efficiently to full-length separase, but significantly less well to any of the deletion mutants (Fig.2.14-A). Thus, the very N-terminus of separase contributes to the inhibitory interaction with securin.

Because only a C-terminal part of securin was used in this binding assay, one could not exclude the possibility of additional contacts between securin and separase. I therefore co-expressed full-length securin and the different separase constructs in yeast and isolated complexes by binding of separase to chitin beads (Fig.2.14-B). Again, only full-length separase interacted efficiently with securin. But a weaker interaction of securin with separase was evident after the N-terminus was deleted. The efficiency of this interaction was similar when separase lacked only 155 N-terminal amino acids or when only the short C-terminal protease domain was expressed (Fig.2.14-B). This shows that while the separase N-terminus is necessary for securin binding, securin also makes contact with the C-terminal protease domain in separase.

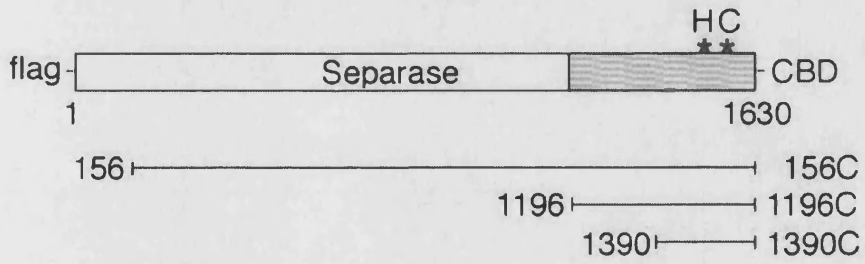

Figure 2.13: Scheme of the separase N-terminal deletion mutants
The separase domain that shows conservation between all species is shaded. The residues histidine, H, and cysteine, C, that are predicted to form the catalytic dyad are marked with asterisks. The scheme is drawn to scale.

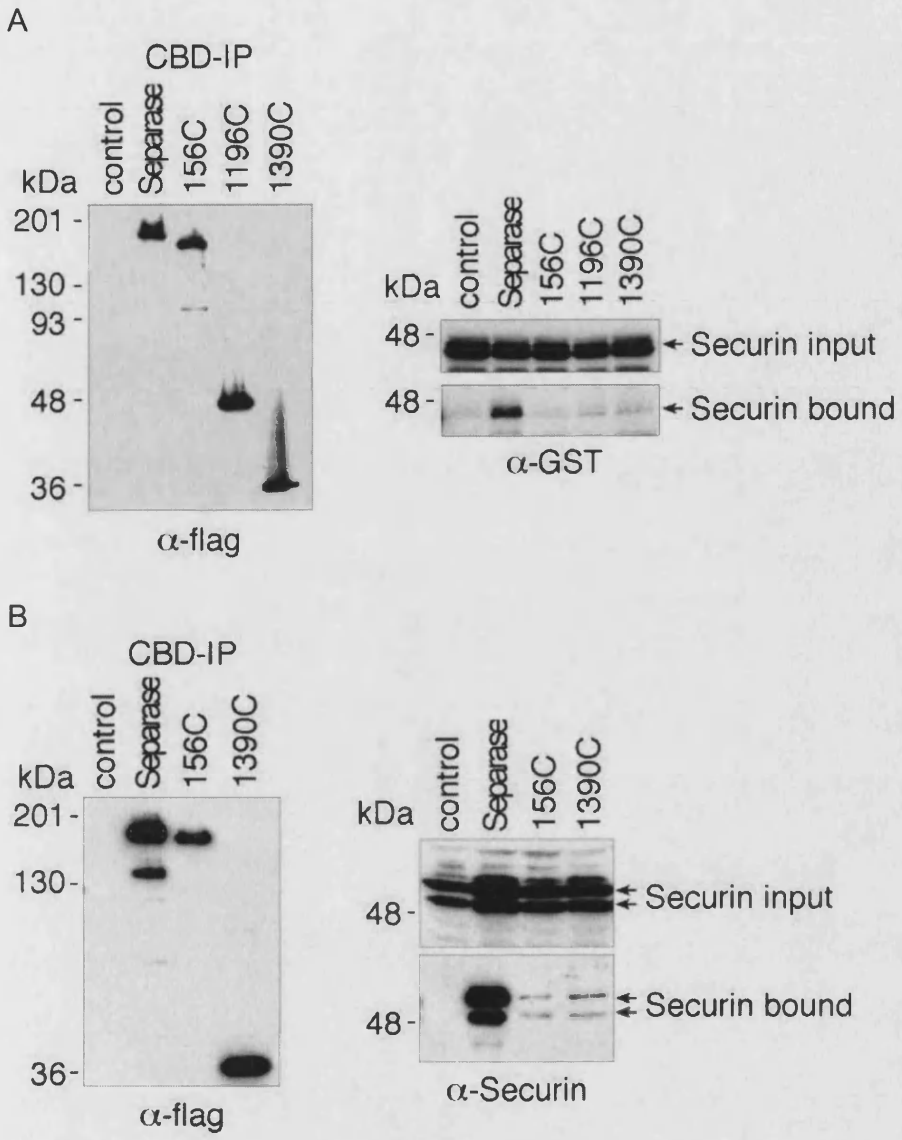

Figure 2.14: Securin interacts with the N-terminus of separase
(A) The strains that expressed these deletion mutants were Y373 (*MATa, GAL1-flag-ESP1(156C)-CBD*), Y367 (*MATa, GAL1-flag-ESP1(1196C)-CBD*), and Y336 (*MATa, GAL1-flag-ESP1(1390C)-CBD*). Separase and the deletion mutants were purified on chitin beads, and binding of the securin fragment was analysed. (B) Separase and the deletion mutants together with full-length securin were co-overexpressed in yeast and their association was analysed after binding separase to chitin beads. Securin was detected using antibody sc-9076.

2.2.4 The separase N-terminus is required for protease activity

What role does the N-terminus play for the activity of separase and its inhibition by securin? To address this question, I now analysed the separase deletion mutants for protease activity against Scc1. After overexpression in

yeast, only full-length separase was capable of cleaving Scc1 while removing the first 155 amino acids completely abolished its protease activity (Fig.2.15-A). This shows that the separase N-terminus plays an essential role in the proteolytic activity of the protein.

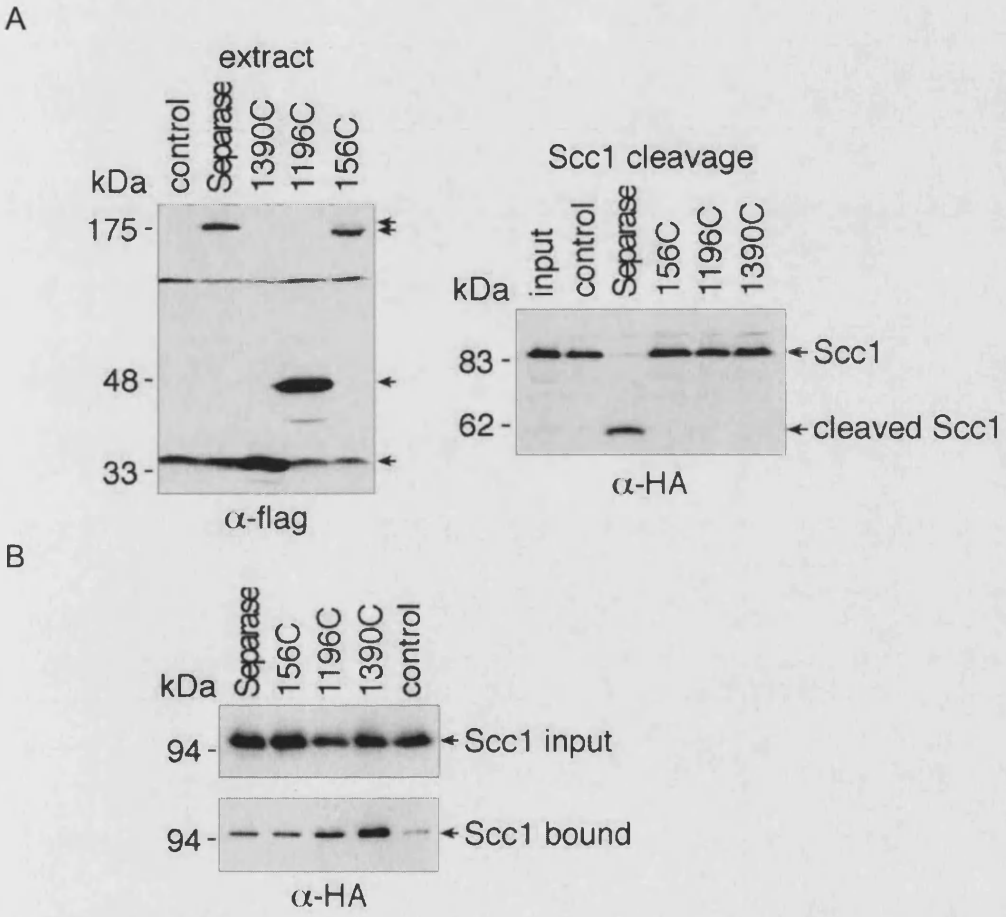

Figure 2.15: The separase N-terminus is required for catalytic activity
(A) Separase and N-terminal deletion mutants were overexpressed in yeast, and separase activity in the extracts was measured using yeast chromatin as the substrate as described [35]. The arrows in the left panel indicate the migration of the individual separase fragments. (B) A catalytically inactive version of full-length separase and the deletion mutants together with Scc1 were co-overexpressed in yeast. Association of Scc1 with separase was measured after binding separase to chitin beads.

It might be that separase lacking the N-terminus can no longer interact with its substrate Scc1. Alternatively the N-terminus might be required for the C-terminus to adopt a proteolytically active conformation. To distinguish between these possibilities I first analysed the ability of the N-terminal separase deletion mutants to interact with Scc1 (Fig.2.15-B). All of the deletion mutants interacted

with Scc1. Indeed the interaction was reproducibly enhanced when only the C-terminal protease domain of separase, 1390C, was expressed (Fig.2.15-B). This demonstrates that the separase N-terminus is not required for interaction with the substrate Scc1. N-terminal sequences might be even involved in loosening the protease substrate interaction to facilitate turnover of processed substrate.

I then analysed the binding of the peptide inhibitor Bio-SVEQGR-amk to the separase deletion mutants which all interacted with Scc1. If the protease domain is in an active state, one would expect the cleavage site peptide inhibitor to be able to bind to these fragments as well. Instead, while full-length separase efficiently bound the peptide inhibitor, binding was strongly reduced in any N-terminal deletion (Fig.2.16).

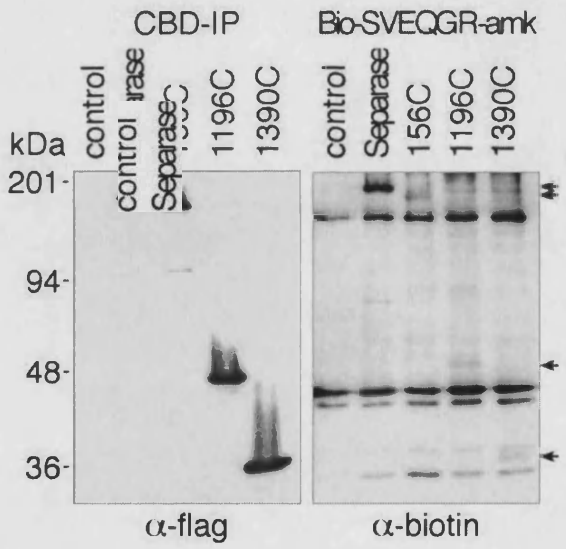

Figure 2.16: The separase N-terminus is required for binding of the cleavage site peptide
Wild-type separase and separase deletion mutants were immobilised on chitin beads and incubated with the cleavage site peptide inhibitor Bio-SVEQGR-amk. Binding of the inhibitor was analysed by probing the Western blot against the biotin moiety of the inhibitor.

This shows that while the N-terminus is not required for overall interaction of separase with its substrate Scc1, it is required for the C-terminal protease active site to react with the peptide inhibitor. The separase N-terminus might be required to stabilise an active conformation of the protease active site. Only the

active conformation would allow access of the cleavage site peptide to the active site groove or its attack by the active site cysteine residue. To achieve this, the N-terminus might have an allosteric effect on the active site. Alternatively, the N-terminus might become itself part of the active site.

2.2.5 Separase N- and C-termini bind each other

The dependence of separase activity on its own N-terminus predicts that separase N- and C-termini may interact. To test whether there might be a direct physical association, I co-overexpressed fragments from both ends of separase in yeast. The C-terminal fragments were purified via the attached chitin binding domain and association with the N-terminal fragments was analysed by Western blotting against the flag epitopes present on both fragments (Fig.2.17-A and B).

I first expressed the entire separase sequence in two parts, the C-terminal separase domain (1196C), together with the N-terminus (N1195). These two fragments of separase associated with each other in stoichiometric amounts, indicating a stable interaction between them (Fig.2.17-B, lane 3). The interaction was not diminished when only the shorter C-terminal protease domain, 1390C, was expressed (Fig.2.17-B, lane 4), indicating that the contact of the N-terminus may occur at the protease domain. When a shorter N-terminal fragment comprising residues 1-370 was expressed, this N370 fragment also interacted with the C-terminal separase domain, although with somewhat reduced efficiency (Fig.2.17-B, lane 5). Therefore, while N370 makes contact with the separase C-terminus, more central parts of the protein may also be involved.

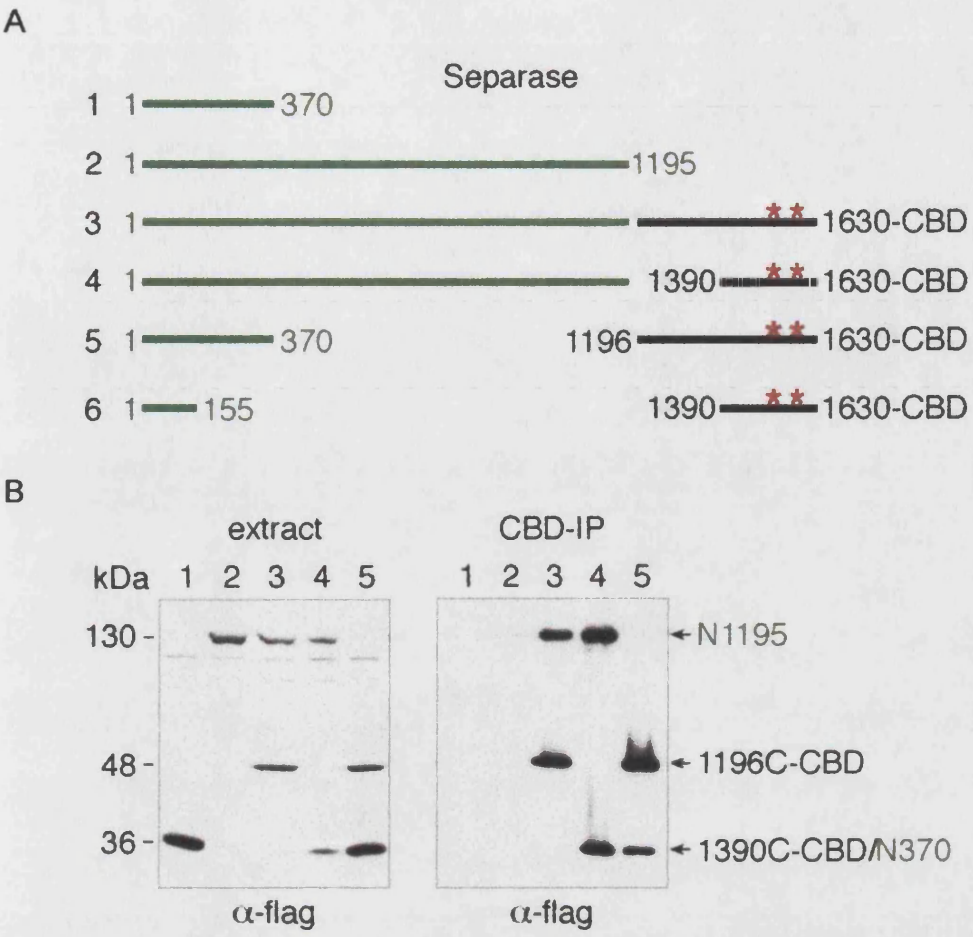

Figure 2.17: The N- and C-termini of separase interact with eachother
(A) Scheme of the separase fragments expressed in the experiment. The strains expressing these fragments were 1 Y538 (*MATa, GAL1-flag-ESP1(N370)*), 2 Y490 (*MATa, GAL1-flag-ESP1(N1195)*), 3 Y533 (*MATa/MATα, GAL1-flag-ESP1(N1195), GAL1-flag-ESP1(1196C)-CBD*), 4 Y532 (*MATa/MATα, GAL1-flag-ESP1(N1195), GAL1-flag-ESP1(1390C)-CBD*), 5 Y541 (*MATa/MATα, GAL1-flag-ESP1(N370), GAL1-flag-ESP1(1196C)-CBD*), 6 Y561 (*MATa/MATα, GAL1-flag-ESP1(N155), GAL1-flag-ESP1(1390C)-CBD*). (B) Extracts from these strains were prepared and interactions between N- and C-terminal pairs were analysed after binding of the C-terminal fragments to chitin beads. The numbers correspond to the combinations of fragments as indicated in (A).

2.2.6 Securin disrupts the separase N/C-terminal interaction

How could the presence of securin influence the interaction between separases' N- and C-termini? To address the question, I expressed 155 N-terminal amino acids (N155) together with the C-terminal protease domain (Fig.2.17-A, raw 6). Expression of the N155 fragment from the *GAL1* promoter

consistently yielded poor expression levels compared to other separase fragments. Nevertheless a clear interaction of this fragment with the C-terminal protease domain (Fig.2.18) was detectable. When securin was co-overexpressed in the same cells, the interaction between the N155 fragment and the protease domain was markedly reduced. Instead, securin now bound to the protease domain. This indicates that securin is capable of displacing the separase N-terminus from the C-terminus. The low levels of N155 still bound to the separase domain in the presence of securin could mean that the displacement was not complete under the experimental conditions. Alternatively it might stem from a trimeric complex in which securin might bind separase N- and C-termini simultaneously. The recovery of a trimeric complex is expected to be poor because of the relatively weak interaction of securin with the separase C-terminus. This demonstrates that securin can interrupt interactions between the separase N- and C-terminus. Therefore securin has the potential to disrupt contacts within separase that may be crucial for the activation of the protease active site.

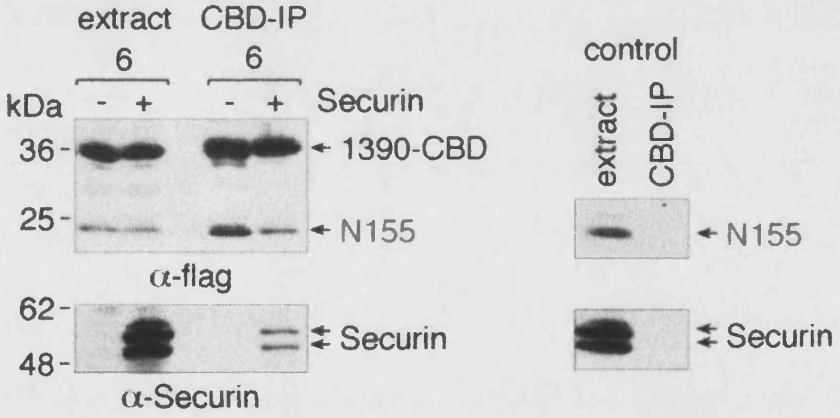

Figure 2.18: The interaction between the separase N- and C-termini is disrupted by securin
As described in Figure 2.16, but securin was co-overexpressed in addition to the separase fragments using strain Y682 (*MATa/MATα, GAL1-PDS1, GAL1-flag-ESP1(N155), GAL1-flag-ESP1(1390C)-CBD*).

2.2.7 Separase activation is intramolecular

Securin could prevent separases' proteolytic activity in two ways: either by preventing an intramolecular activating interaction between separases' N- and C-termini or by interfering with an intermolecular interaction of two separase polypeptides. To investigate if separase forms dimeric or multimeric complexes, I myc-epitope tagged endogenous separase and introduced in the same cell a further HA-epitope tagged separase copy under its endogenous promoter. As in budding yeast separase is active from anaphase throughout G1-phase, I arrested cells in G1 by pheromone treatment to follow a possible oligomerisation of separase during its proteolytic active phase. Immunoprecipitaion with either tag was performed, but did not lead to a pull down of the second separase polypeptide (Fig.2.19). This indicates that separase does not form dimers or multimers, but that it most likely activates itself via an intramolecular interaction between its N-and C-terminus.

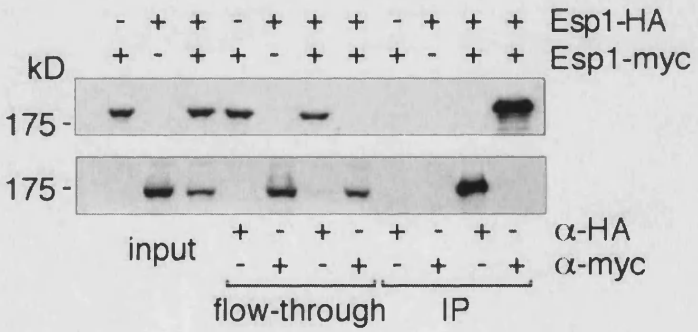

Figure 2.19: Separase activation is intramolecular
Extracts from strains Y1244 (*MATa, ESP1-HA6*), Y1316 (*MATa, ESP1-myc18*), Y1243 (*MATa, ESP1-myc18, Esp1promoter-ESP1-HA6*) were prepared after alpha factor arrest and interactions between the two separase polypeptides were analysed after binding to protein A beads.

Chapter 3

Differential cleavage of chromatin-bound and soluble cohesin

An aspect of cohesin cleavage that has so far received little attention is the apparent ability of separase to discriminate between cohesin bound to chromosomes and soluble cohesin inside cells in mitosis. In vertebrates a large fraction of cohesin is removed from chromosomes already in prophase by a mechanism that does not involve Scc1 cleavage [106, 125]. This 'prophase pathway' of cohesin removal is thought to facilitate individualisation and condensation of chromosome arms as cells enter mitosis. Only a relatively small fraction of cohesin is still bound to chromosomes in metaphase, providing crucial cohesion at centromeres and between condensed sister arms. At anaphase onset, only a similarly small fraction of the total cellular cohesin is cleaved by separase [106], and this fraction therefore most likely corresponds to still chromatin-bound cohesin. During fission yeast anaphase an equally small fraction of the cellular cohesin appears to be cleaved [71]. Targeted cleavage of only chromatin-bound cohesin would make the best use of separase activity to promptly separate sister chromatids at anaphase onset. Furthermore, in both fission yeast and vertebrates cohesin reassociates with chromosomes soon after anaphase. For this it may be important to maintain the soluble pool of cohesin intact and uncleaved during anaphase.

In budding yeast metaphase approximately two thirds of the total cohesin is bound to chromatin, while one third is found in a soluble cellular fraction [52, 126]. In contrast to higher eukaryotes, budding yeast chromosomes condense only slightly in mitosis [127], which may allow a relatively large fraction of cohesin to remain chromatin-bound. Consistently, in anaphase the majority of, but not all, Scc1 is cleaved by separase [38]. It is not known whether budding yeast separase differentiates cleavage of chromosomal and soluble cohesin.

3.1 Separase preferentially cleaves chromatin-bound Scc1 in vitro

3.1.1 Chromatin-bound Scc1 is cleaved faster than soluble Scc1

To address whether chromatin-bound budding yeast cohesin might be preferentially cleaved by separase over cohesin in the soluble cellular fraction, I established an in vitro assay to compare the cleavage rates of Scc1 in these two pools of cohesin. Chromatin and soluble fractions were prepared from two metaphase arrested cultures of budding yeast cells in which endogenous Scc1 was fused to an HA- or myc-epitope tag, respectively. Chromatin and soluble fractions containing reciprocal Scc1 epitope tags were mixed. This resulted in two reactions, one containing chromatin bound Scc1-HA and soluble Scc1-myc, and one with chromatin bound Scc1-myc and soluble Scc1-HA (Fig. 3.1).

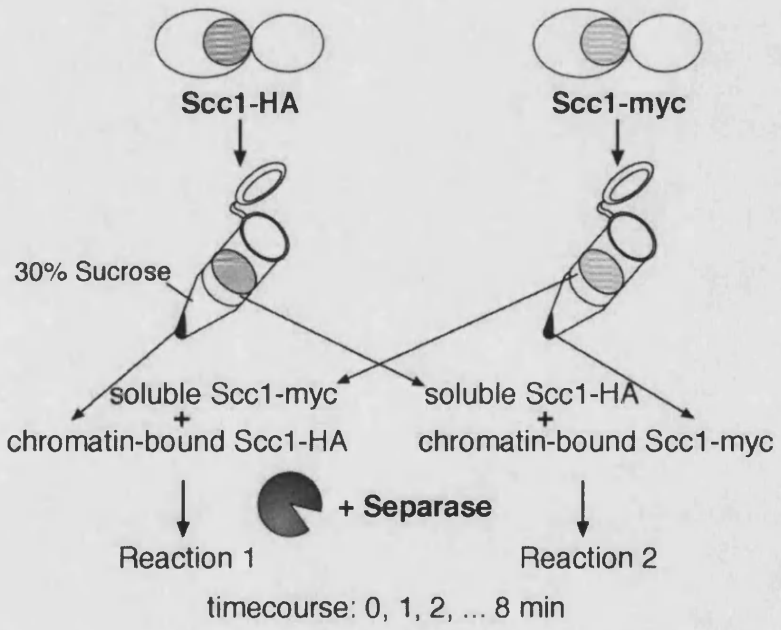

Figure 3.1: Experimental outline to compare the rates of Scc1 cleavage in chromatin-bound versus soluble cohesin
Whole cell extracts of nocodazole arrested cells were fractionated by centrifugation through a 30% sucrose cushion into chromatin-bound and soluble proteins. Chromatin and soluble fractions containing differentially tagged Scc1 were mixed and cell extract containing overexpressed separase was added. The two reciprocal reactions were incubated at 25°C and aliquots retrieved at 1 min intervals for analysis by quantitative Western blotting.

Scc1 cleavage in the mixtures was induced by adding cell extracts containing overexpressed separase and placing the reactions at 25°C. Samples of the cleavage reaction were taken every minute to follow Scc1 cleavage. This allowed cleavage of chromatin-bound and soluble cohesin to be compared within one reaction, distinguished by their differential epitope tags.

The amount of remaining full-length Scc1 with either epitope tag at each time point was analysed by quantitative Western blotting (Fig.3.2). Scc1 cleavage over time adhered closely to the characteristics of a first order reaction, consistent with a bimolecular reaction in which Scc1 is turned over by a constant concentration of separase (Fig.3.3).

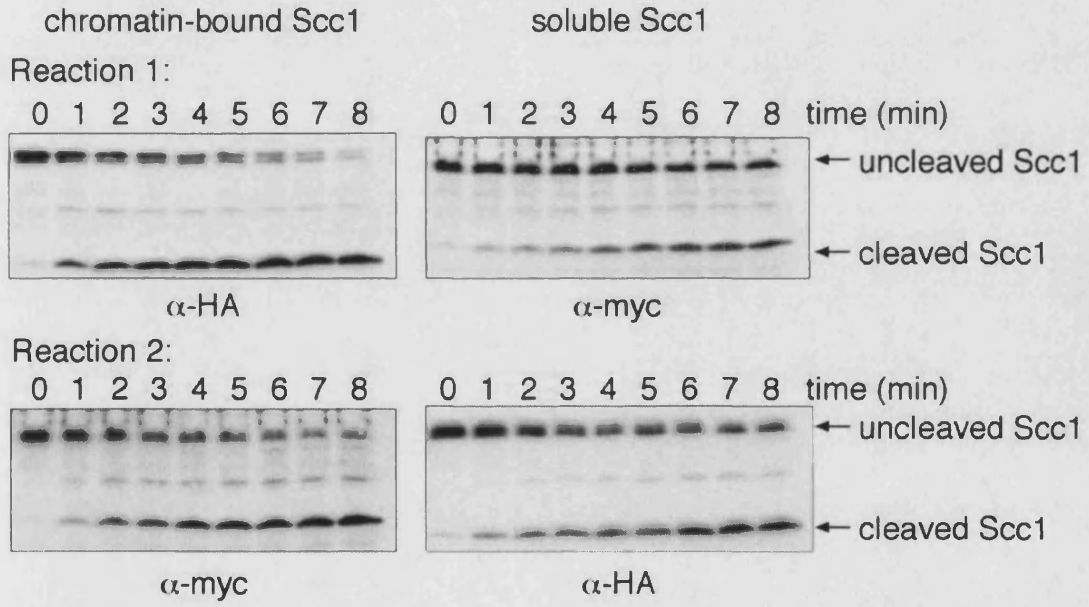

Figure 3.2: Scc1 in chromosomal cohesin is cleaved at faster rate than Scc1 in soluble cohesin
Western blot analysis of the two Scc1 cleavage reactions described in Figure 1. Reaction 1 compares cleavage of chromatin-bound Scc1-HA with soluble Scc1-myc, and reaction 2 compares cleavage of chromatin-bound Scc1-myc with soluble Scc1-HA. The strains were Y58 (*MAT*a, *SCC1-myc18*), and K8869 (*MAT*a, *SCC1-HA6*). Separase overexpression was in strain Y334 (*MAT*a, *GAL-flag-ESP1-CBD*).

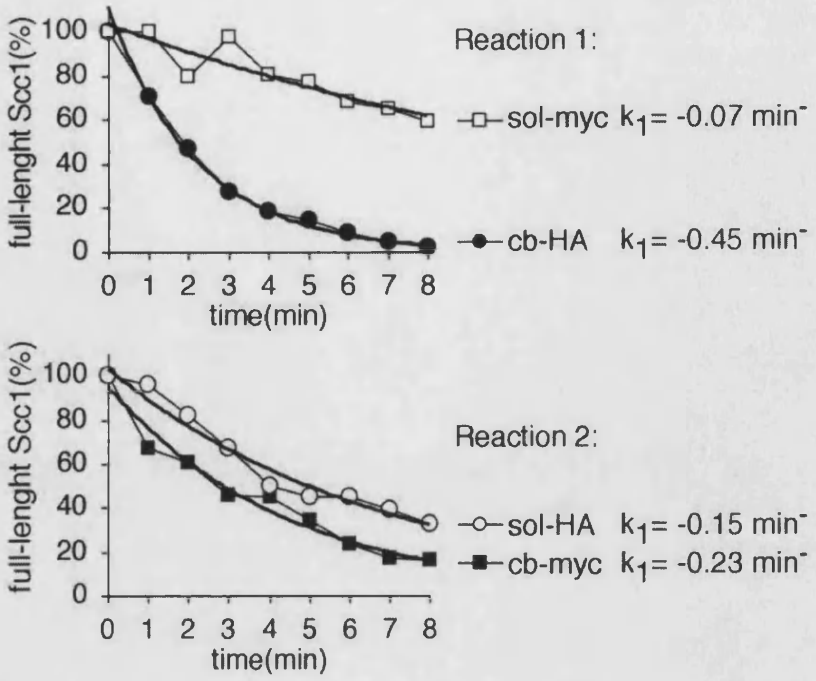

Figure 3.3: Quantification of remaining full-length Scc1 in the chromatin-bound (cb) and soluble (sol) fraction over time
Bands on the Western blot in Figure 3.2 were quantified using an IRDye800 coupled secondary antibody and an Odyssey fluorescence scanner (LI-COR). The graph was fitted with a first order reaction (bold line), and the first order rate constant k_1 was derived.

Comparison of the derived first order rate constants for Scc1 cleavage in each reaction showed that chromatin-bound Scc1 was cleaved significantly faster than soluble Scc1. Chromatin-bound Scc1-HA was cleaved 6 times faster than soluble Scc1-myc, and chromatin-bound Scc1-myc was cleaved about 1.5 times faster than soluble Scc1-HA. Therefore, in both reactions chromatin-bound cohesin was preferentially cleaved by separase. The discrepancy as to the extent of the difference was most likely caused by the differential epitope tags. When compared side by side, cleavage of Scc1-myc occured consistently at reduced rate compared to corresponding fractions containing Scc1-HA (Fig.3.4). This could be due to steric hindrance of cleavage by the myc epitope tag. Together this suggests that the chromatin context enables Scc1 to be cleaved faster as compared to Scc1 in soluble cohesin.

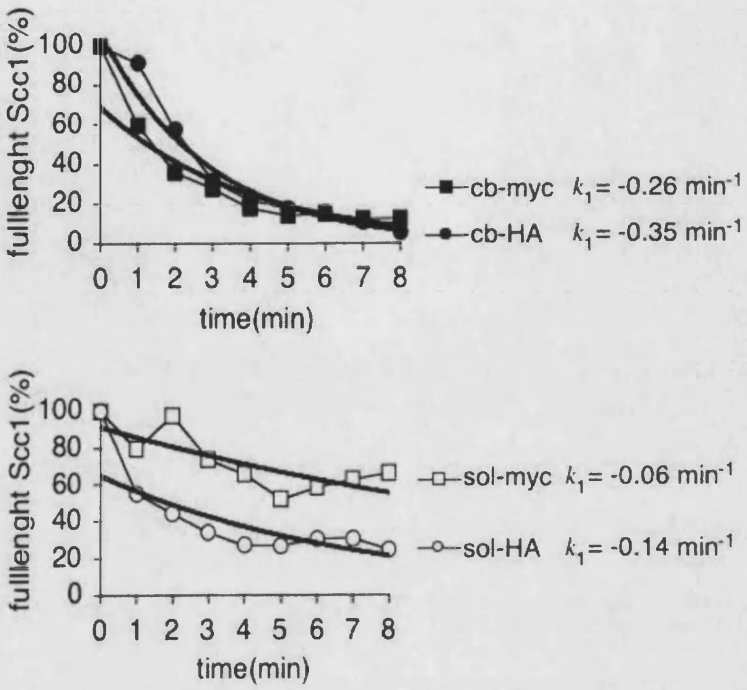

Figure 3.4: Cleavage rates of HA and myc epitope-tagged Scc1 in direct comparison
Cleavage rates of chromatin-bound and soluble Scc1-HA and Scc1-myc were determined as in Figure 3.3, but the reactions compared either chromatin-bound Scc1-HA and chromatin-bound Scc1-myc, or soluble Scc1-HA and soluble Scc1-myc.

3.1.2 Preferred cleavage of chromatin-bound Scc1 is maintained after its solubilisation

The faster cleavage of chromosomal Scc1 could be due to preferential separase targeting by the chromatin environment. Alternatively, chromatin-bound cohesin may aquire a property that facilitates its cleavage independently of the chromosomal context. To distinguish between these possibilities, I solubilised cohesin from chromatin by DNase I treatment. After DNase I digest, no DNA was detectable in the solubilised fraction and the released cohesin was found in a complex indistinguishable in size from soluble cohesin (Fig.3.5, and [52]).

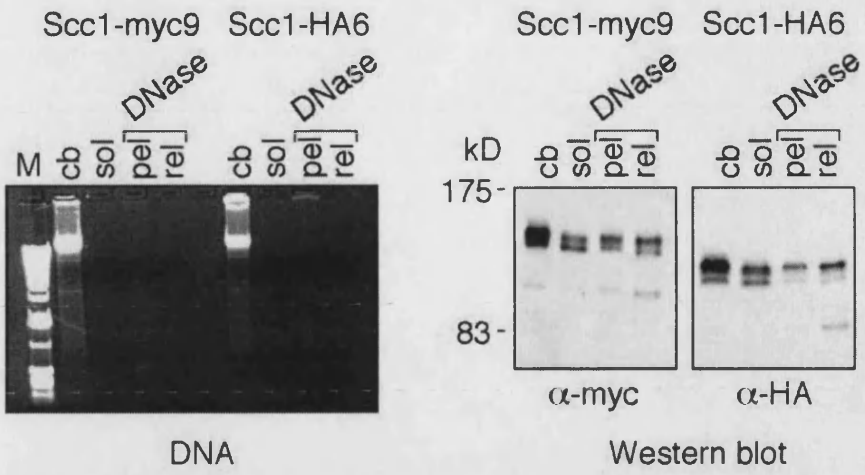

Figure 3.5: Chromatin release of cohesin by DNase I digest
Fractions during the release of cohesin from chromatin were analysed by Western blotting against Scc1. Aliquots were analysed after phenol/chloroform extraction and RNase treatment by TAE/agarose gel electrophoresis, followed by staining with ethidium bromide, to visualise DNA. The starting chromatin-bound (cb) and soluble (sol) fractions are shown, as well as the remaining insoluble material after DNase I treatment (pel) and the released, soluble fraction after DNase I digest (rel).

The rate of cleavage of chromatin-released cohesin was analysed as in the above assay. I compared cleavage of chromatin-released HA-epitope tagged Scc1 with either chromatin-bound or soluble myc-epitope tagged Scc1. Chromatin-released Scc1-HA was still 4 times faster cleaved than Scc1-myc from the soluble cellular fraction. It was also somewhat faster cleaved than Scc1-myc in chromatin-bound cohesin, but the latter difference was not significantly different from the effect of the differential epitope tags (Fig.3.6-A). This suggests that chromatin-released cohesin is cleaved with similar rate to chromatin-bound cohesin. I also compared cleavage of chromatin-released myc-epitope tagged Scc1 with either chromatin-bound or soluble HA-epitope tagged Scc1. Chromatin-released Scc1-myc was now cleaved with similar rate as soluble Scc1-HA, and 2-fold slower than chromatin bound Scc1-HA (Fig.3.6-B). Taking into account that the myc epitope tag by itself slows cleavage, this is consistent with the idea that cohesin released from chromatin is still cleaved at a faster rate than cohesin found in the soluble cellular fraction.

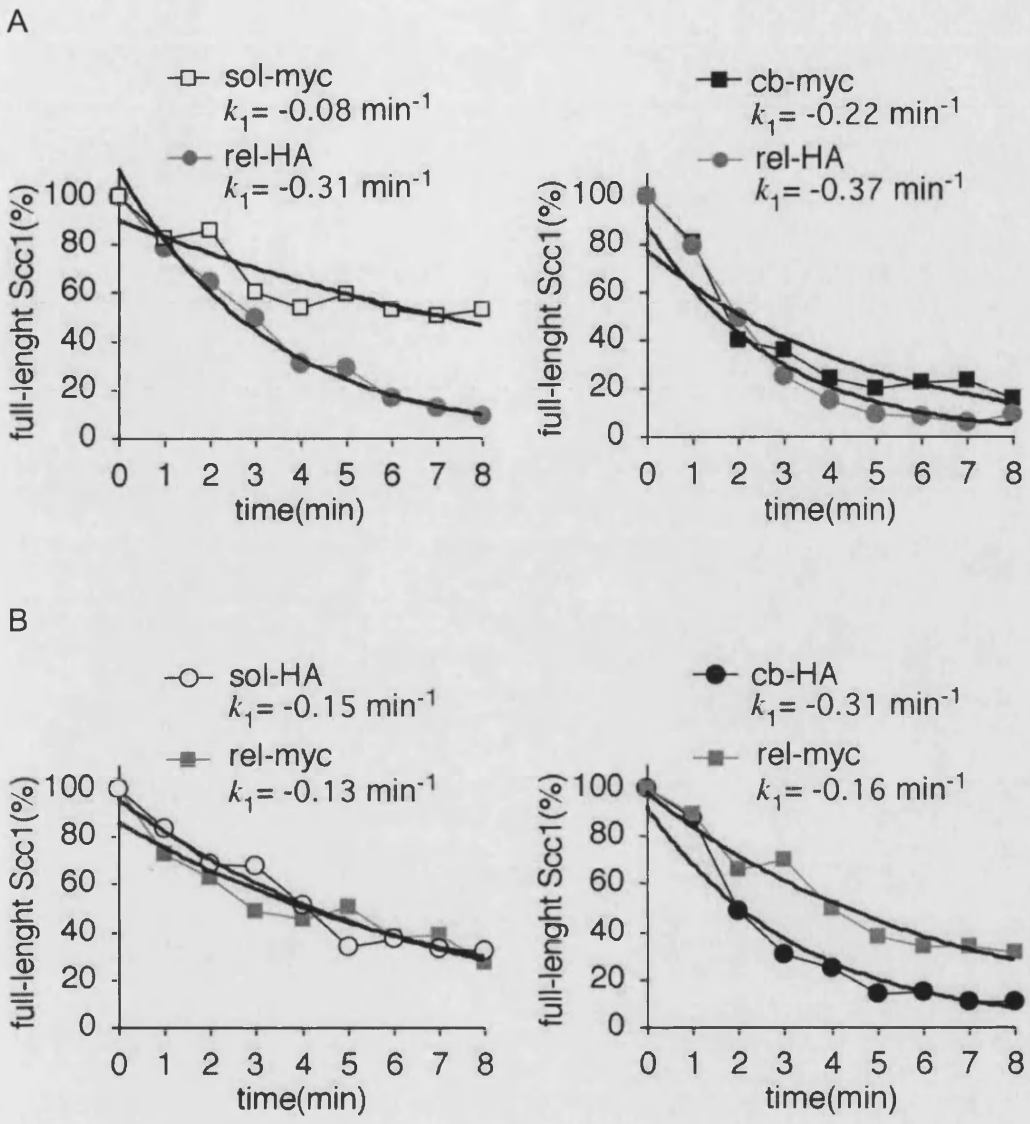

Figure 3.6: Scc1 in cohesin that was released from chromatin by DNase I treatment is cleaved at a similar rate to chromosomal Scc1
(A) Cleavage of chromatin-released Scc1-HA (rel) was compared in the same reaction with soluble (sol) or chromatin-bound (cb) Scc1-myc. (B) Cleavage of chromatin-released Scc1-myc was compared with soluble and chromatin-bound Scc1-HA.

The experiments so far compared cleavage of differentially epitope tagged Scc1 within the same reaction mix. While providing a direct internal comparison, this method suffered from the differential effect of the two epitope tags. Throughout our experiments, I found that cleavage rates between different reactions were highly reproducible, in particular when the source of separase were aliquots of the same separase-enriched cell extract (compare e.g. Fig.3.3 and 3.6). I therefore compared the cleavage rates of chromatin-bound,

chromatin-released, and soluble cohesin containing the same Scc1 epitope tag in parallel reactions. Figure 3.7 shows that both Scc1-HA and Scc1-myc in chromatin-released cohesin are cleaved 2.5 times faster than Scc1 with the same epitope tag in cohesin from the soluble cellular fraction. The cleavage of chromatin-released cohesin was comparable to chromatin-bound cohesin, but somewhat less efficient in the case of Scc1-myc. This suggests that the chromatin context may play some role in facilitating separase cleavage, but mainly that chromatin-bound cohesin has acquired an intrinsic property, maybe a post-translational modification, that allows its efficient cleavage even after chromatin-release.

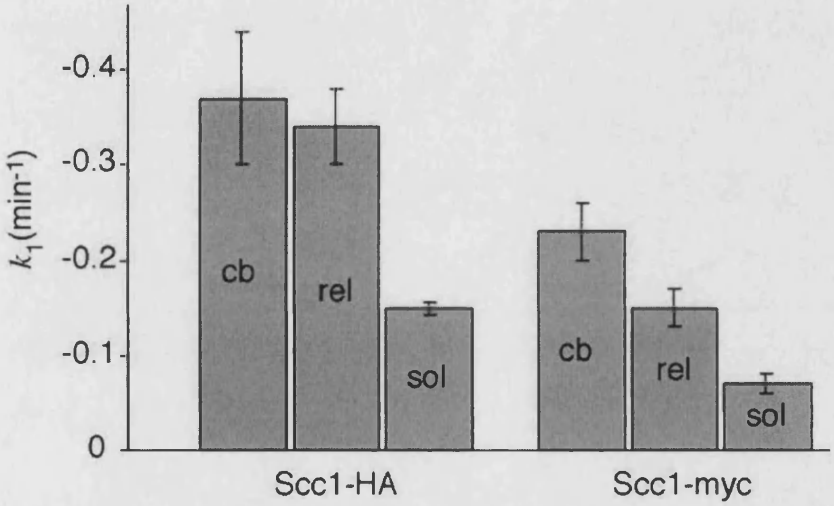

Figure 3.7: Summary of rate constants obtained in parallel reactions for cleavage of Scc1 in chromosomal, chromatin-released, and soluble cohesin
Average rate constants are given together with error bars indicating the standard deviation (n=3 for chromatin-bound and soluble Scc1-HA and Scc1-myc, n=2 for chromatin-released Scc1)

3.2 The preferential cleavage of chromatin-bound Scc1 depends on its phosphorylation status

3.2.1 Chromatin-bound Scc1 is hyperphosphorylated compared to soluble Scc1

Phosphorylation of Scc1, dependent on Polo-like kinase, has been shown to contribute to its efficient cleavage [35, 102]. I therefore analysed

whether chromatin-bound Scc1 may be preferentially phosphorylated. Most Scc1 from chromatin-bound cohesin in metaphase shows slow migration during electrophoresis, indicative of phosphorylation ([102] and Fig.3.10). In contrast, a significant fraction of Scc1 in soluble cohesin migrated faster, suggesting it was less phosphorylated (Fig.3.10, compare lane 1 and 4). It therefore appears that Scc1 in chromatin-bound cohesin is preferentially phosphorylated.

Mass spectroscopy has identified ten serine residues in Scc1 that can be directly phosphorylated by Polo ([102] and Fig.3.8). In order to address the role of Scc1 phosphorylation in preferential cleavage of chromatin-bound cohesin, I mutated these ten serines to alanine, individually and in combination. All mutant proteins were expressed under control of the endogenous *SCC1* promoter and were able to complement for the deletion of the essential wild-type *SCC1* gene. Individual mutations showed only a minor effect, but mutation of all 10 serines (10xS→A) lead to a significant shift in electrophoretic mobility of Scc1 (Fig.3.9, Fig.3.10). A mutant changing two serines near the two separase cleavage sites was described before (S175,263A) [102], and showed an intermediate mobility pattern (Fig.3.10). Slower migrating bands, even though largely reduced, were still evident in the 10xS→A mutant Scc1. These were due to residual phosphorylation as they could be removed by phosphatase treatment (Fig.3.10). In all mutants, as with the wild-type protein, chromatin-bound Scc1 showed a pattern of slower mobility as compared to soluble Scc1. This indicates that Scc1 is preferentially phosphorylated when bound to chromatin, and that phosphorylation can occur at over ten different sites within the protein.

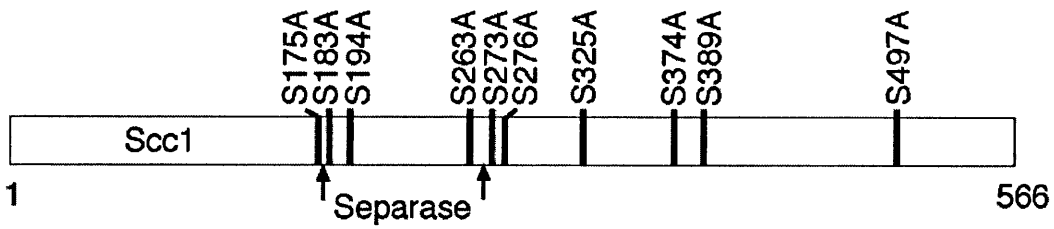

Figure 3.8: Schematic representation of the 10 known Polo phosphorylation sites in Scc1
The two separase cleavage sites are indicated by arrows.

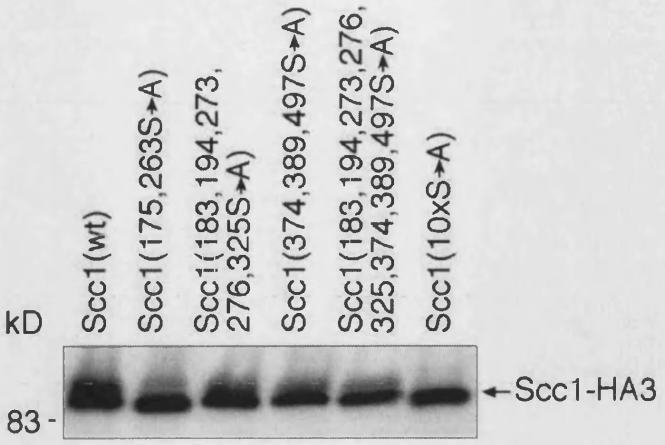

Figure 3.9: Effect of mutations replacing polo phosphorylated serines to alanines
Migration of Scc1 containing different serine to alanine mutations. Whole cell extracts from strains Y1287 (*MAT*a, *GAL-SCC1-myc18, SCC1promoter-SCC1-HA3*), Y1296 (*MAT*a, *GAL-SCC1-myc18, SCC1promoter-SCC1 (S175,263A)-HA3*), Y1633 (*MAT*a, *GAL-SCC1-myc18, SCC1promoter-SCC1 (S183,194,273,276,325A)-HA3*), Y1634 (*MAT*a, *GAL-SCC1-myc18, SCC1promoter-SCC1 (S374,389,497A)-HA3*), Y1635 (*MAT*a, *GAL-SCC1-myc18, SCC1promoter-SCC1 (S183,194,273,276,325,374,389, 497A)-HA3*) and Y1288 (*MAT*a, *GAL-SCC1-myc18, SCC1promoter-SCC1 (S175, 183, 194, 263, 273 ,276, 325, 374, 389, 497A) -HA3*) were analysed by Western blotting.

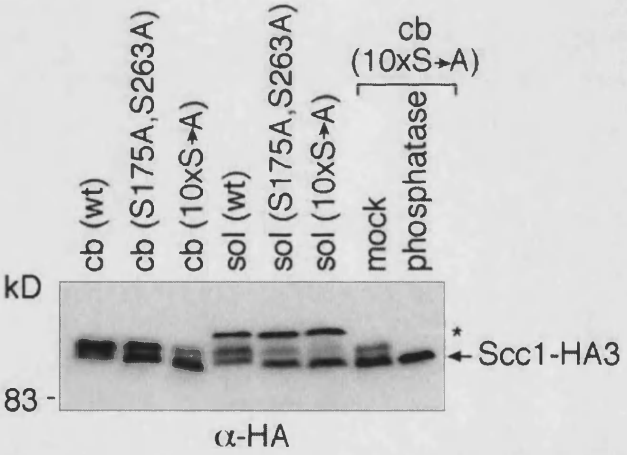

Figure 3.10: Scc1 in chromatin-bound cohesin is hyperphosphorylated compared to Scc1 in soluble cohesin
Migration of chromatin-bound (cb) and soluble (sol) Scc1, and the effect of mutations replacing serines S175 and S263 (S175,263A), or all 10 potential phospho-serine residues to alanine (10xS→A). Chromatin-bound and soluble fractions of nocodazole arrested strains Y1287 (*MAT*a, *GAL-SCC1-myc18, SCC1promoter-SCC1-HA3*), Y1296 (*MAT*a, *GAL-SCC1-myc18, SCC1promoter-SCC1(S175,263A)-HA3*), and Y1288 (*MAT*a, *GAL-SCC1-myc18 SCC1promoter-SCC1(S175,183,194,263,273,276,325,374, 389,497A)-HA3*) were analysed by Western blotting. Remaining slow migration of the chromatin-bound 10xS→A mutant was resolved after treatment with λ-phosphatase. An HA cross-reacting band in the soluble fractions is denoted by a star.

3.2.2 The cleavage rate of chromatin-bound Scc1 is regulated by phosphorylation

To find out whether differential phosphorylation accounts for preferred cleavage of chromatin-bound cohesin, I compared the rates of cleavage of the phosphorylation site mutants. In two sets of experiments cleavage of wild-type, mutant, and phosphatase-treated wild-type cohesin was compared, either chromatin-bound or soluble. Scc1 was tagged with HA epitopes in all cases, and the rates of cleavage were determined in parallel reactions. Myc epitope-tagged wild-type Scc1 was included as an internal control in each reaction and was found cleaved at the same rate in each reaction (data not shown). Figure 3.11 therefore directly compares cleavage of the HA-epitope tagged cohesin variants.

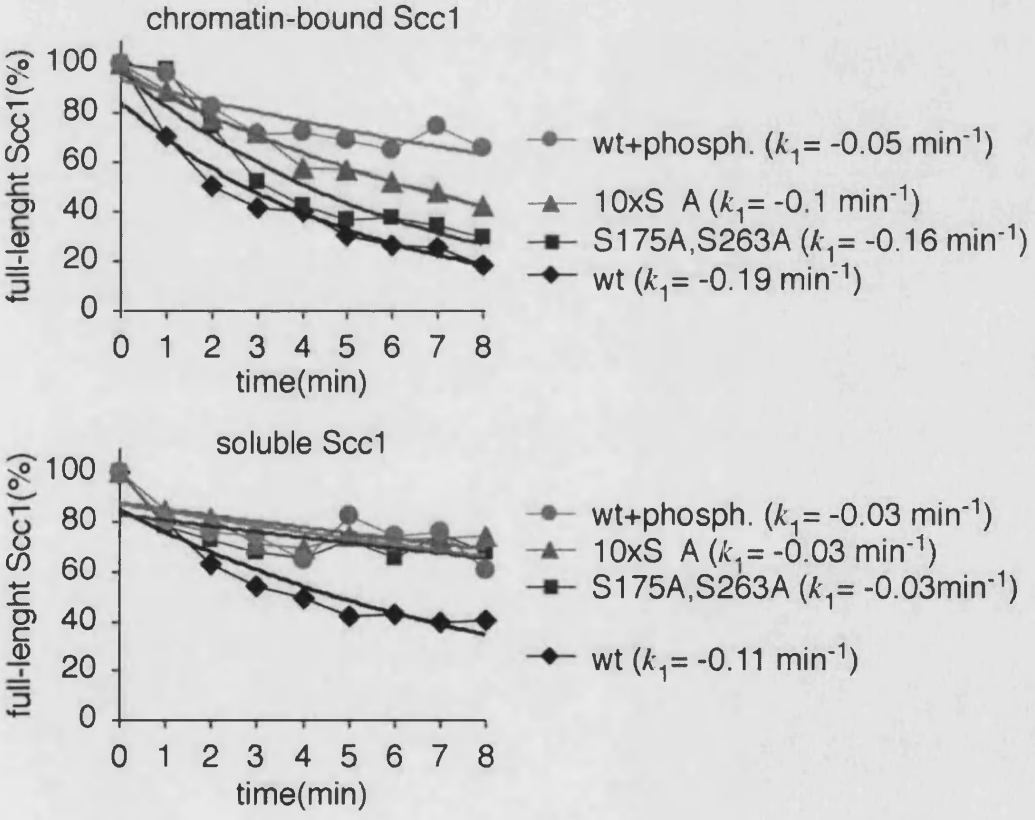

Figure 3.11: Response of the Scc1 cleavage rate to phospho-site mutations and to dephosphorylation by λ-phosphatase
Scc1-HA cleavage was analysed in parallel reactions using chromatin-bound or soluble cohesin preparations.

The efficient cleavage of chromosomal Scc1-HA was reduced by 15% due to the S175,263A mutation, and was down by nearly half as a consequence of the 10xS→A mutation. The reduction in cleavage was most likely due to the absence of phosphorylation, rather than another adverse effect of the mutations, because phosphatase treatment of wild-type chromosomal cohesin also caused a drastic reduction of cleavage. After phosphatase treatment, cleavage was a further two-fold slower than cleavage of the 10xS→A mutant. This is consistent with the possibility that remaining phosphorylation even on the 10xS→A mutant facilitates cleavage to some degree.

Scc1 in soluble wild-type cohesin was cleaved at a rate comparable to the chromatin bound 10xS→A mutant, and any phosphorylation site mutations reduced cleavage to rates similar of phosphatase treated cohesin (Fig.3.11). Together, these results suggest that the phosphorylation status of Scc1 is an important determinant of its rate of cleavage, and that the higher phosphorylation levels of Scc1 in chromatin-bound cohesin might be responsible for its faster cleavage.

3.2.3 Hyperphosphorylation of soluble Scc1 increases its cleavage

If the difference in the rate of cleavage was indeed due to preferential phosphorylation of chromatin-bound Scc1 over soluble Scc1, then enhancing Polo phosphorylation of soluble Scc1 should make it a likewise susceptible cleavage target. To test this I used cells in which, in addition to endogenous Polo, levels of the kinase could be increased under control of the galactose-inducible *GAL* promoter. One hour after Polo induction in metaphase arrested cells, the migration of soluble Scc1 had changed to a pattern similar to chromatin-bound Scc1, indicating increased phosphorylation (Fig.3.12-A). I then compared the cleavage rates of soluble and chromatin bound Scc1 before and after Polo induction. Scc1 was again tagged with HA epitopes, and cleavage rates were obtained in parallel reactions. Similar cleavage rates of Scc1-myc, contained in the reactions as internal standard, confirmed that separase activity was the same in all reactions. Cleavage of soluble cohesin was 2.5 times

accelerated after Polo induction, reaching 80% of the rate of chromatin-bound cohesin (Fig.3.12-B).

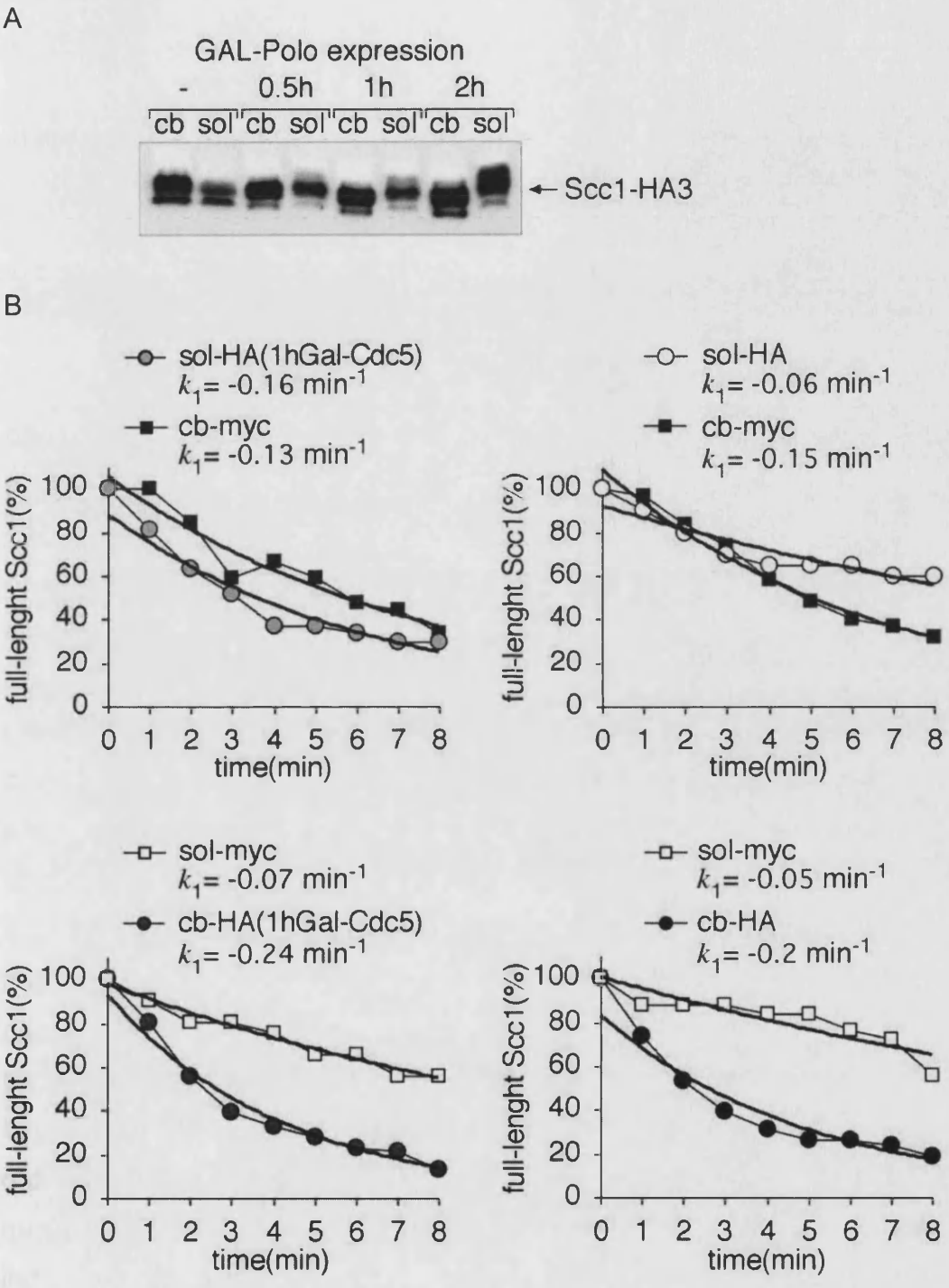

Figure 3.12: Phosphorylation of soluble Scc1 by overexpressed Polo makes its cleavage comparable to chromatin-bound Scc1
(A) Hyperphosphorylation of soluble Scc1 in strain Y1585 (*MAT*a, *SCC1-HA3, GAL-CDC5*) after induction of Polo (encoded by *CDC5*) in metaphase arrested cells. (B) Soluble and chromatin-bound cohesin was prepared 1 hour after Polo induction, and its cleavage was compared to soluble and chromatin-bound cohesin from uninduced cells.

The cleavage rate of chromatin-bound cohesin increased only marginally, in keeping with its pattern of phosphorylation that did not noticeably change after Polo induction. This suggests that the relative under-phosphorylation of soluble cohesin is limiting its rate of cleavage. It also suggests that Polo phosphorylation of chromosomal cohesin is close to its maximum possible level in metaphase cells, thus facilitating its fast cleavage

3.2.4 Scc1 phosphorylation enhances both recognition and cleavage by separase

I next addressed the mechanism responsible for preferential separase cleavage of phosphorylated Scc1. Separase might show enhanced affinity for phosphorylated Scc1, or phosphorylation might in another way facilitate the cleavage reaction. To investigate these possibilities, I first measured cleavage of recombinant phosphorylated Scc1 by purified separase. Recombinant Scc1 can be isolated in a mitotically phosphorylated form after overexpression in insect cells that have been treated with the phosphatase inhibitor okadaic acid [35]. I compared cleavage of mitotically phosphorylated recombinant Scc1 to cleavage of the same protein after dephosphorylation with lambda phosphatase. Separase was purified from yeast via chitin affinity chromatography [41]. Saturating amounts of Scc1 were added to the reaction, and quantitative Western blotting revealed that after 10 minutes at 25°C, separase had cleaved 8 times more mitotically phosphorylated Scc1 as compared to phosphatase treated Scc1. The difference was due to the phosphorylation status of Scc1, rather than an effect of the phosphatase on separase activity, because preincubation of separase with lambda phosphatase did not change its activity (Fig.3.13-A). This result is consistent with previous qualitative experiments that demonstrated a requirement of okadaic acid-induced or Polo-mediated phosphorylation for cleavage of recombinant Scc1 [35, 102].

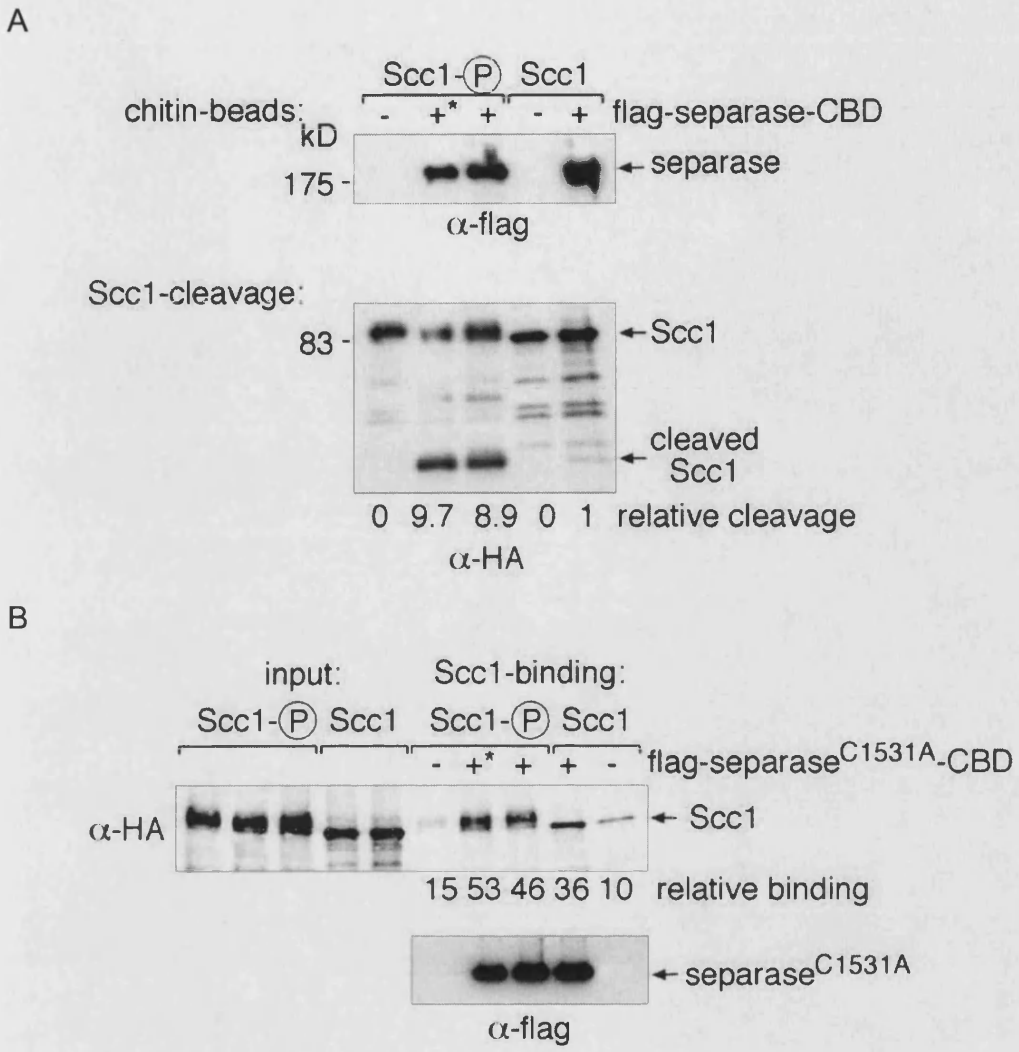

Figure 3.13: Fast cleavage of recombinant, phosphorylated Scc1 is not due to higher affinity for separase
(A) Phosphorylated recombinant Scc1 (Scc1-P) is cleaved faster than phosphatase-treated Scc1 (Scc1). Recombinant Scc1 was incubated with separase, purified by chitin affinity chromatography from strain Y334. Cleavage was analysed by quantitative Western blotting and relative amounts of the cleavage product in each reaction is given. In one reaction, separase was phosphatase treated, denoted by *, before incubation with Scc1. (B) Separase binding to Scc1. Phosphorylated and phosphatase-treated recombinant Scc1 was bound to catalytically inactive separase (C1531A) that was affinity purified on chitin beads. Bound protein was analysed by quantitative Western blotting, binding is indicated relative to the respective input. A reaction in which separase was phosphatase treated is also included, denoted by *.

To analyse whether separase has a higher binding affinity for phosphorylated versus unphosphorylated Scc1, I repeated the experiment, but this time purified a proteolytically inactive separase protein containing a point mutation in the active site cysteine residue (C1531A). This prevented Scc1 cleavage in the reaction and thus enabled the examination of substrate binding.

C1531A mutated separase was bound to chitin beads, similar amounts of mitotically phosphorylated or phosphatase treated recombinant Scc1 were added, and bound Scc1 quantified. Both phosphorylated and phosphatase treated Scc1 associated with separase, but 1.8 times more phosphorylated Scc1 was recovered (Fig.3.13-B).

This indicates that separase possesses higher affinity for phosphorylated Scc1. However, discrimination against binding to unphosphorylated Scc1 did not appear large enough to explain the 8-fold difference in the efficiency of cleavage. Scc1 phosphorylation, in addition to increasing affinity to separase, might therefore facilitate cleavage more directly, maybe by providing substrate induced catalysis.

3.3 Phosphorylation-dependent preferential cleavage of chromatin-bound Scc1 in vivo is important for chromosomal stability

3.3.1 In vivo chromatin-bound Scc1 is preferentially cleaved depending on its phosphorylation

The above data show that chromatin-bound cohesin is preferentially cleaved over soluble cohesin by separase in vitro, and that Scc1 phosphorylation is likely to play a role in determining this difference. I next addressed whether preferred cleavage of chromatin-bound cohesin would take place during budding yeast anaphase in vivo. I arrested cells in metaphase by depletion of the APC activator Cdc20 under control of the galactose inducible *GAL* promoter, and released cells into synchronous anaphase by reinduction of Cdc20 [38]. Anaphase at the normal growth temperature of 25°C occurs very rapidly, therefore release was performed at 16°C to slow mitotic progression and facilitate analysis. Samples were taken every 5 minutes, soluble and chromatin-bound fractions separated, and levels of remaining full-length Scc1 over time were analysed by quantitative Western blotting. Full-length Scc1 started to disappear from the chromatin fraction 15 min after release into anaphase, but a reduction in the soluble fraction only became obvious after 25 min (Fig.3.14). Therefore chromatin-bound cohesin appears to be preferentially

cleaved during budding yeast anaphase. This may aid the rapid resolution of sister chromatid cohesion at anaphase onset.

To investigate whether preferred cleavage of chromosomal cohesin in vivo depended on its phosphorylation, I repeated the experiment with a strain containing the Scc1 10xS→A mutant as the sole source of Scc1. Cleavage of chromatin-bound cohesin was now delayed until 25 minutes after release into anaphase, and both chromatin-bound and soluble full-length Scc1 disappeared with similar kinetics. This suggests that the preferential cleavage of chromatin-bound cohesin in vivo depends on its phosphorylation.

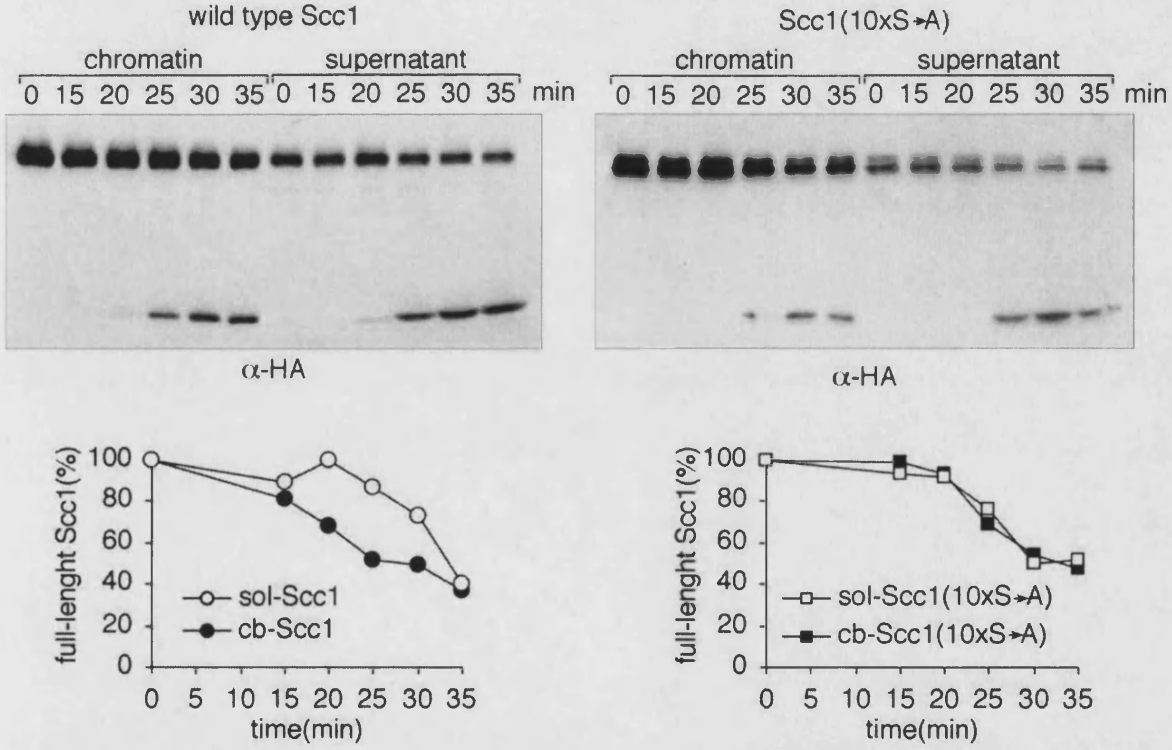

Figure 3.14: Phosphorylation accelerates cleavage of chromosomal Scc1 *in vivo*
Faster cleavage of chromatin-bound Scc1 *in vivo* depends on phospho-serine residues. Strains Y1447 (*MAT*a, *GAL-CDC20, PDS1-myc18, SCC1promoter-SCC1-HA3*) and Y1449 (*MAT*a, *GAL-CDC20, PDS1-myc18, SCC1promoter-SCC1(S175,183,194,263, 273,276,325,374,389,497A)-HA3*) were arrested in metaphase by depleting Cdc20 and released into synchronous anaphase at 16˚C. Soluble and chromatin-bound Scc1 was separated in samples taken at the indicated time points, and full-length Scc1 quantified. Note that cleaved cohesin is released from chromatin, thus the Scc1 cleavage product in the soluble fraction originates partly from chromatin.

I also analysed whether the subcellular distribution of separase could help the preferential cleavage of chromatin-bound versus soluble cohesin. Approximately two thirds of separase was found in the soluble cellular fraction and one third was chromatin-associated (Fig.3.15). Therefore, a pool of separase exists on chromatin, but in contrast to cohesin most separase is found in the soluble cellular fraction.

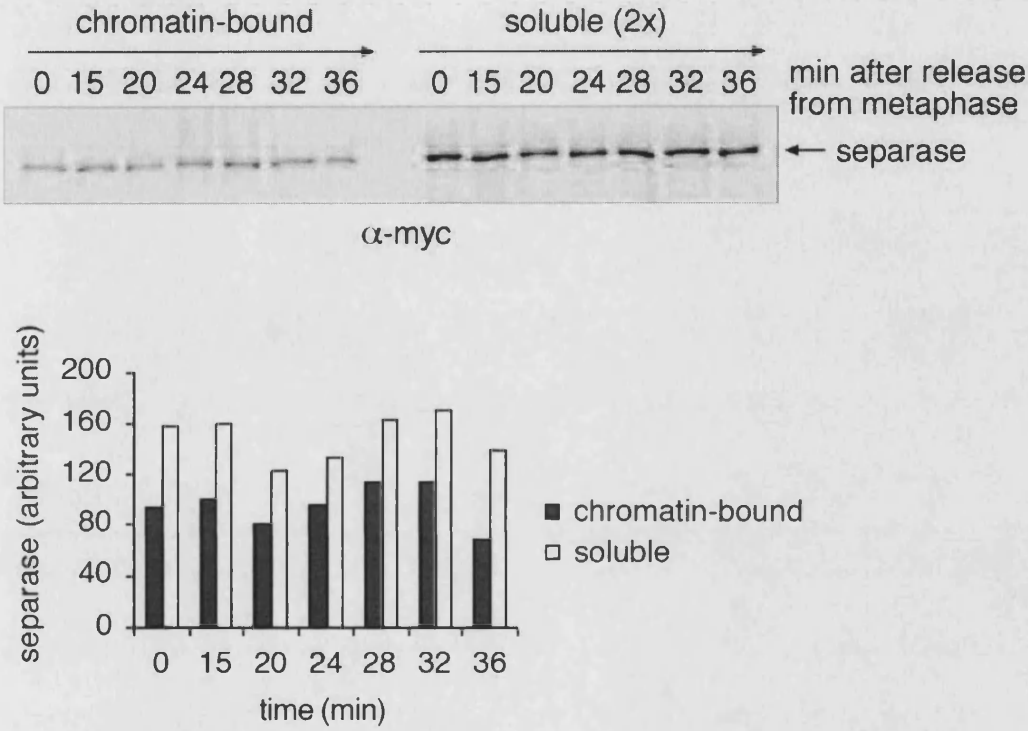

Figure 3.15: Separase distribution between soluble and chromatin-bound fractions
Strain Y1215 (*MATa, GAL-CDC20, ESP1-myc18, SCC1-HA6*) was arrested in metaphase by depletion of Cdc20 (time point 0), and released into synchronous anaphase at 16°C (compare Fig.3.14). Chromatin and soluble fractions were prepared at the indicated times, and levels of separase were compared by quantitative Western blotting against the myc epitope tag fused to separase. Note that twice the comparable amount of the soluble fraction has been loaded on the blot shown above, but that the levels have been normalised to the same cell equivalent in the quantification below.

3.3.2 Delayed cleavage of chromatin-bound cohesin slows anaphase progression and causes chromosomal instability

Does delayed cleavage of chromatin-bound cohesin due to the Scc1 10xS→A mutation has consequences for the faithful progression of mitosis?

Previously, the Scc1 S175,263A mutation has been shown to cause lethality and delay cohesin cleavage by about 30 minutes in cells lacking securin [102], a situation in which separase is mislocalised and shows reduced activity [41]. The Scc1 10xS→A mutation introduced a 10 minutes delay to cleavage of chromatin-bound cohesin in wild-type cells progressing through anaphase at 16°C. When analysing chromosome segregation in these cells, compared to cells containing wild-type Scc1, I found a corresponding delay in the dissociation of cohesin from chromosomes, and of anaphase spindle elongation (Fig.3.16). The time difference was small, but reproducible. I confirmed that separase activation occurred at the exact same time in both strains as judged from the disappearance of nuclear securin.

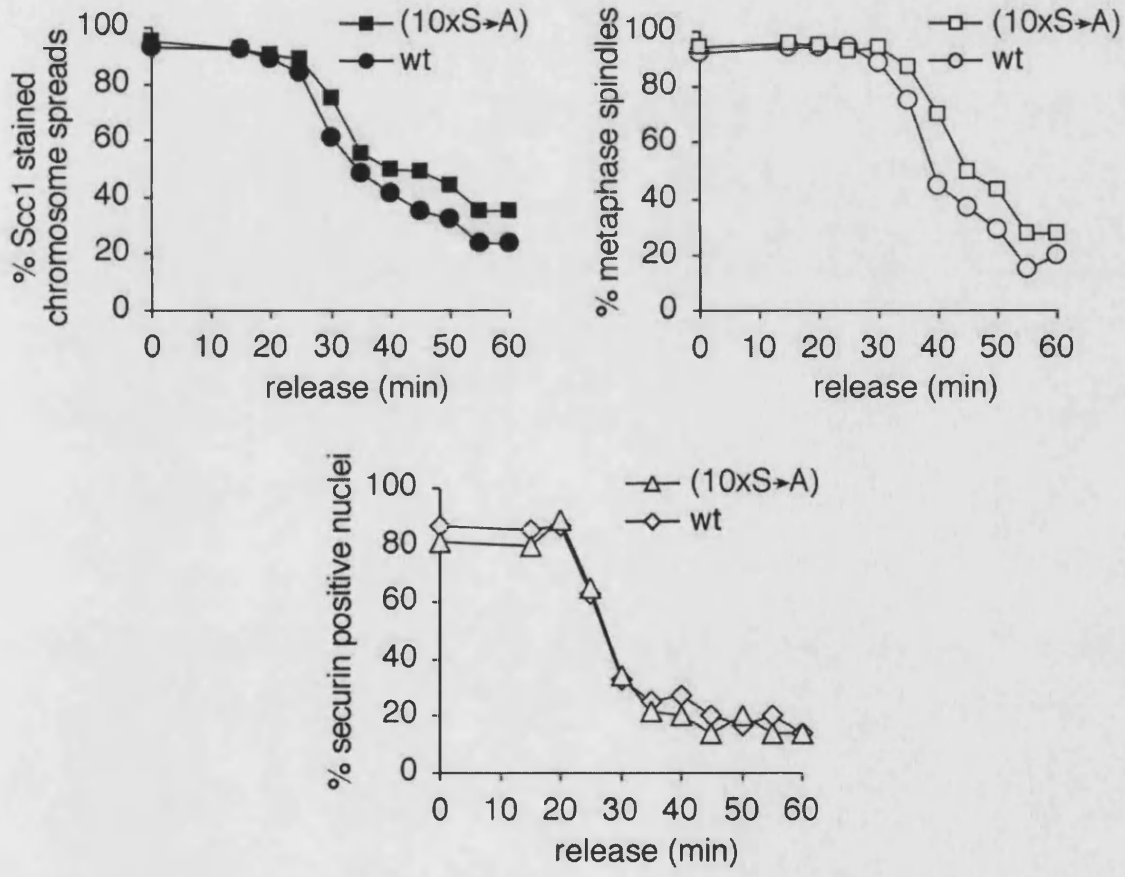

Figure 3.16: 10xS→A mutant Scc1 dissociates from chromatin later and delays elongation of the anaphase spindle
As in Figure 3.14, but degradation of securin and spindle elongation were analysed by indirect immunofluorescence, and Scc1 binding to chromatin was visualised on chromosome spreads.

Cells containing Scc1 10xS→A as the sole source of Scc1 were viable and, apart from a delay, anaphase progression appeared normal. To more rigorously test the effect of this mutation on chromosome segregation, I analysed the rate of chromosome loss using a sensitive colony sectoring assay [128]. This assay indicated that a marker chromosome was lost with twice the frequency of that observed in wild-type strains, suggesting that efficient cleavage of chromatin-bound cohesin at anaphase onset is important for faithful chromosome segregation (Fig.3.17).

chromosome loss

	half red	%	n
wt	9	0.07	12750
10xS→A	21	0.16	12750

Figure 3.17: 10xS→A mutant Scc1 confers increased chromosome loss
Strains Y1305 (*MAT*a, *CFIII (CEN3.L.YPH278), URASUP11, SCC1promoter-SCC1-HA3*) and Y1306 (*MAT*a, *CFIII (CEN3.L.YPH278), URASUP11, SCC1promoter-SCC1-S175,183,194,263,273,276,325,374,389,497A)-HA3*) were grown in medium lacking uracil to maintain a marker chromosome, and plated on rich medium. Half red sectored colonies were counted, indicative of chromosome loss in the first division after plating. Chromosome loss in the strain containing 10xS→A Scc1 is greater than in wild-type with a confidence level greater than 93.75%.

3.4 Polo kinase co-localises with Scc1 on chromatin

The finding that Scc1 is higher phosphorylated when bound to chromosomes offers a plausible explanation for why chromatin-bound cohesin is preferentially cleaved by separase. But how is chromatin-bound Scc1 preferentially phosphorylated in a Polo-dependent manner? To address this, I analysed whether Polo may co-localise with cohesin on chromosomes. In a subcellular fractionation experiment, a significant part of Polo, close to half of the total cellular pool, was found associated with a Triton-insoluble chromatin fraction (Fig.3.18-A).

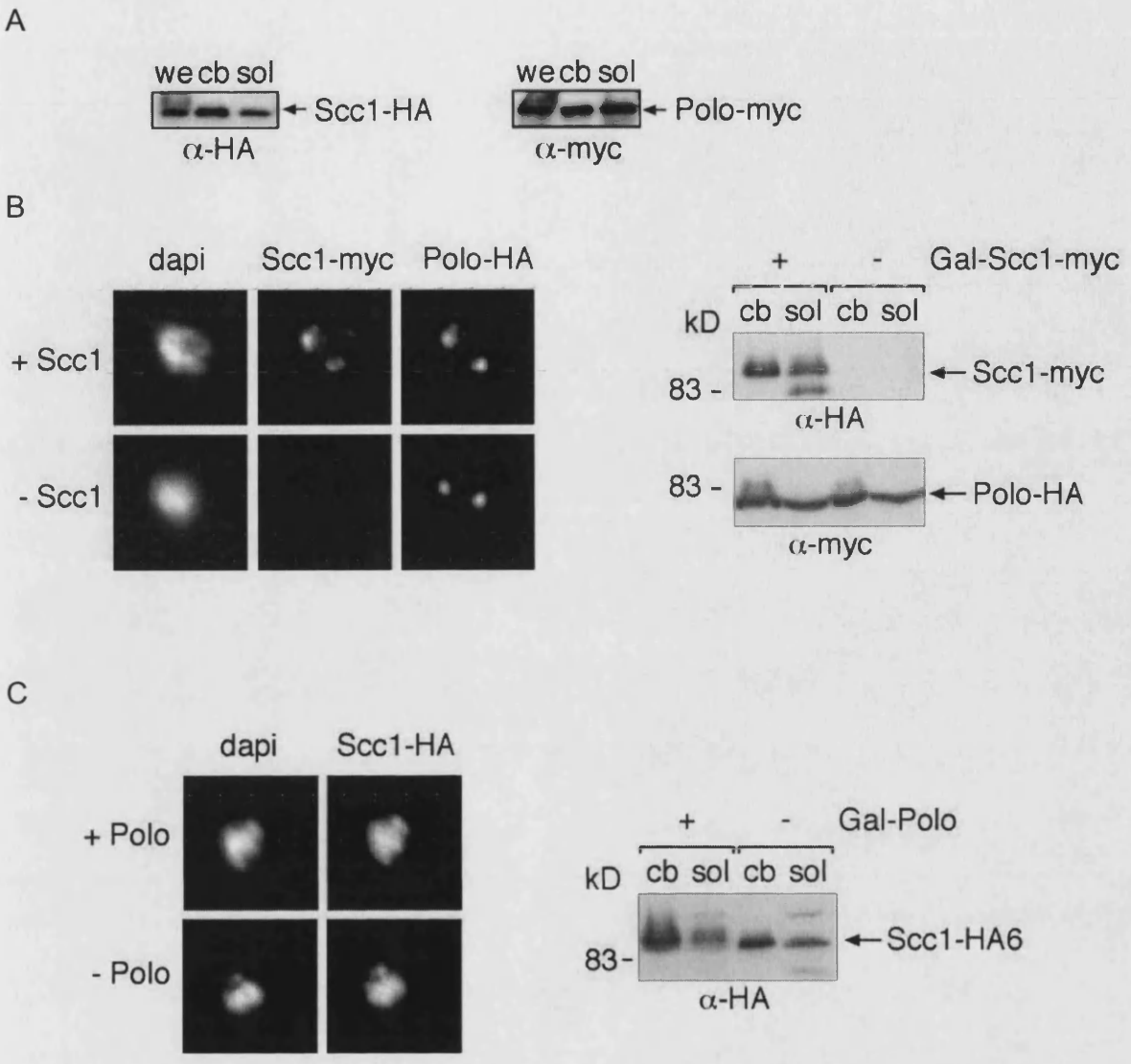

Figure 3.18: Chromatin provides a Polo-rich environment
(A) Polo in the chromatin-bound fraction. Whole extract (we), chromosomal (cb), and soluble (sol) cellular fractions were prepared from strain Y1570 (*MAT*a, *SCC1-HA6, CDC5-myc18*), Scc1 and Polo were detected by Western blotting. (B) Polo associates with chromatin independently of cohesin. Scc1 was depleted from strain Y1571 (*MAT*a, *GAL-SCC1-myc18, CDC5-HA6*) and cells arrested in metaphase by nocodazole treatment. Chromatin binding of Scc1 and Polo were analysed by chromosome spreading, and levels of both proteins in soluble and chromatin-bound fractions confirmed by Western blotting. (C) Cohesin binds chromatin independently of Polo. Cells were arrested by nocodazole treatment after depletion of Polo in strain Y8646 (*MAT*a, *GAL-CDC5, SCC1-HA6*). Polo depletion was confirmed by the fast mobility of hypophosphorylated Scc1. Cohesin binding to chromosomes was analysed by chromosome spreading and cellular fractionation.

The chromosome association of Polo could be confirmed by immunostaining on mitotic chromosome spreads. Interestingly, the staining of

Polo on mitotic chromosomes overlapped the staining of cohesin (Fig.3.18-B). Both proteins were enriched in two foci that most likely correspond to the two clusters of centromeres in mitosis where cohesin is known to accumulate [108]. Polo may associate with chromosomes as a consequence of binding and phosphorylating cohesin. If this was the case, chromosomal cohesin would not be in any advantage over soluble cellular cohesin with which the soluble pool of Polo could likewise associate. I therefore tested whether binding of Polo to chromosomes depended on cohesin. Scc1 was depleted from cells under control of the repressible *GAL* promoter, conditions under which none of cohesin's subunits binds to chromatin [52, 126], but the amount and pattern of Polo association with mitotic chromosomes was unaltered (Fig.3.18-B). This suggests that Polo binds chromosomes independently of cohesin. I also tested whether cohesin binding to chromatin depended on Polo. After Polo-depletion under control of the repressed *GAL* promoter, the phosphorylation-dependent mobility shift in Scc1 was abolished, but the levels of chromatin-bound Scc1 remained unchanged (Fig.3.18-C). Therefore Polo and cohesin bind to chromosomes in a similar pattern, but independently from each other. The pool of chromosomal Polo may thus provide an environment for preferential phosphorylation of cohesin that binds within its vicinity.

Chapter 4

Discussion

4.1 Separase regulation by securin in the yeast Saccharomyces cerevisiae

4.1.1 Securin is a positive regulator of separase

The first interaction studies between separase and securin have been performed in the yeast *Schizosaccharomyces pombe* [30]. In this organism, complex formation between Cut1/separase and Cut2/securin is needed for the loading of Cut1/separase to the spindle in prophase. After securin degradation in metaphase, central and C-terminal regions of Cut1 are needed for its association with the anaphase spindle and the spindle pole bodies [40]. While I performed these studies, a securin dependent nuclear localisation and spindle association of separase has been shown in budding yeast using over-expressed GFP-tagged Esp1 [34]. The here presented study addressed the nuclear localisation of Esp1 under more natural conditions by virtue of myc epitopes that were added to the genomic copy of the *ESP1* gene. This confirmed a dependency of separase nuclear localisation on securin. It also shows a separase concentration on the anaphase spindle, mainly the spindle midzone and the spindle pole bodies. Interestingly, securin deletion mutants still show a reduced chromatin and spindle association of separase in metaphase. In anaphase, this association is limited to the spindle pole region. The association of low levels of separase with chromatin and the mitotic spindle in the absence of securin indicates that separase can enter the nucleus independently of securin, consistent with the fact that securin deleted budding yeast cells are viable. Monitoring the nuclear localisation of separase and securin during one cell cycle revealed a 20-minute delay of separases' nuclear accumulation compared to securin. The above observations led to the model that separase can enter the nucleus independently of securin but that securin

helps separase to accumulate in the nucleus by preventing its nuclear export, possibly by blocking nuclear export sequences within separase. As blocking the nuclear export receptor Crm1/Xpo1 does not prevent separase from leaving the nucleus, these export sequences might be recognised by a mechanism different from the Crm1/Xpo1-mediated nuclear export.

4.1.2 Securin is a direct inhibitor of separase

I analysed the functional relationship between securin and separase, by producing a series of deletion mutants of both proteins. The analysis of separase and securin domains and their interactions shows interesting features. It revealed that securin is a direct inhibitor of separase protease activity. Interestingly, a C-terminal fragment of securin spanning aminoacids 256 to 359 out of the total 373 aminoacids is sufficient to bind and inhibit separases' proteolytic activity. This is in line with studies in fission yeast that show that the C-terminus of Cut2/securin is necessary for binding to separase [40] and studies in *Drosophila* that show that the C-terminal residues 115-199 out of 199 aminoacids are sufficient for binding to THR, the N-terminal domain of separase [39]. N-terminal regions of securin contain the destruction boxes needed for the cell cycle regulated degradation of securin [32, 129].

Studies in fission yeast also showed that the first 300 aminoacids out of the 1828 aminoacid long Cut1/separase polypeptide are sufficient for an interaction with securin [40]. Deletion analysis of separase in this study revealed that the first 156 aminoacids of Esp1/separase are necessary for a tight interaction with the C-terminus of securin. However full-length Pds1/securin is able to interact with C-terminal regions of separase although this interaction is much weaker (aa1390-1630). Similarly, in fission yeast more central regions of securin (aa128-161) are needed for an interaction with separase [30].

If securin binds tightly to the N-terminus of separase, how can it efficiently inhibit the proteolytic activity located at the very C-terminus of the protein separated by over 1500 aminoacids? The presented results suggest that securin competes with Scc1 for binding to separase. The definition of a competitive inhibitor is that it interferes with substrate binding. This study clearly

shows that securin not only hinders binding of the substrate Scc1, but that it is also able to displace separase-bound Scc1, indicative for a competitive inhibition. However a competitive inhibitor usually competes for the active site. This was puzzling as the active site is located at separases' C-terminus and although Scc1 has a strong binding affinity for this C-terminal region, securin's strongest affinity is the very N-terminus of separase. In addition, Scc1 binding happens outside the catalytic side and more N-terminal regions of separase seem to influence the binding of the substrate, weakening the interaction and thereby possibly increasing the turnover of the substrate.

Allosteric inhibitors inhibit enzymes by acting on a site different (allosteric) from the substrate binding site. Interestingly, securin, by binding to the N-terminus of separase, can prevent binding of the small peptide inhibitor that recognises the active site, indicating an allosteric effect of securin on separases' catalytic site. However, it cannot be excluded that securin hinders the binding of the small peptide inhibitor by preventing access to the active site. Indeed, and as discussed above, securin is also able to interact with the C-terminus of separase, although much less efficiently.

A possible answer to this puzzle came through the observation that the N-terminus of separase itself is necessary for its proteolytic activity. An N-terminal deletion of the first 156 aminoacids of separase is unable to bind the small peptide inhibitor, suggesting that these aminoacids are needed to establish the correct configuration of the active site of separase. Securin could therefore act in the following way: it competes with Scc1 for binding to separase and in the same time interferes with an activating interaction between separases' N-and C-termini (Fig.4.1). Indeed N- and C-terminal fragments of separase do interact when co-expressed.

Co-expression of securin with short N-and C-terminal fragments of separase lead to the formation of a trimeric complex with securin in the centre further sustaining the idea that securin interferes with an activating interaction between the N- an the C-terminus of separase. This model also offers a possible explanation for securin's proposed chaperone function. By bridging separases' N-and C-termini, which are separated from each other by over 1500 aminoacids, securin might bring them in juxtaposition, preparing them for interaction upon securin destruction (Fig.4.1).

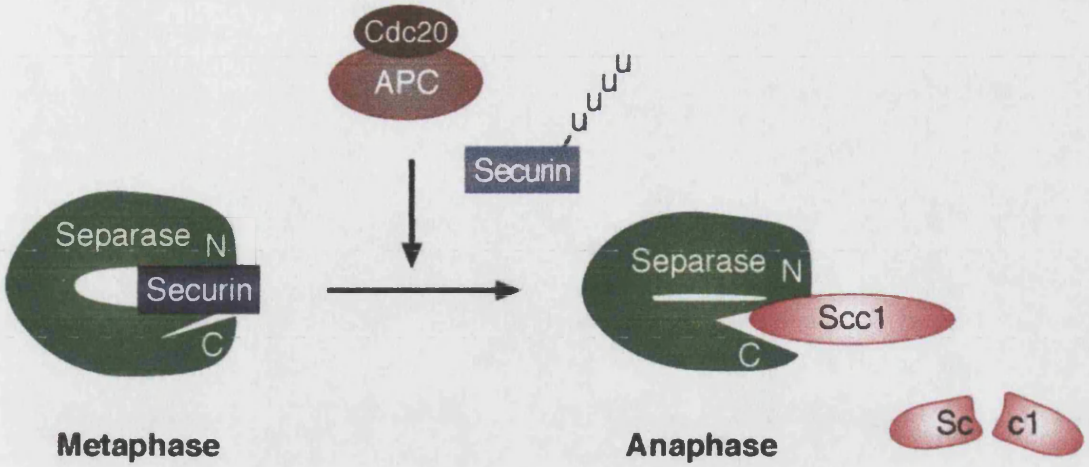

Figure 4.1: Model of separase and its inhibition by securin
Securin binds to both separase N- and C-terminus. Thereby securin may separate these two parts of the protein, acting as a molecular wedge. After securin degradation via ubiquitylation by the anaphase promoting complex (APC) the separase N-terminus is free to interact with the protein's C-terminus. Securin might promote the interaction by pre-positioning the separase termini. The interaction within separase might induce an activating conformational change at the protease active site at the separase C-terminus. Securin, while bound to separase, also prevents access of Scc1 to separase.

The above observations also go some way in explaining why separases are such large proteins. Sequences very close to the N-terminus of the protein are required for protease activity at the protein's C-terminus. What about the sequences in between? The co-expressed fragments from the N- and C-termini of separase efficiently formed complexes, but were unable to reconstitute protease activity. This indicates that the intactness of the middle portion of separase is also important for the function of the protease. Consistent with this, when 10 temperature sensitive alleles of the fission yeast separase Cut1 were sequenced, 8 were found to encode single amino acid changes in the middle of the protein [30]. Therefore this region might also contribute to the proteolytic activity of separase.

The presented model would predict a possible binding competition of securin and the C-terminus of separase to N-terminal regions of separase. Interestingly, a search for sequence homologies between Pds1/securin and separases from different species revealed the following Prosite profile: N-

X(15,16)-{RK}-{IL}-X(8,10)-R-L-P-L-X(12,14)-F-X(15)-{QE}. This consensus sequence located in the C-terminal half of separase, is also present in budding yeast securin and is conserved in the phylogenetic group of the different fungi *S.cerevisiae*, *S.pombe*, *C.albicans* and *E.nidulans* (Fig.4.2).

```
E.nidulans      NVLSLSLSADRAEFVVSRLHRG-CSPFLLRLPLRRGNSE
S.cerevisiae    NVITIDFCPITGNLLLSKLEPRRKRRTHLRLPLIRSNSR
C.albicans      .LVTLDICQNTGDLLISKLTKGSPNPIFMRLPLLRFPS.
S.pombe         NVVSITINNSGEDLFISKIRKG.HSPLIFRLPLQRHNSR
S.cerevisiae    N..TLKYIQGGKEVSPTKRLHT.HAQQQGRLPLAAKDNN
consensus       :::::.....:::::::.:.....****.:..:.

E.nidulans      DEE.EQFTFEDGRDEMKEL.IRLANE (Separase)
S.cerevisiae    DLDEVHLSFPEATKKLLSI.INESNQ (Separase)
C.albicans      .....SLGFQQLMQNFEKI.IDDSN. (Separase)
S.pombe         DADEEILVFTKAQTELFRI.ISKSNQ (Separase)
S.cerevisiae    RSK..SFIFPETSNQSKDADLPQL.Q (Securin)
consensus       ........*.........:.:...:.
```

Figure 4.2: The C-terminus of separase and the N-terminus of securin share a specific profile
The C-terminal regions of separases from the fungi *S.cerevisiae* (aa1167-1230), *S.pombe* (aa1375-1437), *C.albicans* (aa1095-1138) and *E.nidulans* (aa1601-1662) share the following common sequence profile with budding yeast securin (aa59-117): N-X(15,16)-{RK}-{IL}-X(8,10)-R-L-P-L-X(12,14)-F-X(15)-{QE}.

Given the poor overall sequence homology between separase and securin molecules of different species, this alignment could indeed reinforce the model of a trimeric complex. As the consensus sequence in securin is located in the N-terminal half, the C-terminus of securin could be, like in fission yeast, necessary but not sufficient for the interaction with separase. Also, in Drosophila a mutational analysis of aminoacids located in PIM/securin revealed two mutations at the very N-terminus of the protein that were able to abolish the interaction with THR, the N-terminal domain of separase [46]. Although in their analysis most mutations affecting this interaction were located in the C-terminus of securin, the PIM-THR interaction appears to be less dependent on defined residues. Altogether, it is likely that securin form multiple interactions with separase, the N-terminus being the strongest.

Securin prevents separases' proteolytic activity by preventing an intramolecular activating interaction between separases' N- and C-termini. This is in contrast to other members of the CD clan of proteins, the caspases. The initiator caspases 8 and 9 both need to form dimers in order to be active [130]. Dimer formation is achieved by a process of induced proximity and mediated by adaptor molecules like Apaf-1 in the apoptosome or FADD in the DISC (death inducing signaling complex). In both cases the interaction of the prodomains of the caspases with an oligomerised adaptor molecule increases the local caspase concentration and induces the activation of the protease.

Will this model of separase inhibition and activation also be applicable to other organisms? N-terminal regions within PIM/securin (aa 88-114) are particularly important for binding with SSE, the separase domain containing the catalytic site. Additionally, the THR protein in *Drosophila* is required for separase activity [39]. The pattern of interactions of THR with separase and the *Drosophila* securin PIM is reminiscent of the interactions of the budding yeast separase N-terminus with its catalytic C-terminus and securin [39]. Therefore the presented results on the activation of separase's protease activity and its inhibition by securin might be applicable to *Drosophila* as well, supporting a model in which THR activates separase by an interaction that is prevented by PIM (Fig.4.3) [39].

Xenopus and human securin must be degraded for separase activation [33, 106] and human securin promotes inhibition of human separase in vitro [37]. A distinct feature of human separase is that, after its activation by securin degradation, separase cleaves itself into two halves at a position upstream of separases' active site [37]. Processed separase is still active to cleave cohesin. Consistent with the idea that the N-terminus might be required for proteolytic activity, is the observation that the resulting polypeptides stay associated with eachother after cleavage. Taken together, the here proposed interaction between separase and securin appear to be very similar in higher eukaryotes (Fig.4.3).

Another level of regulation of human separase is its inhibition by CDK (CDC2)-dependent phosphorylation. This inhibition is effective even after securin is degraded. The phosphorylation takes place in the centre of separase, and it would be interesting to see whether it influences an interaction between

N- and C-termini or inhibits separase by an alternative mechanism. In budding yeast there is no evidence for self-cleavage and CDK-dependent inhibition of separase. Sister separation proceeds in the presence of high kinase activity and securin destruction is sufficient to promote anaphase onset [31, 102].

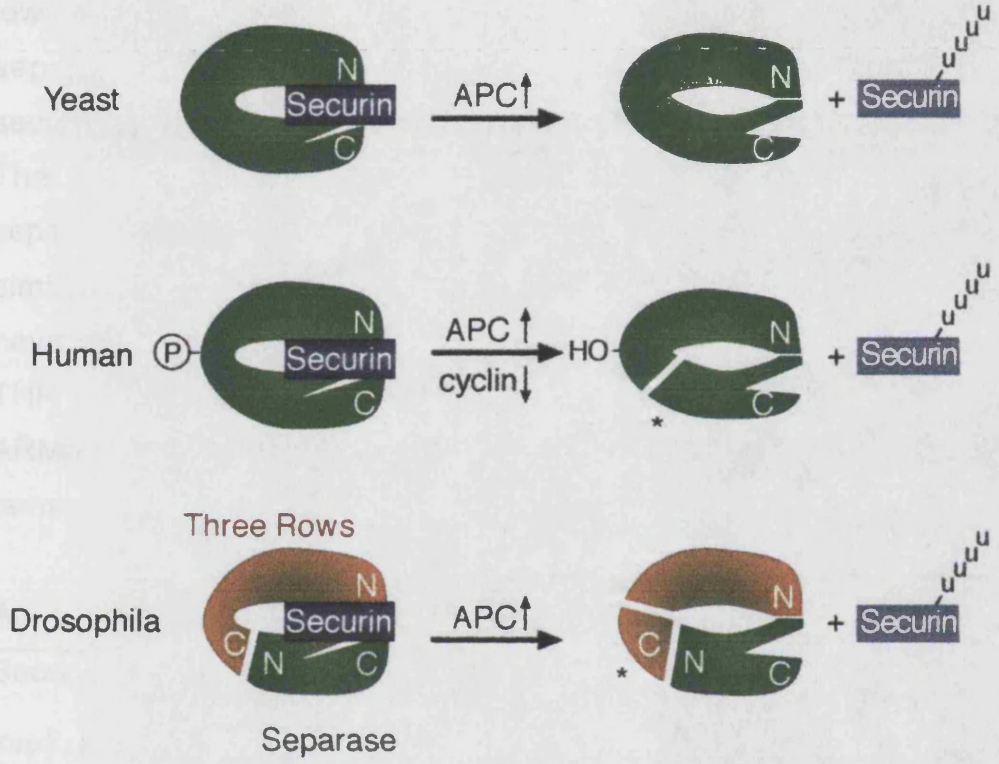

Figure 4.3: Separase regulation at the metaphase to anaphase transition
In budding yeast, securin prevents an interaction of the separase amino terminus with the protease active site at the carboxyl terminus. Securin is degraded at anaphase onset after ubiquitylation by the anaphase promoting complex (APC). This allows an intramolecular interaction within separase that may activate protease activity. Human separase is inactivated by phosphorylation in metaphase. The phosphate has to be removed in anaphase, when cyclin-dependent kinase activity decreases. During anaphase, separase cleaves itself and the carboxy-terminal separase fragment, which contains the protease active site, is rendered unstable (asterisk). In *Drosophila*, separase consists of two polypeptides, called Three Rows and separase. After securin destruction, separase cleaves its own Three Rows component. The carboxy-terminal Three Rows fragment, probably required for separase activity, is thereby destabilised (asterisk) (adapted from F.Uhlmann, Current Biology, Volume 13, 4.2.2003).

Apart from the highly conserved C-termini, separases from different eukaryotes show very little sequence homology (see appendix). Moreover, sequence similarity among securin proteins is restricted to signals that promote the mitotic degradation required for separase activation.

This study and studies in *Drosophila* and humans indicate a very similar tertiary structure of separases and their interactions with securin, despite their low primary sequence similarity. Interestingly, N-terminal regions of human separase are able to interact with the C-terminus of PIM and human securin/PTTG is able to interact with Drosophila THR and separase/SSE [46]. The fact that heterologous interactions between Drosophila and human separase and securin proteins occur, even though significant primary sequence similarities are missing, raised the possibility that these domains might nevertheless adopt a related tertiary structure. Tertiary structure predictions on THR in *Drosophila* indicate an alpha-alpha superhelical structure similar to ARM/HEAT repeat-containing domains. A secondary structure query on the N-termini of Esp1 and Cut1 shows a helical rich structure (Fig.4.4-A).

A

Secondary structure alignment of Esp1 and Cut1:

```
Esp1:MMVKQEEPLNEI-SPNTPMTSKSYLLNDTLSKVHHSGQTRPLTSVLSG-DASSN
Cut1:MSTRSIVTSKVSWTPEKFISALSYPEHCSITLVKRLKASVKLKDLKQNISRDAP
     CCCCCCCCHHHC-CCCCCCCCCHHHHHHHHHHHHHCCCCCCHHHHHCC-CCCCC
     CCCCCCCCHHHCCCCCCCCCCHHHHHHHHHHHHHCCCCCHHHHHCCCCCCCCE

Esp1:SIGILAMHNNIIRDFTKIASNNIDLAIEDITTVDHSLNSIYSLLKSHHMWGHIN
Cut1:SWTFEHLFVAFKCAVSNLAKQWAELSTTDKEKTRRMFCTPSRLNTAHRPEVFYL
     CEEEEECHHHHHHHHHHCCCCCCEEEEEHHHHHHHHHHHHHHHHHCCCCCCH
     EEEEECHHHHHHHHHHCCCCCCEEEEEHHHHHHHHHHHHHHHHHCCCCCCHHH

Esp1:STVKQHLMIIVKLINNNALGLASSEIIFLFNETNLFQAHSLKNILLADFSTWND
Cut1:LECCTYILEQMQVVTKNTSHLYDC-IRSGVSICNRLLDMEIFEPAISLLMKTHK
     HHHHHHHHHHHHHHCCCCCCCCCCCCEEEEECCCCEEEHHCCCCEEEECCCCCCC
     HHHHHHHHHHHHHCCCCCCCCCCCE-EEEECCCCEEEHHCCCCEEEECCCCCCCC

Esp1:YYLSNLKILALQIILKRKLVDEYLPHILELFSHDKRYLLK
Cut1:NLIILLTYRDHDAIPTATLLNPTL-DVSEIQLESCLFVPM
     CHHCCHHHHHHHHHHHHHHHHHHHHHHHHHCCCCEEECC
     HHCCHHHHHHHHHHHHHHHHHHH-HHHHHHCCCCEEECC
```

B

Secondary structure alignment of Esp1 and D12:

```
Esp1:MMVKQEEPLNEISPNTPMTSKSYLLNDTLSKVHHSGQTRPLTSVLSGDASSNSI
D12 :MDEIVKNIREGTHVLLPFYETLPELNLSLGKSPLPSLEYGANYFLQISRVNDLN
     CCCCCCCCHHHCCCCCCCCCCHHHHHHHHHHHHHCCCCCHHHHHCCCCCCCE
     CCCCCCCCHHHCCCCCCCCCCHHHHHHHHHHHHHCCCCCHHHHHCCCCCCCE

Esp1:GILAMHNNIIRDFTKIASNNIDLAIE--DITTVDHSLNSIYSLLKSHHMWGHIN
D12 :RMPTDMLKLFTHDIMLPESDLDKVYEILKINSVKYYGRSTKADAVVADLSARNK
     EEEEECHHHHHHHHHCCCCCEEEE--EHHHHHHHHHHHHHHHHHCCCCCCH
     EEEEECHHHHHHHHHCCCCCEEEEEHHHHHHHHHHHHHHHHHCCCCCCHHH

Esp1:STVKQHLMIIVK-LINNNALGLASSEIIFLFNETNLFQAHSLKNILLADFSTWN
D12  LFKRERDAIKSNNHLTENNLYISDYKMLTFDVFRPLFDFVNEKYCIIKLPTLFG
     HHHHHHHHHHHH-HHCCCCCCCCCCCEEEEECCCCEEEHHCCCCEEEECCCCCC
     HHHHHHHHHHHHCCCCCCCCCCCEEEEECCCCEEEHHCCCCEEEECCCCCCCH

Esp1:DYYLSNLKI---LALQIILKRKLVDEYLPHILELFSHDKRYLLK
D12  RGVIDTMRIYCSLFKNVRLLKCVSDSWLKDSAIMVASD------
     CCHHCCHHH---HHHHHHHHHHHHHHHHHHHHHHCCCCEEECC
     HCCHHHHHHHHHHHHHHHHHHHHHHHHHHCCCCEEECC------
```

Figure 4.4: Secondary structure alignment of Esp1 (*S.cerevisiae*), Cut1 (*S.pombe*) and the D12 subunit of the vaccinia virus mRNA capping enzyme
The secondary structure alignment was performed using the 3D-JIGSAW software.

HEAT repeats in invertebrate and mammalian orthologues average only 13% sequence identity [131]. Thus, the structural features rather than primary sequences are conserved in these cases. In those structures, where the HEAT/ARM-repeat containing proteins have been co-crystallised with a binding partner, the HEAT/ARM-repeat region is involved in protein-protein interactions [131]. It is thus conceivable that the predicted alpha-alpha superhelical domains in THR and separases mediate binding to PIM/SSE and securin/C-terminal separase domains, respectively [46].

Functional instead of structural studies on the N-terminus of Esp1 revealed an unexpected link to the mRNA machinery [132]. The N-terminus of Esp1 is able to complement a temperature-sensitive mutation in the *CEG1* gene encoding the mRNA guanylyltransferase (capping enzyme). The 52-kDa protein resembles that of the vaccinia virus guanylyltransferase. In both cases, GTP reacts with the enzyme-GMP intermediate with concomitant release of pyrophosphate. The enzyme then donates the GMP to a 5' diphosphate-

terminated RNA [133]. Mechanistic similarities between the cellular and viral capping enzyme are echoed at the structural level by regional amino acid sequence conservation. The vaccinia virus mRNA capping enzyme is a heterodimer of D1 (95kDa) and D12 (33kDa) subunits that catalyse all three steps in cap synthesis [133]. The RNA triphosphatase and RNA guanylyltransferase activities reside within the 60kDa N-terminal region of the D1 subunit. The 287 aminoacid D12 subunit, together with the C-terminal 305 aminoacid portion of the D1 subunit, catalyse the cap methylation reaction.
The N-terminus of Esp1 that rescues Ceg1 function and the D12 subunit of the vaccinia virus mRNA capping enzyme show four fragments of sequence similarity arrayed in a collinear fashion in both polypeptides ([132], Fig.4.5).
The last 700 amino acids of Esp1/separase containing the catalytic side are dispensable for the complementation of Ceg1. The D12 protein itself, although essential, has no catalytic activity. Rather it interacts tightly with the D1 subunit and stimulates its RNA-methyltransferase activity by 50- to 100 fold [132].

```
          : *  :: :: : *   **   :  *: :* :**
D12   49:VNDLNRMPTDMLKLFTHDIMLPESDLDKVYEILK:83
Esp1  63:IRDFTKIASNNIDLAIEDITTVDHSLNSIYSLLK:97

          * *: *:*: *:*   :
D12  123:TENNLYISDYKMLTFDV:140
Esp1 156:TWNDYYLSNLKILALQI:173

          **::  * ***  *:*
D12  171:YCSLFKNVRLL-KCVS:186
Esp1 316:YCNMSEN-RLLWSCIS:331

          * **:****
D12  241:INKFLEFSN:250
Esp1 523:ITKFIEFSN:532
```

Figure 4.5: Regions of similarity between the N-terminus of Esp1 (*S.cerevisiae*) and the D12 subunit of the vaccinia virus capping enzyme
Amino acid identity is indicated by a star, similarity is denoted by 2 dots (adapted from B.Schwer and S.Shuman, Gene Expression, Volume 5, 1996).

These mechanistic features seem to be very similar to the proposed activation of separase through its own N-terminus. Interestingly, a secondary structure query in D12 showed a similar helix-coiled-helix distribution as found in the N-termini of Esp1 and Cut1 (Fig.4.4-B). Furthermore a tertiary structure model of D1 shows a similar array of five beta strands as that of gingipain containing the catalytic dyad, the structure predicted for the C-terminus of separase (Fig.4.6).

What role could the N-terminus of Esp1 play in mRNA capping? It is possible that in the screen increased dosage of Esp1 drove a physical interaction with Ceg1, the effect of which is to either stabilise Ceg1 against denaturation or proteolysis at the non-permissive temperature or else to enhance its catalytic activity above a threshold level required for viability. It is conceivable that gene duplication led to the development of two different enzymes using very similar activation mechanisms.

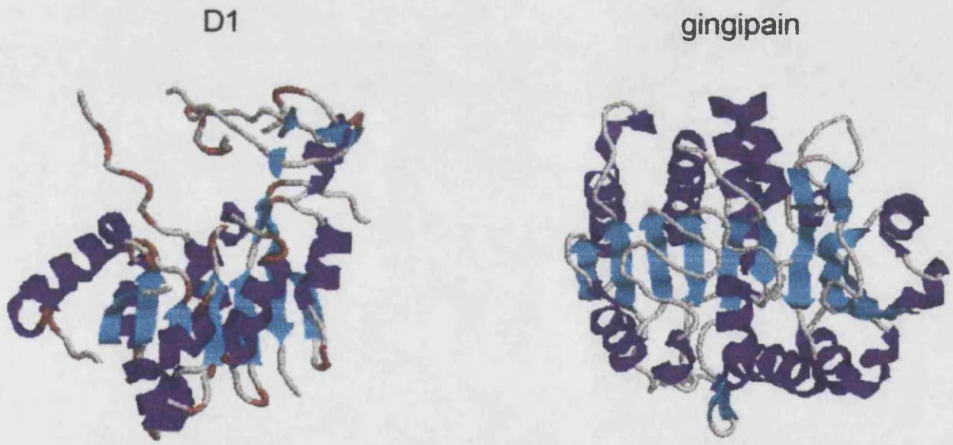

Figure 4.6: The D1 subunit of the vaccinia virus capping enzyme and the Cysteine Proteinase Gingipain (Porphyromonas gingivalis) show a similar tertiary structure
Crystal Structure Of The Arginine Specific Cysteine Proteinase Gingipain (Porphyromonas gingivalis) (Eichinger, A., Embo J., Volume 18, 1999) and the the D1 subunit of the vaccinia virus capping enzyme (Mao, X., et al., Biochemistry, Volume 35, 1996)

4.2 Regulation of cohesion cleavage

Anaphase onset is triggered when the Scc1 subunit of the chromosomal cohesin complex is cleaved by the protease separase. Only part of the total cellular cohesin is bound to chromosomes in metaphase, and it has been suspected separase may specifically recognise and cleave only this fraction to separate sister chromatids, while leaving cohesin in the soluble cellular fraction intact. Direct evidence for preferential cleavage of chromosomal cohesin or suggestions as to a possible targeting mechanism have not been available. The presented study shows that the rate of separase cleavage of chromosomal cohesin in budding yeast is indeed significantly greater when compared to cleavage of cohesin in the soluble cellular fraction, and that this is most likely due to preferential phosphorylation of chromatin-bound cohesin by Polo kinase. In budding yeast, two thirds of cohesin are chromatin-bound in metaphase, and accordingly a relatively large fraction of cohesin is cleaved at anaphase onset. If budding yeast is arrested in G1, or small daughter cells are isolated, little or no uncleaved Scc1 remains detectable in these cells [134, 135]. This suggests that in the course of mitotic progression most budding yeast Scc1, also in the soluble fraction, is cleaved. Nevertheless, preferential cleavage of chromosomal cohesin at anaphase onset will increase the promptness of sister chromatid separation. Some Scc1 may remain uncleaved and can be reused as large mother cells enter the subsequent S-phase soon after mitosis. The origin of cohesin that is unbound to chromosomes in the soluble cellular fraction in budding yeast metaphase is unclear. Not all cohesin may ever bind to chromosomes, and a soluble fraction of cohesin can be detected even during S and G2 phase [52]. In higher eukaryotes, a large fraction of cohesin dissociates from chromatin during chromosome condensation in prophase, leading to a substantial pool of soluble cohesin in metaphase [106]. Whether a fraction of chromatin-bound cohesin becomes soluble during budding yeast chromosome condensation is not known.

In vertebrates, it has been estimated that the amount of cohesin left on chromosomes after condensation is only about 5% of the total [125]. The amount of cohesin cleaved at anaphase onset appears similarly small [106], but it has not been formally shown that the cleaved cohesin in fact corresponds to

chromosomal cohesin. This seems likely to be the case though, because cohesin only promotes sister chromatid cohesion when bound to chromosomes, and cleavage of human cohesin is required for sister chromatid separation [36, 50]. To achieve preferential cleavage, the discrimination of human separase for chromatin-bound cohesin is likely to be greater than the 2-3 fold faster cleavage of chromosomal cohesin observed in budding yeast. The same is probably true in fission yeast, where a relatively small fraction of the total cohesin is cleaved to trigger anaphase [71, 119, 136]. Preferential cleavage of chromatin-bound cohesin in budding yeast depends on its phosphorylation, probably by a high local concentration of chromosome-associated Polo kinase. An alternative explanation for preferential phosphorylation might be that chromatin-bound cohesin is in a distinct conformational state that assists recognition by the kinase. This appears less likely, as overexpression of Polo led to hyperphosphorylation mainly of soluble rather than chromosomal cohesin. This study suggests that preferential modification of chromatin-bound cohesin is due to a high local concentration of a chromosome-associated enzyme. Such a mechanism might also contribute to distinguish chromosomal from soluble cohesin in other organisms.

Could Polo-like kinase be involved in determining preferential cleavage of chromosomal cohesin also in vertebrates? There, Polo promotes separase-independent cohesin removal from chromosomes during condensation [119, 136]. It seems at first sight counterintuitive that Polo could induce cleavage-independent cohesin dissociation, and at the same time mark persisting chromosomal cohesin for preferential separase cleavage. Another chromosomal kinase or enzymatic activity could therefore facilitate cohesin cleavage in vertebrates. Then again, Polo may in fact provide a generic mark for all chromosomal cohesin. Polo may not be specifying cohesin for one of the two pathways of removal from chromosomes, but it may identify all chromosomal cohesin as 'still chromosome-bound'. Such a mark could help both the prophase pathway, as well as cohesin cleavage by separase. Once released from chromosomes, phosphorylation may no longer be maintained. This would ensure that both mechanisms to remove cohesin from chromosomes are specifically targeted at remaining chromosomal cohesin.

In vertebrate, as well as *Drosophila* and fission yeast cells, cohesin reassociates with chromosomes very soon after mitosis, as chromosomes decondense in telophase [106, 120, 125]. Whether cohesin plays a specific role on chromosomes in telophase and the following G1 phase, before cohesion between sister chromatids must be again established in the next round of DNA replication, is not known. Nevertheless, maintenance of a pool of intact soluble cohesin throughout mitosis is clearly required to enable cohesin's fast reassociation with chromosomes when these cells exit from mitosis.

Chapter 5

Materials and methods

This chapter details the experimental methods used throughout this thesis. It also gives details of the contents of buffers and the derivation of strains used.

5.1 Solutions, buffers and media

All media and commonly used solution were provided by Cancer Research UK central services.

Media

L-Broth (LB) 170mM NaCl, 0.5%w/v yeast extract, 1% w/v bactotryptone
Ampicilin was added to a final concentration of 100μg/ml.

YEP-D 1.1%w/v yeast extract, 2.2%w/v bacto-peptone, 2%w/v D-glucose, 0.0055%w/v adenine

YEP-Raff/Gal 1.1%w/v yeast extract, 2.2%w/v bacto-peptone, 2%w/v raffinose, 2%w/v galactose, 0.0055%w/v adenine

YNB 0.32% Yeast Nitrogen Base
For plates 2%w/v agar was added.

Sectoring plates 1%w/v yeast extract, 2%w/v bacto-peptone, 4%w/v D-glucose, 2%w/v agar

Sporulation plates 0.33% Sodium acetate, 0.048% Sodium chloride, 0.076% potassium chloride, 0.014% Magnesium sulphate, 2%w/v agar

PBSA 170mM NaCl, 3mM KCl, 10mM Na_2HPO_4, 2mM KH_2PO_4

Gibco™ Graces Insect Cell Culture Medium (Invitrogen) containing 3.33 mg/l lactalbumin hydrolysate, 3.33 mg/l yeastolate, 1.5% L-glutamine, 10% foetal calf serum and 0.01mg/ml gentamycin.

Molecular biology

TE	10mM TrisHCl pH7.0, 0.1M EDTA
10XDNA loading buffer	60%w/v sucrose, 0.1%w/v bromophenol blue
TAE	40mM Tris-acetate, 1mM EDTA
10xTaq Buffer	200mM TrisHCl pH6.8, 100mM KCl, 30mM $MgSO_4$, (0.5% Triton X-100)
SCE	1M sorbitol, 0.1M sodium citrate pH7.0, 60mM EDTA
SCE/ME/zymolase	1M sorbitol, 0.1M sodium citrate pH7.0, 60mM EDTA, 8µl/ml β-mercaptoethanol, 2mg/ml zymolyase T-20
SDS-solution	100mM TrisHCl pH9.0, 50mM EDTA, 2% SDS
10xTEL	100mM TrisHCl pH7.5, 1mM EDTA, 1M Lithium acetate
TELP	100µl 10xTEL, 100µl H_2O, 800µl 50% PEG (polyethylenglycol 3350 or 4000)

Protein Biochemistry

2X SDS-PAGE- loading buffer	100mM TrisHCl pH6.8, 20% glycerol, 4% SDS, 0.2% Bromophenol blue, 100mM DTT
10x Running buffer	250mM TrisHCl, 2.5M glycine pH8, 1% SDS
Transfer buffer	144g/l glycine, 30g/l Tris base, 10% methanol
Stripping buffer	2% SDS, 50mM DTT, 50mM Tris base pH7
4x Stacking gel buffer	0.5M TrisHCl pH6.8, 0.4% SDS
4x Separating gel buffer	1.5M TrisHCl pH8.8, 0.4% SDS
Wash buffer (protein extraction)	50mM HEPES/KOH pH7.5, 100mM KCl, 2.5mM $MgCl_2$,
Extraction buffer (protein extraction)	50mM HEPES/KOH pH7.5, 100mM KCl, 2.5mM $MgCl_2$, 1mM DTT, 2mM benzamidine, 0.2mg/ml bacitracin, 20mg/ml leupeptine, 2µg/ml aprotinin, 2µg/ml pepstatinA, 1mM PMSF
Wash buffer (chromatin preparation)	50mMHEPES/KOH pH7.5, 100mMKCl, 2.5mM $MgCl_2$, 0.4M sorbitol

EB (chromatin preparation)	50mM HEPES/KOH pH7.5, 100mM KCl, 2.5mM $MgCl_2$, 1mMDTT, 2mM benzamidine, 0.2mg/ml bacitracin, 20mg/ml leupeptine, 2μg/ml aprotinin, 2μg/ml pepstatinA, 1mM PMSF (fresh)
EBX (chromatin preparation)	EB + 0.25% Triton X-100
EBX-S (chromatin preparation)	EBX + 30% sucrose

Protein purification from insect cells:

Wash buffer	50mM HEPES/KOH pH7.5, 10mM KCl, 1.5mM $MgCl_2$, 2mM benzamidine, 0.2mg/ml bacitracin, 20mg/ml leupeptine, 2μg/ml aprotinin, 2μg/ml pepstatinA
H200	50mM HEPES/KOH pH7.5, 200mM NaCl, 1.5mM $MgCl_2$, 0.01% Nonidet P-40
H500	50mM HEPES/KOH pH7.5, 500mM NaCl, 1.5mM $MgCl_2$, 0.01% Nonidet P-40
Elution buffer	50mM HEPES/KOH pH7.5, 200mM NaCl, 1.5mM $MgCl_2$, 0.01% Nonidet P-40, 2mM benzamidine, 0.2mg/ml bacitracin, 20mg/ml leupeptine, 2μg/ml aprotinin, 2μg/ml pepstatinA, 50mM DTT

Microscopy

Formaldehyde buffer	100mM KH_2PO_4 pH6.4, 0.5mM $MgCl_2$, 3.7% formaldehyde
Wash buffer	100mM KH_2PO_4 pH7.4, 0.5mM $MgCl_2$, 1.2M sorbitol
Spheroplasting buffer	100mM KH_2PO_4 pH7.4, 0.5mM $MgCl_2$, 1.2M sorbitol, 0.2% β-mercaptoethanol, 0.04% zymolase T-100
Blocking buffer	1% BSA (bovine serum albumin) in PBS
Sol1	100mM KH_2PO_4 pH7.4, 0.5mM $MgCl_2$, 1.2M sorbitol
Sol2	0.1M MES (2-(N-morpholino) ethane sulfonic acid), 1mM EDTA, 0.5mM $MgCl_2$, 1M sorbitol pH6.4

Fixative	4% paraformaldehyde (dissolved in water at 60-80°C (minute amounts of NaOH are eventually added to dissolve), 3.4% sucrose (kept in dark at 4°C)
Blocking buffer	0.5% BSA, 0.5% gelatine in PBS (warmed up in a microwave oven to dissolve gelatine)

5.2 Molecular Biological techniques

Molecular biological techniques were used as described (Maniatis, 1982) including growth and transformation of bacterial cells, gel electrophoresis of DNA in TAE buffer, restriction enzyme digests, minipreps and preparation of competent bacteria.

Nucleic Acid preparation and manipulation

Yeast genomic DNA for PCR genotyping was prepared from fresh patches of the strain of interest. A toothpick of cells was incubated in 200µl SC/ME/zymolase for 45min at 37°C on a shaking thermomixer. 200µl SDS-solution was added and the mix was heated up for 5min at 65°C. 200µl 5M KAc was added at room temperature. After 10min centrifugation at 12000rpm the supernatant was treated with 800µl EtOH. After a further centrifugation at 6000rpm for 2min, the pellet was washed with 70% EtOH and dissolved in 200µl H_20. For PCR, 0.5-1µl of the genomic DNA was used.

Enzymatic digestion of DNA with restriction enzymes was carried out as recommended by the suppliers (New England Biolabs).

DNA fragments were examined on 1%, 1.5% and occasionally, where fragments were very small, 2% (w/v) agarose in 1XTAE buffer. Gels were run at 100V in 1XTAE buffer in Anachem electrophoresis cells.

Polymerase Chain Reaction:

Non Mutagenic PCR

Normal PCR reactions were carried out using Vent (New England Biolabs) or Expand High Fidelity (Roche) polymerases with buffers supplied by the

manufacturers. dNTPs were supplied at 0.2mM in reaction volumes of 50 or 100µl. A reaction volume of 100µl contained 5 units of enzyme.

For colony PCR, samples were prepared in a similar manner. A toothpick full of yeast colony was suspended in the reaction mix heated to 95°C for 5 minutes. Subsequently enzyme was added and PCR started.

All PCRs were performed in a Peltier Thermal Cycler-200. Reactions were checked on DNA agarose gels for product size and precipitated in 1/10 volume of NaAc and 2.5 volumes of EtOH for further use.

PCR based site directed mutagenesis

Generation of site specific mutated DNA fragments was performed by PCR using overlap extension mutagenesis with Expand High Fidelity polymerase. For a first round of PCR (15 cycles: 5 cycles with an annealing temperature of at 56°C, 10 cycles with an annealing temperature of 60°C) 100ng template was used. Two sets of primers were used for two parallel reactions. The two sets contained the forward and reverse primers carrying the site specific mutation and a downstream reverse primer and an upstream forward primer respectively, needed for cloning. The two resulting PCR fragments were purified after running on an agarose gel using the Qiagen gel extraction kit. Equal amounts of PCR product (total amount 100ng) were used as templates for a second round of PCR (15 cycles: 5 cycles with an annealing temperature of 56°C, 10 cycles with an annealing temperature of 60°C) using only the outside primers. The resulting PCR fragment was either purified after running on an agarose gel or precipitated in 1/10 volume of NaAc and 2.5 volumes of EtOH. The mutagenesis was checked by sequencing.

Gene Disruption

All genes were disrupted using PCR generated fragments [137]. A marker gene (*LEU2*, *URA3*, *HIS3*, *TRP1*) was amplified with flanking sequences corresponding to the 5' and 3' ends of the relevant genes. Fragments were transformed into a strain lacking the selective marker. Colonies were selected on plates lacking the selective marker. The marker genes came from

heterologous sources (*K.lactis*, *S.pombe*) to prevent gene conversion of the mutant marker in *S.cerevisiae*.

Overexpression and C-terminal epitope tagging of genes in their chromosomal location

Glucose repressible promoters were integrated into the genome in front of the initiator ATG codon of genes by a PCR-based gene targeting method [137]. C terminal tagging of genes with HA, Myc or GFP eptiopes was also carried out using PCR generated fragments as described [137]. All tagging was confirmed by western blotting with specific antibodies.

Transformation and isolation of plasmid DNA in E. coli

Competent *E. coli* stored at –70°C were thawed on ice and incubated 20 minutes with 10ng of plasmid DNA. Cells were heat shocked at 42°C for 90s after which 1ml of LB media was added. The cells were allowed to recover at 37°C for 30 minutes to 1 hour before being plated onto LB plates containing the selective marker carried by the plasmid.

Chromosome loss assay

The assay to determine the frequency of chromosome loss was adapted from Spencer et al 1990 [128]. Strains were grown on medium lacking uracil and plated on rich medium. Half red sectored colonies were counted as they lost the extra chromosome in the first mitotic division.

5.3 Protein Biochemistry

Western blot analysis

Budding yeast protein extract were either prepared using glass beads disruption or NaOH lysis. For glass bead disruption between 10^6–10^8 cells were resuspended in protein extraction buffer and boiled in 250µl 2xSDS-loading buffer. Cells were then broken on a IKA Vibrax shaker for 10min. Following lysis with glass beads the extract was boiled again for 5 min, then clarified by centrifugation, and the protein concentration measured using the Bradford

Assay (BioRad). 5-10μl (20μg) of protein extracts were boiled in 2xSDS-loading buffer for 5 minutes and then run on 8% or 10% SDS-polyacrylamide gels.
For NaOH lysis of yeast cells between 10^6 –10^8 cells were used per sample. Cells were harvested by centrifugation and washed once with water. 100μl of chilled water and 100μl of 0.2M NaOH were then added to the cells, which were incubated at room temperature for 5 minutes before centrifugation. The supernatant was discarded and cell pellet resuspended in 50μl of 2xSDS-loading buffer. After boiling for 5 minutes, 5-10μl of protein extract was run on an SDS-polyacrylamide gel as above.
Blotting of gels was carried out as follows. Proteins were first transferred onto Protran (Schleicher and Schuell) transfer membrane. Semidry transfer was used for 3 hours at 1.2mA/cm^2 gel. After blocking for 1hr in 5% Milk PBSA solution with 0.01% Tween, antibodies were added in the same solution. Membranes were incubated for 1-2h (for quantitative western blots overnight at 4°C), washed and secondary antibody of Horseradish peroxidase conjugated goat anti-rabbit or goat anti-mouse IgG were incubated with the blot. A chemiluminescence system (ECL) was used to detect the bound antibodies.

Chromatin preparation

A crude Triton X-100-insoluble chromatin preparation was adapted from Liang & Stillman, 1997 [138].
200 ml of yeast cultures were grown in YEP-D medium at 25°C to a density of 1x 10^8 cells/ml. Cells were pelleted by centrifugation and resuspended in 6 ml 100 mM PIPES/KOH (pH 9.3), 10 mM dithiothreitol, and 0.1% sodium azide, and incubated at room temperature for 10 min. Cell were collected again by centrifugation and resuspended in 4 ml of 50 mM potassium phosphate (pH 7.5), 0.6 M sorbitol, 0.5 mM MgCl2, and 10 mM dithiothreitol. Zymolase T-100 (ICN Biochemicals) was added to a final concentration of 40μg/ml and spheroplasting was at 37°C for 10 min. Cells were collected again, washed in wash buffer, and resuspended in 350μl buffer EB. Spheroplasts were lysed by the addition of 0.25% Trition X-100 for 3 min on ice. This whole cell extract was layed on 100μl EBX-S and centrifuged 10min at 12000rpm. The upper phase of the supernatant containing the soluble material was removed carefully and

stored at –80°C for further analysis. The sucrose was removed by aspiration and the chromatin pellet resuspended in 100µl EBX. For storage at –80°C, 10% glycerol was added to the chromatin pellet.

In vitro assay for Esp1 activity

The Esp1 activity assay was adapted from Uhlmann et al. [35]. 200 ml of yeast cultures containing the *ESP1* gene under the inducible galactose promoter were grown in YEP medium with 2% raffinose as carbon source at 25°C. At a density of 2.5 x 10^6 cells/ml, the *GAL* promoter was induced by the addition of 2% galactose for 3 h before cells were harvested. As overexpression of Esp1 from the *GAL* promoter is toxic to cells, extracts with overproduced Esp1 were prepared 3 h after induction with galactose. One culture was left uninduced as a control for the purification. Cells were resuspended in 6 ml 100 mM PIPES/KOH (pH 9.3), 10 mM dithiothreitol, and 0.1% sodium azide, and incubated at room temperature for 10 min. Cell were collected again by centrifugation and resuspended in 4 ml of 50 mM potassium phosphate (pH 7.5), 0.6 M sorbitol, 0.5 mM MgCl2, and 10 mM dithiothreitol. Zymolase T-100 (ICN Biochemicals) was added to a final concentration of 40µg/ml and spheroplasting was at 37°C for 10 min. Cells were collected again, washed in wash buffer, and resuspended in 350µl buffer EB. Spheroplasts were lysed by the addition of 0.25% Trition X-100 for 3 min on ice.

A crude Triton X-100-insoluble chromatin preparation was obtained from yeast cells containing epitope tagged Scc1 as described above. The pelleted chromatin was resuspended in the above extracts containing overexpressed Esp1. Reactions were incubated for 10 min at 25°C with gentle shaking, and stopped on ice. The chromatin fraction was separated again from the supernatant by centrifugation, and resuspended in buffer EBX. Equivalent aliquots of supernatant and chromatin pellet were analysed by SDS-PAGE and western blotting. HA-tagged Scc1 was detected using monoclonal antibody 16B12, myc-tagged Scc1 with monoclonal antibody 9E10.

Purification of Scc1 Expressed in Baculovirus Infected Insect Cells

Purification of Scc1 from baculovirus infected insect cells was adapted from Uhlmann et al 2000. The Scc1 coding sequence was cloned into the baculovirus transfer vector pFastBac1 (Gibco Life Technologies). At the C terminus, a Flag and HA epitope tag was added followed by a cassette containing the yeast VMA intein and a chitin binding domain (New England Biolabs). Recombinant baculoviruses were obtained according to the manufacturer's instructions, and HiFive insect cells (Invitrogen) grown in monolayers to confluency were infected at a multiplicity of infection of 2. To obtain metaphase-like phosphorylation, 0.1 μM Okadaic acid was added 40 hr after infection. 43 hours after infection, cells were harvested. Cytoplasmic and nuclear extracts were obtained as described [139]. When Scc1 was purified after treatment of the cells with Okadaic acid, 5 mM NaF and 5 mM sodium pyrophosphate was added to the extraction buffer. Combined cytoplasmic and nuclear extracts from cells in 10 T250 flasks (8 ml, 100 mg protein) were loaded onto 1 ml bead volume of chitin beads (New England Biolabs), equilibrated in buffer H200. Loading was for 2 hr by rocking at 4°C. The chitin resin was then washed in a column with 20 column volumes each of buffer H500 and H200 (index indicates the concentration of NaCl). The column was then flushed with 3 column volumes of buffer H200 containing 50mM dithiothreitol and closed for cleavage of the intein overnight. The eluate containing Scc1 released from the column was directly loaded onto a MonoQ HR 5/5 column (Amersham Pharmacia), and the column was developed with a gradient from H200 to H1000 in 10 ml. Fractions containing Scc1 were detected by SDS-PAGE followed by Coomassie staining and Western blotting against the Flag epitope or the HA epitope. Pooled fractions were diluted to 200 mM NaCl by adding buffer H 0, and chromatography on the MonoQ column was repeated. This step was necessary to remove traces of a contaminating protein that copurified with Scc1 and was identified as Hsp70 from the insect host cells by mass spectrometry. The final eluate was dialyzed against buffer H 100 and concentrated by ultrafiltration. This protocol yielded 25 μg of purified Scc1 or purified metaphase-like phosphorylated Scc1.

Overexpression and Purification of Esp1 from Yeast Cells

200 ml of yeast culture were grown in YEP medium with 2% raffinose as carbon source at 25°C. At a density of 2.5 x 10^6 cells/ml, the *GAL* promoter was induced by the addition of 2% galactose for 5 hr before cells were harvested. One culture was left uninduced as a control for the purification. Cells were resuspended in 6 ml 100 mM PIPES/KOH (pH 9.3), 10 mM dithiothreitol, and 0.1% sodium azide, and incubated at room temperature for 10 min. Cell were collected again by centrifugation and resuspended in 4 ml of 50 mM potassium phosphate (pH 7.5), 0.6 M sorbitol, 0.5 mM MgCl2, and 10 mM dithiothreitol. Zymolase T-100 (ICN Biochemicals) was added to a final concentration of 40 μg/ml and spheroplasting was at 37°C for 10 min. Cells were collected again, washed in 2 ml of 50 mM HEPES/KOH (pH 7.5), 100 mM KCl, 2.5 mM MgCl2, and 0.4 M Sorbitol, and resuspended in 350 μl buffer FB (50 mM HEPES/KOH (pH 7.5), 250 mM NaCl, 1 mM $MgCl_2$, 1 mM $CaCl_2$, and 1 mM dithiothreitol, plus protease inhibitors as described [138]. Cells were lysed by the addition of 0.25% Trition X-100 for 3 min on ice, and the lysate was cleared by centrifugation. The extracts were loaded onto 50μl bead volume of chitin beads and equilibrated in buffer FBX (FB plus 0.05% Triton X-100) for 2 hr on a rotating wheel. Beads were transferred into a chromatography column and washed with 5 ml each of FBX1000, and FBX100, containing 1 M and 100 mM NaCl, respectively. Beads were then resuspended in a total volume of 100 μl FBX100 and 20 μl aliquots of the suspension were distributed. Beads were sedimented by gravity and 10 μl supernatant was retrieved and discarded. For detection of purified Esp1, 10 μl of SDS-PAGE loading buffer was added to the beads, boiled for 5 min, and 10 μl of the SDS eluate was loaded for SDS-PAGE.

For immunoprecipitations of Esp1, Pds1 and Scc1 the same protocol was followed up to the cell lysis. Buffer EB was used instead of buffer FB. Protein A beads were used for binding of myc- and HA-epitope tagged protein, chitin beads for binding of CBD epitope tagged protein. Antibodies were added at the concentrations listed below.

Cleavage of Purified Scc1 in Yeast Extracts

Scc1 cleavage-competent yeast extracts after overexpression of Esp1 and control extracts were obtained as described above. 6 μl (20 ng/μl) purified Scc1 or Scc1-P in H200 was added to 12 μl of control or Esp1 containing extracts, or to mixtures at different ratios between these extracts. Incubation was for 10 min at 25°C. The reaction was stopped by adding SDS-PAGE loading buffer, and aliquots were analysed by SDS-PAGE and Western blotting against the Flag and HA-epitope [35].

Scc1 Cleavage by Esp1 Bound to Chitin Affinity Beads

10 μl (20 ng/μl) of purified Scc1 or Scc1-P in FBX100 supplemented with 0.1 mg/ml BSA was added to 10μl of Esp1-bound chitin beads obtained as described above. The reaction was incubated for 15 min at 25°C with continuous shaking. Beads were sedimented by brief centrifugation and 10 μl supernatant was retrieved and loaded for SDS-PAGE. In experiments where the peptide inhibitor was used, 10μl of a 20μM dilution of the small protease inhibitor Bio-SVEQGR-amk (uhlmann cell 2000) was added to 10 μl of chitin beads and incubated 10 min at 25°C. Then, 10μl of supernatant was retrieved again, and Scc1 was added and incubated as above. To detect the proteins on the beads labeled by the inhibitor, the beads were boiled with 10μl of SDS-PAGE loading buffer and the eluate was loaded for SDS-PAGE. After electrophoresis, the gel was transferred to a nitrocellulose membrane and biotinylated proteins were detected as described [140].

To investigate the effect of securin on Scc1 cleavage by Esp1, amino acids 256-359 of securin were cloned into the bacterial expression vector pGEX-KG [141] by PCR using genomic DNA as the template. The binding of the GST-securin fragment to Esp1 was analysed incubating 1 μg of GST-securin with 20 μl of chitin beads, to which Esp1 had been bound as above, in a reaction volume of 25 μl of FBX buffer. Incubation was for 10 min on ice with agitation, after which the beads were washed and the bound protein eluted in SDS-PAGE loading buffer. To analyse the binding of recombinant Scc1 to separase, 0.2 μg Scc1 was added to the separase-containing beads for 10 min at 25°C. For binding of Scc1 to separase deletion mutants, both proteins were co-

overexpressed in the same strain. To detect interactions between N- and C-terminal fragments of separase the fragments in question were co-overexpressed in a diploid strain obtained by crossing strains expressing the individual fragments.

Analysis of Scc1 cleavage kinetics

Exponentially growing cells were arrested in metaphase by addition of 5 μg/ml nocodazole. Soluble and chromatin fractions were prepared after spheroplast lysis as previously described. The Scc1 in vitro cleavage assay was modified as follows [142]: chromatin-bound and soluble fractions containing equivalent amounts of reciprocally tagged Scc1 were mixed, ensuring chromatin was thoroughly resuspended. Chromatin-released cohesin was also included that was obtained as described, and phosphatase treatment of chromosomal cohesin was as described [35]. An aliquot of this mix was taken as the time point 0. Then extract containing overexpressed separase was added and the mix was incubated at 25°C with light agitation. Aliquots were taken every minute and the reaction stopped by injecting the samples directly into preheated SDS-PAGE loading buffer. Samples were subjected to quantitative Western blotting: After Western transfer, membranes were blocked with Odyssey buffer (LI-COR):PBS (1:1), and incubated with 12CA5 and 9E10 mouse monoclonal antibodies against the HA and myc epitope, respectively, and a goat anti-mouse IRDye800 coupled secondary antibody (LI-COR). The fluorescent signal was quantified using the Odyssey infrared imager (LI-COR) and Infrared Imaging System software. Scc1 at time point 0 was set to 100% and remaining full-length Scc1 was plotted over time. Scc1 cleavage by separase adhered closely to the characteristics of a first order reaction, and graphs were fitted with exponential regression (R^2 typically > 0.9) using Excel software.

Dephosphorylation of Scc1 on Chromatin

Chromatin obtained from 50μl cell lysate was resuspended in 200μl phosphatase buffer (50 mM Tris/HCl pH 7.5, 100 mM KCl, 0.1 mM EDTA, 2 mM $MnCl_2$, 5 mM dithiothreitol, 0.1% Triton X-100), and 2000 units lambda protein phosphatase (New England Biolabs) was added. Incubation was for 12 min at

30°C, then the chromatin was recovered by centrifugation and washed once before it was used for the Scc1 cleavage assay [38]. To exclude that the effect observed after phosphatase treatment of the chromatin was due to residual amounts of phosphatase carried into the subsequent cleavage reaction, a control reaction was carried out in which 200 units of lambda phosphatase were added to the cell extract. This had no effect on the efficiency of Scc1 cleavage in the assay.

Hyperphosphorylation by Polo of Scc1 in soluble cohesin

Cells containing an extra copy of the CDC5 gene, encoding Polo kinase, under control of the galactose inducible GAL promoter, were grown in raffinose and arrested in metaphase by addition of 5 μg/ml nocodazole for 2.5 hours. During this period, Polo expression was induced by adding 2% galactose 2h, 1h or 0.5h before the final arrest point.

Phosphorylation shift assay

Strains containing phosphorylation site mutation were assayed for a phosphorylation band shift. Extracts were prepared using the glass bead method described above and run on a specialised 10% SDS-polyacrylamide gel containing an increased concentration of acrylamide to bis-acrylamide, which allowed greater separtation of proteins.

The ratio of acrylamide was increased from 29:1 to 200:1 by the addition of pure 30% acrylamide solution to the gel mixture before pouring.

In vivo cleavage of chromatin-bound versus soluble Scc1

Arrest in metaphase and release into synchronous anaphase using CDC20 under GAL promoter control was as described [38], but cultures were cooled to 16°C before release. Aliquots of $5x10^8$ cells were harvested in 5 min intervals and resuspended in ice-cold wash buffer. After completion of the time course, cells were resuspended in 200μl EB buffer, added to 500μl glass beads and broken on an IKA-Vibrax shaker for 10 min. The crude cell extract was retrieved and separated into chromatin-enriched and supernatant fractions by centrifugation at 12,000 x g for 10 min. Small chromatin fragments in the soluble

fraction were removed by a second round of centrifugation at 100,000 x g for 10 min. The chromatin pellet was washed in EB buffer supplemented with 0.25% Triton X-100 to remove detergent soluble material, and resuspended in 200 µl of the same buffer for analysis by quantitative Western blotting as above.

Separase binding and cleavage of recombinant Scc1

Purification of phosphorylated Scc1 after overexpression in baculovirus infected insect cells, treated with Okadaic acid, was as described above. Dephosphorylation of purified Scc1 was performed using λ-phosphatase (New England Biolabs). Separase and separase (C1531A) was purified after overexpression in yeast by chitin affinity chromatography as described [41]. Scc1 was added to separase decorated chitin beads, and cleavage or binding was analysed after 10 minutes at 25°C. SDS-PAGE loading buffer was directly added to stop the cleavage reaction, while the beads were washed extensively with EB buffer containing 0.25% Triton X-100 before bound Scc1 was analysed in SDS-PAGE loading buffer.

5.4 Microscopy

In situ immunofluorescence

In situ immunofluorescence was adapted from Michaelis et al. [134]. $1x10^5$ cells were resuspended in 1ml icecold formaldehyde buffer and either fixed over night at 4°C or immediately for 1h at 30°C. After washing in washing buffer the fixed cells were incubated at 30°C for 30min for spheroplastation in spheroplasting buffer. Cells were washed again and resuspended in 100-200µl of wash buffer. For immunostaining 5-10µl of cells were pipetted on 15 well slides pretreated with 0.1% polylysine. Cells were left to adhere for 5min, then excess cells and liquid were removed, plunged into icecold methanol for 3min, and then transferred to icecold acetone for 10sec. Slides were blocked in blocking buffer in a moist chamber for 20min. Incubation of the first and secondary antibody (concentrations are listed below) were for 1 hour interrupted by 3x washing with blocking buffer. After the secondary antibody incubation,

slides were washed 4x in blocking buffer and 0.1μg/ml DAPI in antifade mounting medium was added to each well. The slides were covered with a cover slip and sealed with nail polish.
Immunofluorescence images were viewed with a Zeiss Co, Axioplan 2 imaging microscope attached to a Princeton Instrument cooled CCD digital camera. A laser scanning confocal microscope LSM510 (Zeiss Co.) was also used. Images were processed using IPlab software and Adobe ® Photoshop versions 6 or 7.

Chromosome spreads

Yeast chromosome spreading was adapted from Michaelis et al. [134]. $1x10^6$ cells were resuspended in 1ml of Sol1, then incubated for 5-10min at 37°C in Sol1 adding 20μl 1M DTT and 14μl 10mg/ml zymolase T-100. The reaction was stopped by adding 1ml icecold Sol2. Cells were resuspended in 100-200μl Sol2. Menzel SuperFrost slides were used for spreading. 20μl of cell suspension was pipetted onto the slide, followed by 40μl of fixative, 80μl of 1% lipsol and another 80μl of fixative. The drop was distributed over the slide by moving a glass rod gently parallel to the slide. The slides were dried over night. After drying, the slides were washed in PBS, blocked in blocking buffer and incubated with first and second antibody (concentrations are listed below) for 2 hours interrupted by 10min washing in PBS. After the second antibody incubation, the slides were washed in PBS for 10min and 0.1μg/ml DAPI in antifade mounting medium was added to each well. The slides were covered with a cover slip and sealed with nail polish.
Immunofluorescence images were viewed with a Zeiss Co, Axioplan 2 imaging microscope attached to a Princeton COOL CCD digital camera. Images were processed using IPlab software and Adobe ® Photoshop versions 6 or 7.

5.5 Antibodies used in Western blot, Immunoprecipitation (IP) analysis and Immunohistochemistry (in situ)

C-Myc9E10	mouse mono	Babco	1/2000 western

			1/1000 IP
			1/1000 in situ
C-Myc	rabbit poly	Gramsch	1/100 in situ
HA12CA5	mouse mono	CRUK	1/5000 western
			1/1000 IP
HA16B12	mouse mono	CRUK	1/15000 western
			1/1000 IP
			1/1000 in situ
FLAG-M2	mouse mono	Sigma	1/1000 western
			1/100 IP
GST	mouse mono	Sigma	1/3000 western
Scc1	rabbit mono	Dr.A.Strunikow	1/3000 western
		NIH Bethesda	1/100 IP
Sc Pds1	rabbit mono	Santa Cruz	1/200 western
GFP	rabbit mono	MBL, Japan	1/500 in situ
α-tubulin	rat mono	Serotec	1/200 in situ
Peroxidase	mouse mono	Sigma	1/2000 western
Mouse IgG	goat	Rockland via Tebu	1/5000 western
(For Odyssey Infrared Imaging System)		Biosiences	
Mouse IgG	goat	FluoroLink Cy2	1/200 in situ
		Amersham Pharmacia Biotech	
Mouse IgG	goat	FluoroLink Cy3	1/1000 in situ
		Amersham Pharmacia Biotech	
Mouse IgG	sheep	Amersham	1/5000 western
(For ECL detection)		Pharmacia Biotech	
Rabbit IgG	goat	FluoroLink Cy2	1/200 in situ
		Amersham Pharmacia Biotech	
Rabbit IgG	goat	FluoroLink Cy3	1/1000 in situ
		Amersham Pharmacia Biotech	
Rabbit IgG	donkey	Amersham	1/5000 western
(For ECL detection)		Pharmacia Biotech	

5.6 Yeast physiology

Budding yeast nomenclature

The gene names of budding yeast are typically shown as 3 upper italicised case letters and a number e.g. *PDS1*, a mutant allele is italicised and shown lower case letters e.g. *pds1*. Temperature sensitive mutant alleles of a gene are indicated by a suffix of *ts* in superscript. Proteins are named using the same three letters indicative of the gene but are not written in italics. Gene deletions which have been achieved using a specific marker are shown by the gene name followed by :: and the replacement marker gene name. E.g. *pds1::URA3*. A gene deletion can also be annotated by a Δ symbol.

Strain growth and maintenance

S. *cerevisiae* cells were grown in either liquid media or on agar plates containing 2% agar. The contents of different media are shown above. Stocks of yeast strains were stored in 15% glycerol and maintained at –80 °C.

Insect cells were grown in Gibco™ Graces Insect Cell Culture Medium (Invitrogen).

Bacteria were grown in LB-medium containing 100μg/ml ampicillin.

Transformation of budding yeast

Transformations of plasmid DNA into yeast cells were carried out using Lithium Acetate and Poly Ethylene Glycol (PEG) as previously described (ref: Ito, 1983). 50-100μl cells ($1x10^8$) grown to mid logphase were spun down, washed in water, then washed in 1xTEL and resuspended in 100μl 1xTEL. Approximately 1 μg of plasmid DNA or PCR product was used for integrative transformations. 0.05mg/ml denaturised salmon sperm DNA was added together with the plasmid or PCR DNA to 50μl of cell suspension in TEL. 300μl TELP was added followed by a short vortex. After an incubation of 2-4 hours at 25°C, the transformations were heat shocked for 15 min at 42°C and plated on selective medium. Selective markers used in plasmid and integrant transformations were *LEU2, URA3, HIS3, TRP1.*

Synchronous cultures:

G1 synchrony

Cells were grown to mid log phase in rich media, diluted to $1x10^6$ cells/ml and 1μg/ml of the pheromone α-factor was added. After 1 and 2 hours another 0.5μg/ml were added. G1 synchrony was checked under the microscope (budding index). To release cells form the arrest, cells were filtered and washed with YEP media, then resuspended in rich media. Synchrony was measured by flow cytometric analysis (FACS).

Flow cytometry

10^6-10^7 cells/ml from relevant cultures were fixed in 70% ethanol. Cells were pelleted and rehydrated in 3ml 50mM Na_3citrate and then resuspended in 1ml 50mM Na_3citrate containing 0.1mg RNase A, 2μg/ml propidium iodide and incubated for 4hrs at 37°C. Before analysis cells were sonicated for 30s at setting 5 (soniprep 150 sonicator MSE). Flow cytometry was performed as described previously [143] using a Becton-Dickinson FAC Scan with an excitation wavelength of 488nm and a detection wavelength of 510-550nm. Data analysis used the CELL QUEST software package.

S-phase arrest

Cells were grown to mid log phase in rich media ($1x10^8$/ml). 100mM hydroxyurea (HU) was added and large budded cells, indicating an S-phase arrest, were scored under the microscope after 2 hours.

G2 synchrony

Cells were grown to mid log phase in rich media ($1x10^8$/ml). 5μg/ml nocodazole (sigma) with 1% DMSO was added and large budded cells, indicating a metaphase arrest, were scored under the microscope after 2 hours.

Strains expressing Cdc20 from the *GAL1-10* promoter were grown in complete medium containing 2% raffinose as carbon source. The *GAL1-10* promoter was induced by adding 2% galactose. Metaphase arrest due to Cdc20 depletion was obtained in cells with *CDC20* under control of the *GAL1-10* promoter by shifting to medium containing raffinose only. For release from the arrest, 2% galactose

was added back to the culture.

5.7 Budding yeast strains

Name	Description	Derivation
699	MATa, ade2-1, can1-100, trp1-1, leu2-3,112, his3-11,15, ura3, GAL, psi+,	Kim Nasmyth
700	MATalpha, ade2-1, can1-100, trp1-1, leu2-3,112, his3-11,15, ura3, GAL, psi+,	Kim Nasmyth
58	MATa, Scc1-myc18::TRP, ura3::URA3 tetOs, leu2::LEU2 his::HIStetR-GFP, leu2-3, 112	Frank Uhlmann
157	MATa, ade2-101, CAN+, lys2-801, trp1-1, leu2D1,112, his3D200, CFIII (CEN3.L.YPH278) URA3SUP11	P.Hieter/ Christine
192	MATa, ura3::3xURA3 teto112, his::HIStetR-GFP	Attila Toth
189	MATa, Esp1-myc18::TRP, ade2-1, can1-100, leu2-3,112, his3-11,15, ura3, GAL, psi+,	Rafal Ciosk
8869	MATa, ade2-1, can1-100, trp1-1, leu2-3,112, Scc1-HA6::HIS, ura3, GAL, psi+,	Gabriela Alexandru
8646	MATa, ade2-1, can1-100, trp1-1, leu2-3,112, GALCDC5::HIS3, Scc1-HA6::HIS, cdc5::URA3, GAL, psi+,	Gabriela Alexandru
291	MATa, pds1::URA3, Scc1-HA3::TRP, ura3::URA3 tetOs, leu2::LEU2 tetR-GFP, Esp1-myc18::HIS3	this study
292	MATa, tetR-GFP:LEU2, TetOx200:URA3, Esp1myc18::HIS3	this study
334	MATa, tetR-GFP:LEU2, TetOx200: GAL-Flag-Esp1-CBD::TRP1,his::HIStetR-GFP	this study
335	MATa, pds1::URA3, ura3::URA3 tetOs, leu2::LEU2, GAL-Flag-Esp1-CBD:TRP1	this study
336	MATa, GAL-Flag-ESP1(1391-1630)-CBD, tetR-GFP:LEU2, TetOx200:URA3, TRP1	this study
358	MATa, ESP1-myc18::TRP1, GAL1-PDS1-mdb on pRS305 LEU2	this study
363	MATa, ade2-1, can1-100, leu2-3, 112, his3-11,15, ura3, GAL, psi+, pep4::URA3, bar1::hisG, GAL-Flag-Esp1-CBD::TRP1	this study
364	MATa, ade2-1, can1-100, leu2-3,112, his3-11,15, ura3, GAL, psi+, pep4::URA3, bar1::hisG, GAL-Flag-Esp1(H1505A)-CBD::TRP1	this study
367	MATa, GAL-Flag-ESP1(1196-1630)-CBD, tetR-GFP:LEU2, TetOx200:URA3, TRP1	this study
373	MATalpha, GAL-Flag-ESP1(156-1630)-CBD, esp1-1, ura3::URA3 tetOs, leu2::LEU2 tetR-GFP, his3-11, TRP1	this study
455	MATa, tetR-GFP:LEU2, TetOx200:URA3, Esp1-myc18::HIS3, Pds1-HA3::TRP	this study

456	Mat a, clb1 del, clb3::TRP1, clb4::HIS3, clb2-VI rt 37 C, Esp1-myc18:URA	this study
463	MATa, ade2-1, can1-100, leu2-3,112, GAL-Esp1(1390-1630)::TRP, his3-11,15, ura3, GAL, psi+	this study
465	MATa, ade2-1, can1-100, leu2-3,112, GAL-Esp1(1196-1630)::TRP, his3-11,15, ura3, GAL, psi+	this study
467	MATa, ade2-1, can1-100, leu2-3,112, GAL-Esp1(156-1630)::TRP, his3-11,15, ura3, GAL, psi+	this study
480	MATa, ade2-1, can1-100, his3-11,15, ura3, GAL, psi+, pep4::URA3, bar1::hisG, GAL-Flag-Esp1-CBD::TRP1, GAL-SCC1-HA3::LEU2	this study
483	MATa, ade2-1, can1-100, his3-11,15, ura3, GAL, psi+, pep4::URA3, bar1::hisG, GAL-Flag-Esp1(H1505A)-CBD::TRP1, GAL-SCC1-HA3::LEU2	this study
487	MATa, ade2-1, can1-100, leu2-3,112, ura3, GAL, psi+, pep4::URA3, bar1::hisG, GAL-Flag-Esp1(H1505A)-CBD):TRP1, Scc1-HA6::HIS5	this study
488	MATa, ade2-1, trp1-1, can1-100, leu2-3,112, his3-11,15, GAL, psi+, Esp1-myc18::URA3	this study
490	MATalpha,ade2-1,trp1-1,can1-100, his3-11,15, ura3, GAL, psi+, GAL-Flag-ESP1(1-1195)::LEU2	this study
491	MATa, ade2-1, can1-100, leu2-3,112, Esp1(156-1630)::TRP, his3-11,15, ura3, GAL, psi+	this study
492	MATa, ade2-1, can1-100, GAL-Flag-Esp1(1390-1630)::TRP, his3-11,15, ura3, GAL, psi+, GAL-SCC1-HA3 (LEU2)	this study
494	MATa, ade2-1, can1-100, GAL-Flag-Esp1(1196-1630)::TRP, his3-11,15, ura3, GAL, psi+ , GAL-SCC1-HA3 (LEU2)	this study
496	MATa, ade2-1, can1-100, GAL-Flag-Esp1(156-1630)::TRP, his3-11,15, ura3, GAL, psi+, GAL-SCC1-HA3 (LEU2)	this study
498	MATa, Crm1T539C, ade2-1, trp1-1, can1-100, leu2-3,112, his3-11,15, ura3, GAL, psi+	this study
499	MATa, Crm1T539C, ade2-1, trp1-1, can1-100, leu2-3,112, ura3, GAL, psi+, Esp1myc18::HIS	this study
532	MATa/Matalpha, ade2-1/ade2-1, can1-100/can1-100, his3-11,15/his3-11,15, ura3/ura3, GAL-Flag-ESP1(1390-1630)::TRP1/trp1-1, GAL-Flag-ESP1(1-1195)::LEU2/leu2-3,112, GAL/GAL, psi+/psi+	this study
533	MATa/Matalpha, ade2-1/ade2-1, can1-100/can1-100, his3-11,15/his3-11,15, ura3/ura3, GAL-Flag-ESP1(1196-1630)::TRP1/trp1-1, GAL-Flag-ESP1(1-1195)::LEU2/leu2-3,112, GAL/GAL, psi+/psi+	this study
538	MATalpha,GAL-Flag-ESP1(1-370)::LEU,ade2-1,trp1-1, can1-100, his3-11,15,ura3,GAL,psi+	this study

539	MATalpha,GAL-Flag-ESP1(1-175)::LEU,ade2-1,trp1-1, can1-100, his3-11,15,ura3,GAL,psi+	this study
540	MATa/Matalpha, ade2-1/ade2-1, can1-100/can1-100, his3-11,15/his3-11,15, ura3/ura3, GAL-Flag-ESP1(1390-1630)::TRP1/trp1-1, GAL-Flag-ESP1(1-370)::LEU2/leu2-3,112, GAL/GAL, psi+/psi+	this study
541	MATa/Matalpha, ade2-1/ade2-1, can1-100/can1-100, his3-11,15/his3-11,15, ura3/ura3, GAL-Flag-ESP1(1196-1630)::TRP1/trp1-1, GAL-Flag-ESP1(1-370)::LEU2/leu2-3,112, GAL/GAL, psi+/psi+	this study
542	MATa, Crm1T539C, ade2-1, trp1-1, can1-100, leu2-3,112, GAL, psi+ , Esp1myc18::HIS, deltapds1::URA	this study
543	MATa, ESP1-myc18::TRP1, pds1::URA	this study
561	MATa/Matalpha, ade2-1/ade2-1, can1-100/can1-100, his3-11,15/his3-11,15, ura3/ura3, GAL-Flag-ESP1(1390-1630)::TRP1/trp1-1, GAL-Flag-ESP1(1-175)::LEU2/leu2-3,112, GAL/GAL, psi+/psi+	this study
562	MATa/Matalpha, ade2-1/ade2-1, can1-100/can1-100, his3-11,15/his3-11,15, ura3/ura3, GAL-Flag-ESP1(1196-1630)::TRP1/trp1-1, GAL-Flag-ESP1(1-175)::LEU2/leu2-3,112, GAL/GAL, psi+/psi+	this study
576	MATa, ESP1-myc18::TRP1, GAL1-PDS1-mdb on pRS305 LEU2, pds1::URA3	this study
610	MATalpha,YIp128 GAL-Flag-ESP1(156-1195), ade2-1, trp1-1,can1-100,his3-11,15,ura3,GAL, psi+	this study
611	MATa/Matalpha, ade2-1/ade2-1, can1-100/can1-100, his3-11,15/his3-11,15, ura3/ura3, GAL-Flag-ESP1(1390-1630)::TRP1/trp1-1, GAL-Flag-ESP1(156-1195)::LEU2/leu2-3,112, GAL/GAL, psi+/psi+	this study
612	MATa/Matalpha, ade2-1/ade2-1, can1-100/can1-100, his3-11,15/his3-11,15, ura3/ura3, GAL-Flag-ESP1(1196-1630)::TRP1/trp1-1, GAL-Flag-ESP1(156-1195)::LEU2/leu2-3,112, GAL/GAL, psi+/psi+	this study
644	MATa, tetR-GFP:LEU2, TetOx200:URA3, GAL-Flag-ESP1(K809N)(K810N)(K811N)-HA6:TRP	this study
646	MATa, pds1::URA3, ura3::URA3 tetOs, leu2::LEU2 tetR-GFP, GAL-Flag-ESP1(K809N)(K810N)(K811N)-HA6:TRP	this study
682	MATa, ade2-1, can1-100, ura3, GAL-Flag-ESP1(1390-1630)::TRP1/trp1-1, GAL-Flag-ESP1(156-1195)::LEU2/leu2-3, HIS/ his3-11,15 GAL-Pds1::LEU/leu2-3,112, GAL, psi+	this study
717	Mat alpha, ade2-1, ura3-1, his3-11,15, leu2-3,112, can1-100, xpo1::LEU2(pKW457-xpo1-1-HIS3), Esp1myc18::TRP	this study
718	Mat alpha, ade2-1, his3-11,15, leu2-3,112, can1-100, xpo1::LEU2(pKW457-xpo1-1-HIS3), Esp1myc18::TRP, pds1::URA	this study

727	MATalpha,GAL-Flag-ESP1(1-175)::LEU,ade2-1, trp1-1, can1-100, ura3, HIS, GAL, psi+	this study
730	Mata, ade2-1, his3-11,15, can1-100, xpo1::LEU2(pKW457-xpo1-1-HIS3), Esp1myc18::TRP, tetR-GFP:LEU2, TetOx200:URA3	this study
759	MATa, tetR-GFP:LEU2, TetOx200:URA3, GAL-Flag-ESP1(L163A,L166A,L169A)-CBD::TRP	this study
760	MATa, pds1::URA3, ura3::URA3 tetOs, leu2::LEU2 tetR-GFP, GAL-Flag-ESP1(L163A,L166A,L169A)-CBD::TRP	this study
761	MATa, ade2-1, can1-100, Esp1(1196-1630)::TRP, GAL1-PDS1-mdb on pRS305::LEU2, his3-11,15, ura3, GAL, psi+	this study
762	MATa, ade2-1, can1-100, Esp1(156-1630)::TRP, GAL1-PDS1-mdb on pRS305::LEU2, his3-11,15, ura3, GAL, psi+	this study
763	MATa, GAL-PDS1-mdb::LEU, GAL-Flag-ESP1-CBD::TRP, ade2-1, can1-100, his3-11,15, ura3, GAL, psi+	this study
764	MATa, ade2-1, GAL-SCC1-HA3::TRP1, can1-100, leu2-3,112, his3-11,15, ura3, GAL, psi+	this study
765	MATa, ade2-1, GAL-SCC1-HA3::TRP1,GAL1-PDS1-mdb on pRS305::LEU2, can1-100, his3-11,15, ura3, GAL, psi+	this study
1134	MATa, Scc1myc18::HIS3, Gal-Scc1-HA3::TRP, tetR-GFP:LEU2, TetOx200:URA3	this study
1135	MATa, Scc1myc18::HIS3, Gal-Scc1(S183A)-HA3::TRP, tetR-GFP:LEU2, TetOx200:URA3	this study
1136	MATa, Scc1myc18::HIS3, Gal-Scc1(S194A)-HA3::TRP, tetR-GFP:LEU2, TetOx200:URA3	this study
1137	MATa, Scc1myc18::HIS3, Gal-Scc1(S273A,S276A)-HA3::TRP, tetR-GFP:LEU2, TetOx200:URA3	this study
1138	MATa, Scc1myc18::HIS3, Gal-Scc1(S325A)-HA3::TRP, tetR-GFP:LEU2, TetOx200:URA3	this study
1139	MATa, Scc1myc18::HIS3, Gal-Scc1(S374A)-HA3::TRP, tetR-GFP:LEU2, TetOx200:URA3	this study
1140	MATa, Scc1myc18::HIS3, Gal-Scc1(S389A)-HA3::TRP, tetR-GFP:LEU2, TetOx200:URA3	this study
1141	MATa, Scc1myc18::HIS3, Gal-Scc1(S497A)-HA3::TRP, tetR-GFP:LEU2, TetOx200:URA3	this study
1142	MATa, Scc1myc18::HIS3, Gal-Scc1(S183A,S273A,S276A,S325A)-HA3::TRP, tetR-GFP:LEU2, TetOx200:URA3	this study
1143	MATa, Scc1myc18::HIS3, Gal-Scc1(S374,S389A)-HA3::TRP, tetR-GFP:LEU2, TetOx200:URA3	this study
1144	MATa, Scc1myc18::HIS3, Gal-Scc1(S374,S389A,S497A)-HA3::TRP, tetR-GFP:LEU2, TetOx200:URA3	this study
1145	MATa, Scc1myc18::HIS3, Gal-Scc1(S183A,374A,S389A)-HA3::TRP, tetR-GFP:LEU2, TetOx200:URA3	this study

1146	MATa, Scc1myc18::HIS3, Gal-Scc1(S183A,374A,S389A,S497A)-HA3::TRP, tetR-GFP:LEU2, TetOx200:URA3	this study
1147	MATa, Scc1myc18::HIS3, Gal-Scc1(S273A,S276A,S374A,S389A)-HA3::TRP, tetR-GFP:LEU2, TetOx200:URA3	this study
1148	MATa, Scc1myc18::HIS3, Gal-Scc1(S273A,S276A,S374A, S389A,S497A)-HA3::TRP, tetR-GFP:LEU2, TetOx200:URA3	this study
1149	MATa, Scc1myc18::HIS3, Gal-Scc1(S183A,S273A,S276A, S325A,S374A,S389A)-HA3::TRP, tetR-GFP:LEU2, TetOx200:URA3	this study
1150	MATa, Scc1myc18::HIS3, Gal-Scc1(S183A,S273A,S276A, S325A,S374A,S389A)-HA3::TRP, tetR-GFP:LEU2, TetOx200:URA3	this study
1151	MATa, Scc1myc18::HIS3, Gal-Scc1(S183A,S273A,S276A, S325A,S374A,S389A,S497A)-HA3::TRP, tetR-GFP:LEU2, TetOx200:URA3	this study
1186	MATa, Scc1myc18::HIS3, tetR-GFP:LEU2, TetOx200:URA3, Scc1promoterScc1-HA3 ::TRP	this study
1187	MATa, Scc1myc18::HIS3, tetR-GFP:LEU2, TetOx200:URA3, Scc1promoterScc1(S183A)-HA3 ::TRP	this study
1188	MATa, Scc1myc18::HIS3, tetR-GFP:LEU2, TetOx200:URA3, Scc1promoterScc1(S194A)-HA3 ::TRP	this study
1189	MATa, Scc1myc18::HIS3, tetR-GFP:LEU2, TetOx200:URA3, Scc1promoterScc1(S273A,S276A)-HA3 ::TRP	this study
1190	MATa, Scc1myc18::HIS3, tetR-GFP:LEU2, TetOx200:URA3, Scc1promoterScc1(S325A)-HA3 ::TRP	this study
1191	MATa, Scc1myc18::HIS3, tetR-GFP:LEU2, TetOx200:URA3, Scc1promoterScc1(S374A)-HA3 ::TRP	this study
1192	MATa, Scc1myc18::HIS3, tetR-GFP:LEU2, TetOx200:URA3, Scc1promoterScc1(S389A)-HA3 ::TRP	this study
1193	MATa, Scc1myc18::HIS3, tetR-GFP:LEU2, TetOx200:URA3, Scc1promoterScc1(S497A)-HA3 ::TRP	this study
1215	MATa, ade2-1, can1-100, leu2-3,112, psi+, Esp1-myc18::URA3, GAL1-CDC20::TRP, Scc1-HA6::HIS	this study
1216	MATa, Scc1myc18::HIS3, Gal-Scc1(S183A,S194A,S263A, S273A,S276A,S325A,S374A,S389A)-HA3::TRP, tetR-GFP:LEU2, TetOx200:URA3	this study
1217	MATa, Scc1myc18::HIS3, Gal-Scc1(S175A,S183A,S194A, S263A,S273A,S276A,S325A,S374A,S389A)-HA3::TRP, tetR-GFP:LEU2, TetOx200:URA3	this study

1218	MATa, Scc1myc18::HIS3, GalScc1(S175A,S183A,S194A, S263A,S273A,S276A,S325A,S374A,S389A, S497A)-HA3::TRP, tetR-GFP:LEU2, TetOx200:URA3	this study
1243	MATa, ade2-1, trp1-1, can1-100, his3-11,15, GAL, psi+, Esp1-myc18::URA3, Esp1promoter-Esp1-HA6::LEU	this study
1244	MATa, ade2-1, trp1-1, can1-100, leu2-3, Esp1-HA6::HIS, ura3, GAL, psi+	this study
1287	MATa, ade2-1, can1-100, leu2-3,112, his3-11,15, GAL, psi+, bar-, Scc1promoter-Scc1-HA3::TRP,GAL-SCC1myc18, scc1::URA3	this study
1288	MATa, ade2-1, can1-100, leu2-3,112, his3-11,15, GAL, psi+, bar-, Scc1promoter-Scc1(S175A,S183A, A194A,S263A, S273A,S276A,S325A,S374A,S389A,S497A)-HA3::TRP, GAL-SCC1myc18, scc1::URA3	this study
1295	MATa, ura3-52, lys2-801, ade2-101, CAN+, his3Δ200, leu2Δ1, CFIII (CEN3.L.YPH278) URA3SUP11, Scc1promoter-SCC1-HA3::TRP	this study
1296	MATa, ade2-1, can1-100, trp1-1, his3-11,15, GAL, psi+, bar-, Scc1promoter-Scc1(S175A,S263A)-HA3::LEU, GAL-SCC1myc18, scc1::URA3	this study
1297	MATa, ura3-52, lys2-801, ade2-101, CAN+, his3Δ200, leu2Δ1, CFIII (CEN3.L.YPH278) URA3SUP11, Scc1promoter SCC1(S175A,S183A,A194A,S263A,S273A, S276A, S325A,S374A,S389A,S497A)-HA3::TRP	this study
1306	MATa, ura3-52, lys2-801, ade2-101, CAN+, his3Δ200, leu2Δ1, CFIII (CEN3.L.YPH278) URA3SUP11, Scc1promoter-SCC1(S175A,S183A,A194A,S263A,S273A, S276A, S325A, S374A,S389A,S497A)-HA3::TRP, ΔScc1::HIS	this study
1316	MATa, ade2-1, ura3, can1-100, leu2-3, his3-11,15, GAL, psi+, Esp1-myc18::TRP	this study
1444	MATa, ade2-1, can1-100, his3-11,15, Pds1-myc18::URA, GAL-CDC20::TRP, Scc1promoterScc1(S175A,S263A)-HA3 (LEU2), psi+	this study
1445	MATa, ade2-1, can1-100, Pds1-myc18::URA, GAL-CDC20::TRP, Scc1promoterScc1(S175A,S263A)-HA3 (LEU2),scc1::HIS, psi+	this study
1446	MATa, ade2-1, can1-100, his3-11,15, Pds1-myc18::URA, GAL-CDC20::LEU, Scc1promoterScc1-HA3 (TRP), psi+	this study
1447	MATa, ade2-1, can1-100, Pds1-myc18::URA, GAL-CDC20::LEU, Scc1promoterScc1-HA3 (TRP), scc1::HIS, psi+	this study

1448	MATa, ade2-1, can1-100, his3-11,15, Pds1-myc18::URA, GAL-CDC20::LEU, Scc1promoter-SCC1(S175A,S183A,A194A,S263A,S273A,S276A,S325A, S374A,S389A,S497A)-HA3 (TRP1), psi+	this study
1449	MATa, ade2-1, can1-100, Pds1-myc18::URA, GAL-CDC20::LEU, Scc1promoter-SCC1(S175A,S183A, S194A,S263A,S273A,S276A,S325A,S374A,S389A,S497A)-HA3::TRP1, scc1::HIS, psi+	this study
1540	MATa, SCC1-HA6::HIS3, Gal-Cdc5::URA	this study
1569	MATa, ade2-1, can1-100, leu2-3, his3-11,15, ura3, GAL, psi+, Scc1-HA3::TRP	this study
1570	MATa, SCC1-HA6::HIS3, CDC5-myc18::URA	this study
1571	MATa, ade2-1, trp1-1, can1-100, leu2-3,112, GAL, psi+, bar-, GAL-SCC1myc18, scc1::URA3, CDC5 HA6::HIS	this study
1572	MATalpha,ade2-1,can1-100,leu2-3,112,his3-11,15,ura3,GAL,psi+, Scc1promoter-SCC1(S175A,S183A,A194A,S263A,S273A,S276A,S325A,S374A,S389A,S497A)-HA3::TRP1	this study
1576	MATalpha,ade2-1,can1-100,leu2-3,112,ura3,GAL,psi+, Scc1promoter-SCC1(S175A,S183A,A194A,S263A,S273A, S276A,S325A,S374A,S389A,S497A)-HA3::TRP1, ΔScc1::HIS	this study
1585	MATa, ade2-1, can1-100, leu2-3,112, his3-11,15, GAL, psi+, Scc1-HA3::TRP, GAL-CDC5::URA	this study
1633	MATa, Scc1myc18::HIS3, Scc1promoterScc1(S183A,S194A,S273A,S276A,S325A)-HA3::TRP, tetR-GFP:LEU2, TetOx200:URA3	this study
1634	MATa, Scc1myc18::HIS3, Scc1promoterScc1(S374A,S389A,S497A)-HA3::TRP, tetR-GFP:LEU2, TetOx200:URA3	this study
1635	MATa, Scc1myc18::HIS3, Scc1promoterScc1(S183A,S194A,S273A,S276A,S325A,S374A,S389A,S497A)-HA3::TRP, tetR-GFP:LEU2, TetOx200:URA3	this study

5.8 Plasmids

Name	Description	Derivation
1	YIplac128 LEU2 based integrative vector (see Gietz and Sugino 1988, Gene 74, p. 527)	Gietz and Sugino
2	YIplac204 TRP1 based integrative vector	Gietz and

	(see Gietz and Sugino 1988, Gene 74, p. 527)	Sugino
3	YIplac211 URA3 based integrative vector (see Gietz and Sugino 1988, Gene 74, p. 527)	Gietz and Sugino
9	pRS303 HIS3 based integrative vector (see Sikorski and Hieter 1989, Genetics 122, p. 19)	Sikorski and Hieter
13	YIp128GAL GAL1-10 promoter between EcoRI and BamHI of YIp128 (towards BamHI is the GAL1 side; both EcoRI and BamHI are still available)	Frank Uhlmann
14	YIp204GAL GAL1-10 promoter between EcoRI and BamHI of YIp204 (towards BamHI is the GAL1 side; both EcoRI and BamHI are still available)	Frank Uhlmann
15	YIp211GAL GAL1-10 promoter between EcoRI and BamHI of YIp211 (towards BamHI is the GAL1 side; both EcoRI and BamHI are still available)	Frank Uhlmann
17	pGEX-KG cloning vector for bacterial expression, adding a GST-tag plus a glycine linker and thrombin site	Neil McDonald
22	pFastBac1 Baculovirus transfer cloning vector	GIBCO
29	pTYB2 Bacterial expression vector, introducing an Intein-Chitin binding domain tag.	New England Biolabs
33	myc9-KITRP1 in pUC19 for one step tagging	Wolfgang Zachariae
34	myc18-KITRP1 in pUC19 for one step tagging	Wolfgang Zachariae
35	HA3-KITRP1 in pUC19 for one step tagging	Wolfgang Zachariae
36	HA6-SpHIS5 in pUC19 for one step tagging (SpHIS5 complements ScHIS3)	Gustav Ammerer
37	HA3-SpHIS5 in pUC19 for one step tagging (SpHIS5 complements ScHIS3)	Wolfgang Zachariae
38	myc18-SpHIS5 in pUC19 for one step tagging (SpHIS5 complements ScHIS3)	Wolfgang Zachariae
39	myc18-KIURA3 in pUC19 for one step tagging derived from 34: TRP1 cut out with BglII + StuI and replaced by K. lactis URA3 as a BglII, StuI PCR fragment	Frank Uhlmann
40	HA3-KIURA3 in pUC19 for one step tagging derived from 35: TRP1 cut out with BglII + StuI and replaced by K. lactis URA3 as a BglII, StuI PCR fragment	Frank Uhlmann
68	YIp204 GAL-SCC1myc9 (TRP1) Spe1 myc9 cassette in 67	Frank Uhlmann
69	YIp128 GAL-SCC1-NotI (LEU2) XbaI-SphI PCR fragment of entire Scc1 with NotI before Stop in 13. XbaI in frame with start (TCT AGA ATG ...), NotI before Stop is (.GC GGC CGC TAA).	Frank Uhlmann
70	YIp128 GAL-SCC1-HA3 (LEU2) NotI HA3 cassette in 69 cut with EcoRV for integration at LEU2	Frank Uhlmann

86	Yip128 Scc1promoterScc1-HA3 (LEU2) EcoRI-XbaI promoter fragment from 77 and XbaI-SphI Scc1-HA3 fragment from 70 in Yip128	Frank Uhlmann
90	Yip128 Scc1promoterScc1(S175A,S263A)-HA3 (LEU2) S175A,S263A mutations in 86	Frank Uhlmann
91	Yip204 GAL-SCC1-HA3 (TRP1) XbaI-SphI fragment containing Scc1-HA3 from 70 into 14	Frank Uhlmann
94	Yip204 GAL-SCC1(S175A,S263A)-HA3 (TRP1) S175A,S263A double mutation in 91	Frank Uhlmann
98	pFastBac Scc1-FLAG-InteinCBD XbaI-XhoI fragment of 76 cloned into SpeI-XhoI of pFB1 (22)	Frank Uhlmann
135	Yip204 GAL-ESP1-Flag C-terminal Flag tag by linker insertion into the BstEII site close to the end of ESP1 in 133	Frank Uhlmann
136	Yip204 GAL-Flag-ESP1-XhoI XhoI site introduced into ESPI before Stop by linker insertion into the BstEII site close to the end of ESP1 in 134	Frank Uhlmann
140	Yip204 GAL-Flag-ESP1-CBD CBD amplified from pTYB2 (29) without the intein. XhoI introduced 5' of CBD and SalI after Stop. Placed into XhoI in 136. Linearise with BstXI for integration at TRP1	Frank Uhlmann
141	Yip204 GAL-Flag-ESP1-CBD CBD amplified from pTYB2 (29) without the intein. XhoI introduced 5' of CBD and SalI after Stop. Placed into XhoI in 136. (two amino acids in the linker between Esp1 and the CBD changed through PCR mutation. Fully functional.)	Frank Uhlmann
142	Yip204 GAL-Flag-ESP1(H1505A)-CBD H1505A mutation in 141, by exchanging a NcoI (ESP1), XhoI (end of ESP1) fragment.	Frank Uhlmann
143	Yip204 GAL-Flag-ESP1(C1531A)-CBD C1531A mutation in 141, by exchanging a NcoI (ESP1), XhoI (end of ESP1) fragment.	Frank Uhlmann
193	Yip204GAL-Flag-ESP1(1391-1630)-CBD Xba/Xho1	This study
194	Yip204GAL-Flag-ESP1(1196-1630)-CBD Xba/Xho1	This study
197	Yip204GAL-Flag-ESP1(156-1630)-CBD Xba/Xho1	This study
220	Yiplac211 (URA3 based integrative vector), Crm1 (PvuII cut) is cloned into the PvuII site of this vector	This study
233	Yip128 GAL-Flag-ESP1(1-370), XbaI-flag-ESP1-Xho1-TAA-HindIII	This study
234	Yip128 GAL-Flag-ESP1(1-175), XbaI-flag-ESP1-Xho1-TAA-HindIII	This study
243	Yip204,GAL-Flag-ESP1-HA6	This study

	HA6 cloned in Xho1 site of 136	
244	YIp204 GAL-Flag-ESP1 (K809N)(K810N)(K811N)-HA6NLS mutated and XhoI site used to put in HA6-tag	This study
311	YIp128 GAL-Flag-ESP1(156-1195), XbaI-flag-ESP1-TAA-HindIII	This study
330	YIp204 GAL-Flag-ESP1(L163A,L166A,L169A)-CBD putative NES mutation that is proteolytically inactive, but did not lead to nuclear accumulation	This study
331	YIp204 GAL-Flag-ESP1(K526A,E529A,S531A)-CBD	This study
332	YIp204 GAL-Flag-ESP1(S1144A,E1148A,R1151A)-CBD	This study
387	YIp204 Scc1promoterScc1-HA3 (TRP) EcoRI-XbaI promoter fragment and XbaI-SphI Scc1-HA3 fragment from 86 in YIp204	This study
404	YIp204 Scc1promoterScc1(S183A)-NotI-STOP (TRP)	This study
405	YIp204 Scc1promoterScc1(S194A)-NotI-STOP (TRP)	This study
406	YIp204 Scc1promoterScc1(S273A,S276A)-NotI-STOP (TRP)	This study
407	YIp204 Scc1promoterScc1(S325A)-NotI-STOP (TRP)	This study
408	YIp204 Scc1promoterScc1(S183A,S194A,S273A,S276A,S325A) -HA3-STOP (TRP)	This study
409	YIp204 Scc1promoterScc1(S389A)-NotI-STOP (TRP)	This study
410	YIp204 Scc1promoterScc1(S497A)-NotI-STOP (TRP)	This study
411	YIp204 Scc1promoterScc1(S183A)-HA3-STOP (TRP) HA3 casette into NotI of 404	This study
412	YIp204 Scc1promoterScc1(S194A)-HA3-STOP (TRP) HA3-casette into NotI of 405	This study
413	YIp204 Scc1promoterScc1(S273A,S276A)-HA3-STOP (TRP) HA3-casette into NotI of 406	This study
414	YIp204 Scc1promoterScc1(S325A)-HA3-STOP (TRP) HA3-casette into NotI of 407	This study
415	YIp204 Scc1promoterScc1(S374A)-HA3-STOP (TRP) HA3-casette into NotI of 408	This study
416	YIp204 Scc1promoterScc1(S389A)-HA3-STOP (TRP) HA3-casette into NotI of 409	This study
417	YIp204 Scc1promoterScc1(S497A)-HA3-STOP (TRP)	This study

	HA3-casette into NotI of 410	
418	YIp204 GAL-SCC1(S183A)-HA3 (TRP1) HindIII fragment from 411 into 67	This study
419	YIp204 GAL-SCC1(S194A)-HA3 (TRP1) HindIII fragment from 412 into 67	This study
420	YIp204 GAL-SCC1(S273A,S276A)-HA3 (TRP1) HindIII fragment from 413 into 67	This study
421	YIp204 GAL-SCC1(S325A)-HA3 (TRP1) HindIII fragment from 414 into 67	This study
422	YIp204 GAL-SCC1(S374A)-HA3 (TRP1) HindIII fragment from 415 into 67	This study
423	YIp204 GAL-SCC1(S389A)-HA3 (TRP1) HindIII fragment from 416 into 67	This study
424	YIp204 GAL-SCC1(S497A)-HA3 (TRP1) HindIII fragment from 417 into 67	This study
463	YIp204 GAL-SCC1(S183A,S273A,S276A,S325A)-HA3 (TRP1)	This study
464	YIp204 GAL-SCC1(S374A,S389A)-HA3 (TRP1)	This study
465	YIp204 GAL-SCC1(S374A,S389A,S497A)-HA3 (TRP1)	This study
467	YIp204 GAL-SCC1(S183A,S374A,S389A)-HA3 (TRP1)	This study
468	YIp204 GAL-SCC1(S183A,S374A,S389A,S497A)-HA3 (TRP1)	This study
469	YIp204 GAL-SCC1(S273A,S276A,S374A,S389A)-HA3 (TRP1)	This study
471	YIp204 GAL-SCC1(S183A,S273A,S276A,S325A,S374A,S389A)-HA3 (TRP1)	This study
472	YIp204 GAL-SCC1(S183A,S273A,S276A,S325A,S374A,S389A,S497A)-HA3 (TRP1)	This study
485	YIp204 GAL-SCC1(S175A,S183A,S273A,S276A,S325A,S374A,S389A,S497A)-HA3 (TRP1) Acc1 fragment from 94(S175A) into 472	This study
487	YIp204 GAL-	This study

	SCC1(S183A,S194A,S273A,S276A,S325A)-HA3 (TRP1)	
488	YIp204 GAL-SCC1(S175A,S183A,S194A,S273A,S276A,S325A)-HA3 (TRP1)	This study
489	YIp204 GAL-SCC1(S183A,S194A,S273A,S276A,S325A,S374A,S389A)-HA3 (TRP1)	This study
490	YIp204 GAL-SCC1(S175A,S183A,S194A,S273A,S276A,S325A,S374A,S389A)-HA3 (TRP1)	This study
491	YIp204 Scc1promoterScc1(S374A,S389A,S497A)-HA3 (TRP1)	This study
492	YIp204 Scc1promoterScc1(S183A,S194A,S273A,S276A,S325A,S374A,S389A,S497A)-HA3 (TRP1)	This study
493	YIp128 GAL-SCC1(S175A,S183A,A194A,S263A,S273A,S276A,S325A,S374A,S389A,S497A)-HA3 (LEU) Xba/Sph1 fragment form 505 into 70	This study
496	YIp204 GAL-SCC1(S183A,S194A,S263A,S273A,S276A,S325A,S374A,S389A)-HA3 (TRP1)	This study
502	YIp204 GAL-SCC1(S175A,S183A,S194A,S263A,S273A,S276A,S325A,S374A,S389A)-HA3 (TRP1)	This study
505	YIp204 GAL-SCC1(S175A,S183A,A194A,S263A,S273A,S276A,S325A,S374A,S389A,S497A)-HA3 (TRP1)	This study
509	YIplac128-Esp1promoter-ESP1-HA6 (wt) 430 was Xho1 cut and the proteinA-tag was replaced by the HA-tag of 243	This study
524	YIp204 Scc1promoter-SCC1(S175A,S183A,S194A,S263A,S273A,S276A,S325A,S374A,S389A)-HA3 (TRP1) HindIII fragment from 502 into 387	This study
525	YIp204 Scc1promoter-SCC1(S175A,S183A,A194A,S263A,S273A,S276A,S325A,S374A,S389A,S497A)-HA3 (TRP1) HindIII-fragment from 505 into387	This study

Bibliography

1. Masui, Y. and C.L. Markert, *Cytoplasmic control of nuclear behavior during meiotic maturation of frog oocytes.* J Exp Zool, 1971. **177**(2): p. 129-45.
2. Evans, T., et al., *Cyclin: a protein specified by maternal mRNA in sea urchin eggs that is destroyed at each cleavage division.* Cell, 1983. **33**(2): p. 389-96.
3. Nurse, P., P. Thuriaux, and K. Nasmyth, *Genetic control of the cell division cycle in the fission yeast Schizosaccharomyces pombe.* Mol Gen Genet, 1976. **146**(2): p. 167-78.
4. Hartwell, L.H., et al., *Genetic control of the cell division cycle in yeast.* Science, 1974. **183**(120): p. 46-51.
5. Mendenhall, M.D. and A.E. Hodge, *Regulation of Cdc28 cyclin-dependent protein kinase activity during the cell cycle of the yeast Saccharomyces cerevisiae.* Microbiol Mol Biol Rev, 1998. **62**(4): p. 1191-243.
6. Gautier, J., et al., *cdc25 is a specific tyrosine phosphatase that directly activates p34cdc2.* Cell, 1991. **67**(1): p. 197-211.
7. Russell, P. and P. Nurse, *Negative regulation of mitosis by wee1+, a gene encoding a protein kinase homolog.* Cell, 1987. **49**(4): p. 559-67.
8. King, R.W., et al., *How proteolysis drives the cell cycle.* Science, 1996. **274**(5293): p. 1652-9.
9. Hoyt, M.A., *Eliminating all obstacles: regulated proteolysis in the eukaryotic cell cycle.* Cell, 1997. **91**(2): p. 149-51.
10. Townsley, F.M. and J.V. Ruderman, *Proteolytic ratchets that control progression through mitosis.* Trends Cell Biol, 1998. **8**(6): p. 238-44.
11. Peters, J.M., *SCF and APC: the Yin and Yang of cell cycle regulated proteolysis.* Curr Opin Cell Biol, 1998. **10**(6): p. 759-68.
12. Hochstrasser, M., *Ubiquitin-dependent protein degradation.* Annu Rev Genet, 1996. **30**: p. 405-39.
13. Glotzer, M., A.W. Murray, and M.W. Kirschner, *Cyclin is degraded by the ubiquitin pathway.* Nature, 1991. **349**(6305): p. 132-8.

14. Visintin, R., S. Prinz, and A. Amon, *CDC20 and CDH1: a family of substrate-specific activators of APC-dependent proteolysis.* Science, 1997. **278**(5337): p. 460-3.
15. Schwab, M., A.S. Lutum, and W. Seufert, *Yeast Hct1 is a regulator of Clb2 cyclin proteolysis.* Cell, 1997. **90**(4): p. 683-93.
16. Lim, H.H., P.Y. Goh, and U. Surana, *Cdc20 is essential for the cyclosome-mediated proteolysis of both Pds1 and Clb2 during M phase in budding yeast.* Curr Biol, 1998. **8**(4): p. 231-4.
17. Shirayama, M., et al., *The Polo-like kinase Cdc5p and the WD-repeat protein Cdc20p/fizzy are regulators and substrates of the anaphase promoting complex in Saccharomyces cerevisiae.* Embo J, 1998. **17**(5): p. 1336-49.
18. Jaspersen, S.L., J.F. Charles, and D.O. Morgan, *Inhibitory phosphorylation of the APC regulator Hct1 is controlled by the kinase Cdc28 and the phosphatase Cdc14.* Curr Biol, 1999. **9**(5): p. 227-36.
19. Moll, T., et al., *The role of phosphorylation and the CDC28 protein kinase in cell cycle-regulated nuclear import of the S. cerevisiae transcription factor SWI5.* Cell, 1991. **66**(4): p. 743-58.
20. Toyn, J.H., et al., *The Swi5 transcription factor of Saccharomyces cerevisiae has a role in exit from mitosis through induction of the cdk-inhibitor Sic1 in telophase.* Genetics, 1997. **145**(1): p. 85-96.
21. Verma, R., et al., *Phosphorylation of Sic1p by G1 Cdk required for its degradation and entry into S phase.* Science, 1997. **278**(5337): p. 455-60.
22. Visintin, R., et al., *The phosphatase Cdc14 triggers mitotic exit by reversal of Cdk-dependent phosphorylation.* Mol Cell, 1998. **2**(6): p. 709-18.
23. Nigg, E.A., *Polo-like kinases: positive regulators of cell division from start to finish.* Curr Opin Cell Biol, 1998. **10**(6): p. 776-83.
24. Carmena, M., et al., *Drosophila polo kinase is required for cytokinesis.* J Cell Biol, 1998. **143**(3): p. 659-71.
25. Ohkura, H., I.M. Hagan, and D.M. Glover, *The conserved Schizosaccharomyces pombe kinase plo1, required to form a bipolar*

spindle, the actin ring, and septum, can drive septum formation in G1 and G2 cells. Genes Dev, 1995. **9**(9): p. 1059-73.

26. Cohen-Fix, O., et al., *Anaphase initiation in Saccharomyces cerevisiae is controlled by the APC-dependent degradation of the anaphase inhibitor Pds1p.* Genes Dev, 1996. **10**(24): p. 3081-93.
27. Alexandru, G., et al., *Sister chromatid separation and chromosome re-duplication are regulated by different mechanisms in response to spindle damage.* Embo J, 1999. **18**(10): p. 2707-21.
28. Yamamoto, A., V. Guacci, and D. Koshland, *Pds1p is required for faithful execution of anaphase in the yeast, Saccharomyces cerevisiae.* J Cell Biol, 1996. **133**(1): p. 85-97.
29. Yamamoto, A., V. Guacci, and D. Koshland, *Pds1p, an inhibitor of anaphase in budding yeast, plays a critical role in the APC and checkpoint pathway(s).* J Cell Biol, 1996. **133**(1): p. 99-110.
30. Funabiki, H., K. Kumada, and M. Yanagida, *Fission yeast Cut1 and Cut2 are essential for sister chromatid separation, concentrate along the metaphase spindle and form large complexes.* Embo J, 1996. **15**(23): p. 6617-28.
31. Ciosk, R., et al., *An ESP1/PDS1 complex regulates loss of sister chromatid cohesion at the metaphase to anaphase transition in yeast.* Cell, 1998. **93**(6): p. 1067-76.
32. Funabiki, H., et al., *Cut2 proteolysis required for sister-chromatid seperation in fission yeast.* Nature, 1996. **381**(6581): p. 438-41.
33. Zou, H., et al., *Identification of a vertebrate sister-chromatid separation inhibitor involved in transformation and tumorigenesis.* Science, 1999. **285**(5426): p. 418-22.
34. Jensen, S., et al., *A novel role of the budding yeast separin Esp1 in anaphase spindle elongation: evidence that proper spindle association of Esp1 is regulated by Pds1.* J Cell Biol, 2001. **152**(1): p. 27-40.
35. Uhlmann, F., et al., *Cleavage of cohesin by the CD clan protease separin triggers anaphase in yeast.* Cell, 2000. **103**(3): p. 375-86.
36. Hauf, S., I.C. Waizenegger, and J.M. Peters, *Cohesin cleavage by separase required for anaphase and cytokinesis in human cells.* Science, 2001. **293**(5533): p. 1320-3.

37. Stemmann, O., et al., *Dual inhibition of sister chromatid separation at metaphase.* Cell, 2001. **107**(6): p. 715-26.
38. Uhlmann, F., F. Lottspeich, and K. Nasmyth, *Sister-chromatid separation at anaphase onset is promoted by cleavage of the cohesin subunit Scc1.* Nature, 1999. **400**(6739): p. 37-42.
39. Jager, H., et al., *Drosophila separase is required for sister chromatid separation and binds to PIM and THR.* Genes Dev, 2001. **15**(19): p. 2572-84.
40. Kumada, K., et al., *Cut1 is loaded onto the spindle by binding to Cut2 and promotes anaphase spindle movement upon Cut2 proteolysis.* Curr Biol, 1998. **8**(11): p. 633-41.
41. Hornig, N.C., et al., *The dual mechanism of separase regulation by securin.* Curr Biol, 2002. **12**(12): p. 973-82.
42. Agarwal, R. and O. Cohen-Fix, *Phosphorylation of the mitotic regulator Pds1/securin by Cdc28 is required for efficient nuclear localization of Esp1/separase.* Genes Dev, 2002. **16**(11): p. 1371-82.
43. McGrew, J.T., et al., *Requirement for ESP1 in the nuclear division of Saccharomyces cerevisiae.* Mol Biol Cell, 1992. **3**(12): p. 1443-54.
44. Uzawa, S., et al., *The fission yeast cut1+ gene regulates spindle pole body duplication and has homology to the budding yeast ESP1 gene.* Cell, 1990. **62**(5): p. 913-25.
45. Baum, P., et al., *A yeast gene essential for regulation of spindle pole duplication.* Mol Cell Biol, 1988. **8**(12): p. 5386-97.
46. Jager, H., et al., *Structure predictions and interaction studies indicate homology of separase N-terminal regulatory domains and Drosophila THR.* Cell Cycle, 2004. **3**(2): p. 182-8.
47. Herzig, A., C.F. Lehner, and S. Heidmann, *Proteolytic cleavage of the THR subunit during anaphase limits Drosophila separase function.* Genes Dev, 2002. **16**(18): p. 2443-54.
48. Haering, C.H., et al., *Molecular architecture of SMC proteins and the yeast cohesin complex.* Mol Cell, 2002. **9**(4): p. 773-88.
49. Hirano, T., *Chromosome cohesion, condensation, and separation.* Annu Rev Biochem, 2000. **69**: p. 115-44.

50. Ciosk, R., et al., *Cohesin's binding to chromosomes depends on a separate complex consisting of Scc2 and Scc4 proteins.* Mol Cell, 2000. **5**(2): p. 243-54.
51. Sumara, I., et al., *Characterization of vertebrate cohesin complexes and their regulation in prophase.* J Cell Biol, 2000. **151**(4): p. 749-62.
52. Weitzer, S., C. Lehane, and F. Uhlmann, *A model for ATP hydrolysis-dependent binding of cohesin to DNA.* Curr Biol, 2003. **13**(22): p. 1930-40.
53. Arumugam, P., et al., *ATP hydrolysis is required for cohesin's association with chromosomes.* Curr Biol, 2003. **13**(22): p. 1941-53.
54. Buonomo, S.B., et al., *Disjunction of homologous chromosomes in meiosis I depends on proteolytic cleavage of the meiotic cohesin Rec8 by separin.* Cell, 2000. **103**(3): p. 387-98.
55. Kerrebrock, A.W., et al., *Mei-S332, a Drosophila protein required for sister-chromatid cohesion, can localize to meiotic centromere regions.* Cell, 1995. **83**(2): p. 247-56.
56. Moore, D.P., et al., *The cohesion protein MEI-S332 localizes to condensed meiotic and mitotic centromeres until sister chromatids separate.* J Cell Biol, 1998. **140**(5): p. 1003-12.
57. Goldstein, L.S., *Mechanisms of chromosome orientation revealed by two meiotic mutants in Drosophila melanogaster.* Chromosoma, 1980. **78**(1): p. 79-111.
58. Davis, B.K., *Genetic analysis of a meiotic mutant resulting in precocious sister-centromere separation in Drosophila melanogaster.* Mol Gen Genet, 1971. **113**(3): p. 251-72.
59. Kitajima, T.S., S.A. Kawashima, and Y. Watanabe, *The conserved kinetochore protein shugoshin protects centromeric cohesion during meiosis.* Nature, 2004. **427**(6974): p. 510-7.
60. Rabitsch, K.P., et al., *Two fission yeast homologs of Drosophila Mei-S332 are required for chromosome segregation during meiosis I and II.* Curr Biol, 2004. **14**(4): p. 287-301.
61. Marston, A.L., et al., *A genome-wide screen identifies genes required for centromeric cohesion.* Science, 2004. **303**(5662): p. 1367-70.

62. Kerrebrock, A.W., et al., *The Drosophila mei-S332 gene promotes sister-chromatid cohesion in meiosis following kinetochore differentiation.* Genetics, 1992. **130**(4): p. 827-41.
63. Tang, T.T., et al., *Maintenance of sister-chromatid cohesion at the centromere by the Drosophila MEI-S332 protein.* Genes Dev, 1998. **12**(24): p. 3843-56.
64. Sullivan, M., C. Lehane, and F. Uhlmann, *Orchestrating anaphase and mitotic exit: separase cleavage and localization of Slk19.* Nat Cell Biol, 2001. **3**(9): p. 771-7.
65. Varshavsky, A., *The N-end rule: functions, mysteries, uses.* Proc Natl Acad Sci U S A, 1996. **93**(22): p. 12142-9.
66. Rao, H., et al., *Degradation of a cohesin subunit by the N-end rule pathway is essential for chromosome stability.* Nature, 2001. **410**(6831): p. 955-9.
67. Bachmair, A., D. Finley, and A. Varshavsky, *In vivo half-life of a protein is a function of its amino-terminal residue.* Science, 1986. **234**(4773): p. 179-86.
68. Winey, M., et al., *Three-dimensional ultrastructural analysis of the Saccharomyces cerevisiae mitotic spindle.* J Cell Biol, 1995. **129**(6): p. 1601-15.
69. Waizenegger, I., et al., *Regulation of human separase by securin binding and autocleavage.* Curr Biol, 2002. **12**(16): p. 1368-78.
70. Zou, H., et al., *Anaphase specific auto-cleavage of separase.* FEBS Lett, 2002. **528**(1-3): p. 246-50.
71. Tomonaga, T., et al., *Characterization of fission yeast cohesin: essential anaphase proteolysis of Rad21 phosphorylated in the S phase.* Genes Dev, 2000. **14**(21): p. 2757-70.
72. Sullivan, M., et al., *Studies on substrate recognition by the budding yeast separase.* J Biol Chem, 2004. **279**(2): p. 1191-6.
73. Tanaka, T.U., et al., *Evidence that the Ipl1-Sli15 (Aurora kinase-INCENP) complex promotes chromosome bi-orientation by altering kinetochore-spindle pole connections.* Cell, 2002. **108**(3): p. 317-29.

74. Tanaka, T., et al., *Cohesin ensures bipolar attachment of microtubules to sister centromeres and resists their precocious separation.* Nat Cell Biol, 2000. **2**(8): p. 492-9.
75. Adams, R.R., et al., *Essential roles of Drosophila inner centromere protein (INCENP) and aurora B in histone H3 phosphorylation, metaphase chromosome alignment, kinetochore disjunction, and chromosome segregation.* J Cell Biol, 2001. **153**(4): p. 865-80.
76. Kallio, M.J., et al., *Inhibition of aurora B kinase blocks chromosome segregation, overrides the spindle checkpoint, and perturbs microtubule dynamics in mitosis.* Curr Biol, 2002. **12**(11): p. 900-5.
77. Murata-Hori, M. and Y.L. Wang, *The kinase activity of aurora B is required for kinetochore-microtubule interactions during mitosis.* Curr Biol, 2002. **12**(11): p. 894-9.
78. Fraschini, R., et al., *Bub3 interaction with Mad2, Mad3 and Cdc20 is mediated by WD40 repeats and does not require intact kinetochores.* Embo J, 2001. **20**(23): p. 6648-59.
79. Wassmann, K. and R. Benezra, *Mitotic checkpoints: from yeast to cancer.* Curr Opin Genet Dev, 2001. **11**(1): p. 83-90.
80. Charles, J.F., et al., *The Polo-related kinase Cdc5 activates and is destroyed by the mitotic cyclin destruction machinery in S. cerevisiae.* Curr Biol, 1998. **8**(9): p. 497-507.
81. Sanchez, Y., et al., *Control of the DNA damage checkpoint by chk1 and rad53 protein kinases through distinct mechanisms.* Science, 1999. **286**(5442): p. 1166-71.
82. Liu, Q., et al., *Chk1 is an essential kinase that is regulated by Atr and required for the G(2)/M DNA damage checkpoint.* Genes Dev, 2000. **14**(12): p. 1448-59.
83. Gardner, R., C.W. Putnam, and T. Weinert, *RAD53, DUN1 and PDS1 define two parallel G2/M checkpoint pathways in budding yeast.* Embo J, 1999. **18**(11): p. 3173-85.
84. Bardin, A.J., R. Visintin, and A. Amon, *A mechanism for coupling exit from mitosis to partitioning of the nucleus.* Cell, 2000. **102**(1): p. 21-31.

85. McCollum, D. and K.L. Gould, *Timing is everything: regulation of mitotic exit and cytokinesis by the MEN and SIN.* Trends Cell Biol, 2001. **11**(2): p. 89-95.

86. Pereira, G., et al., *The Bub2p spindle checkpoint links nuclear migration with mitotic exit.* Mol Cell, 2000. **6**(1): p. 1-10.

87. Lee, S.E., et al., *Order of function of the budding-yeast mitotic exit-network proteins Tem1, Cdc15, Mob1, Dbf2, and Cdc5.* Curr Biol, 2001. **11**(10): p. 784-8.

88. Cheng, L., L. Hunke, and C.F. Hardy, *Cell cycle regulation of the Saccharomyces cerevisiae polo-like kinase cdc5p.* Mol Cell Biol, 1998. **18**(12): p. 7360-70.

89. Golsteyn, R.M., et al., *Cell cycle regulation of the activity and subcellular localization of Plk1, a human protein kinase implicated in mitotic spindle function.* J Cell Biol, 1995. **129**(6): p. 1617-28.

90. Herrmann, S., I. Amorim, and C.E. Sunkel, *The POLO kinase is required at multiple stages during spermatogenesis in Drosophila melanogaster.* Chromosoma, 1998. **107**(6-7): p. 440-51.

91. Arnaud, L., J. Pines, and E.A. Nigg, *GFP tagging reveals human Polo-like kinase 1 at the kinetochore/centromere region of mitotic chromosomes.* Chromosoma, 1998. **107**(6-7): p. 424-9.

92. Jaspersen, S.L. and D.O. Morgan, *Cdc14 activates cdc15 to promote mitotic exit in budding yeast.* Curr Biol, 2000. **10**(10): p. 615-8.

93. Bardin, A.J. and A. Amon, *Men and sin: what's the difference?* Nat Rev Mol Cell Biol, 2001. **2**(11): p. 815-26.

94. Asakawa, K., et al., *A novel functional domain of Cdc15 kinase is required for its interaction with Tem1 GTPase in Saccharomyces cerevisiae.* Genetics, 2001. **157**(4): p. 1437-50.

95. Mah, A.S., J. Jang, and R.J. Deshaies, *Protein kinase Cdc15 activates the Dbf2-Mob1 kinase complex.* Proc Natl Acad Sci U S A, 2001. **98**(13): p. 7325-30.

96. Shou, W., et al., *Exit from mitosis is triggered by Tem1-dependent release of the protein phosphatase Cdc14 from nucleolar RENT complex.* Cell, 1999. **97**(2): p. 233-44.

97. Visintin, R., E.S. Hwang, and A. Amon, *Cfi1 prevents premature exit from mitosis by anchoring Cdc14 phosphatase in the nucleolus.* Nature, 1999. **398**(6730): p. 818-23.

98. Visintin, R. and A. Amon, *Regulation of the mitotic exit protein kinases Cdc15 and Dbf2.* Mol Biol Cell, 2001. **12**(10): p. 2961-74.

99. Pereira, G., et al., *Regulation of the Bfa1p-Bub2p complex at spindle pole bodies by the cell cycle phosphatase Cdc14p.* J Cell Biol, 2002. **157**(3): p. 367-79.

100. Stegmeier, F., R. Visintin, and A. Amon, *Separase, polo kinase, the kinetochore protein Slk19, and Spo12 function in a network that controls Cdc14 localization during early anaphase.* Cell, 2002. **108**(2): p. 207-20.

101. Sullivan, M. and F. Uhlmann, *A non-proteolytic function of separase links the onset of anaphase to mitotic exit.* Nat Cell Biol, 2003. **5**(3): p. 249-54.

102. Alexandru, G., et al., *Phosphorylation of the cohesin subunit Scc1 by Polo/Cdc5 kinase regulates sister chromatid separation in yeast.* Cell, 2001. **105**(4): p. 459-72.

103. Jallepalli, P.V., et al., *Securin is required for chromosomal stability in human cells.* Cell, 2001. **105**(4): p. 445-57.

104. Mei, J., X. Huang, and P. Zhang, *Securin is not required for cellular viability, but is required for normal growth of mouse embryonic fibroblasts.* Curr Biol, 2001. **11**(15): p. 1197-201.

105. Wang, Z., R. Yu, and S. Melmed, *Mice lacking pituitary tumor transforming gene show testicular and splenic hypoplasia, thymic hyperplasia, thrombocytopenia, aberrant cell cycle progression, and premature centromere division.* Mol Endocrinol, 2001. **15**(11): p. 1870-9.

106. Waizenegger, I.C., et al., *Two distinct pathways remove mammalian cohesin from chromosome arms in prophase and from centromeres in anaphase.* Cell, 2000. **103**(3): p. 399-410.

107. Nasmyth, K., J.M. Peters, and F. Uhlmann, *Splitting the chromosome: cutting the ties that bind sister chromatids.* Science, 2000. **288**(5470): p. 1379-85.

108. Blat, Y. and N. Kleckner, *Cohesins bind to preferential sites along yeast chromosome III, with differential regulation along arms versus the centric region.* Cell, 1999. **98**(2): p. 249-59.

109. Laloraya, S., V. Guacci, and D. Koshland, *Chromosomal addresses of the cohesin component Mcd1p.* J Cell Biol, 2000. **151**(5): p. 1047-56.
110. Megee, P.C., et al., *The centromeric sister chromatid cohesion site directs Mcd1p binding to adjacent sequences.* Mol Cell, 1999. **4**(3): p. 445-50.
111. Tanaka, T., et al., *Identification of cohesin association sites at centromeres and along chromosome arms.* Cell, 1999. **98**(6): p. 847-58.
112. Bernard, P., et al., *Requirement of heterochromatin for cohesion at centromeres.* Science, 2001. **294**(5551): p. 2539-42.
113. Chai, B., et al., *Yeast RSC function is required for organization of the cellular cytoskeleton via an alternative PKC1 pathway.* Genetics, 2002. **161**(2): p. 575-84.
114. Cairns, B.R., et al., *Two actin-related proteins are shared functional components of the chromatin-remodeling complexes RSC and SWI/SNF.* Mol Cell, 1998. **2**(5): p. 639-51.
115. Huang, J., J.M. Hsu, and B.C. Laurent, *The RSC nucleosome-remodeling complex is required for Cohesin's association with chromosome arms.* Mol Cell, 2004. **13**(5): p. 739-50.
116. Bernard, P. and R. Allshire, *Centromeres become unstuck without heterochromatin.* Trends Cell Biol, 2002. **12**(9): p. 419-24.
117. Nonaka, N., et al., *Recruitment of cohesin to heterochromatic regions by Swi6/HP1 in fission yeast.* Nat Cell Biol, 2002. **4**(1): p. 89-93.
118. Losada, A., M. Hirano, and T. Hirano, *Identification of Xenopus SMC protein complexes required for sister chromatid cohesion.* Genes Dev, 1998. **12**(13): p. 1986-97.
119. Sumara, I., et al., *The dissociation of cohesin from chromosomes in prophase is regulated by Polo-like kinase.* Mol Cell, 2002. **9**(3): p. 515-25.
120. Warren, W.D., et al., *The Drosophila RAD21 cohesin persists at the centromere region in mitosis.* Curr Biol, 2000. **10**(22): p. 1463-6.
121. Klein, F., et al., *Localization of RAP1 and topoisomerase II in nuclei and meiotic chromosomes of yeast.* J Cell Biol, 1992. **117**(5): p. 935-48.

122. Tanaka, T., D. Knapp, and K. Nasmyth, *Loading of an Mcm protein onto DNA replication origins is regulated by Cdc6p and CDKs.* Cell, 1997. **90**(4): p. 649-60.

123. Fitch, I., et al., *Characterization of four B-type cyclin genes of the budding yeast Saccharomyces cerevisiae.* Mol Biol Cell, 1992. **3**(7): p. 805-18.

124. Stade, K., et al., *Exportin 1 (Crm1p) is an essential nuclear export factor.* Cell, 1997. **90**(6): p. 1041-50.

125. Losada, A., et al., *Identification and characterization of SA/Scc3p subunits in the Xenopus and human cohesin complexes.* J Cell Biol, 2000. **150**(3): p. 405-16.

126. Toth, A., et al., *Yeast cohesin complex requires a conserved protein, Eco1p(Ctf7), to establish cohesion between sister chromatids during DNA replication.* Genes Dev, 1999. **13**(3): p. 320-33.

127. Guacci, V., E. Hogan, and D. Koshland, *Chromosome condensation and sister chromatid pairing in budding yeast.* J Cell Biol, 1994. **125**(3): p. 517-30.

128. Spencer, F., et al., *Mitotic chromosome transmission fidelity mutants in Saccharomyces cerevisiae.* Genetics, 1990. **124**(2): p. 237-49.

129. Funabiki, H., et al., *Fission yeast Cut2 required for anaphase has two destruction boxes.* Embo J, 1997. **16**(19): p. 5977-87.

130. Salvesen, G.S. and M. Renatus, *Apoptosome: the seven-spoked death machine.* Dev Cell, 2002. **2**(3): p. 256-7.

131. Andrade, M.A., C. Perez-Iratxeta, and C.P. Ponting, *Protein repeats: structures, functions, and evolution.* J Struct Biol, 2001. **134**(2-3): p. 117-31.

132. Schwer, B. and S. Shuman, *Multicopy suppressors of temperature-sensitive mutations of yeast mRNA capping enzyme.* Gene Expr, 1996. **5**(6): p. 331-44.

133. Shuman, S., *Capping enzyme in eukaryotic mRNA synthesis.* Prog Nucleic Acid Res Mol Biol, 1995. **50**: p. 101-29.

134. Michaelis, C., R. Ciosk, and K. Nasmyth, *Cohesins: chromosomal proteins that prevent premature separation of sister chromatids.* Cell, 1997. **91**(1): p. 35-45.

135. Guacci, V., D. Koshland, and A. Strunnikov, *A direct link between sister chromatid cohesion and chromosome condensation revealed through the analysis of MCD1 in S. cerevisiae.* Cell, 1997. **91**(1): p. 47-57.
136. Losada, A., M. Hirano, and T. Hirano, *Cohesin release is required for sister chromatid resolution, but not for condensin-mediated compaction, at the onset of mitosis.* Genes Dev, 2002. **16**(23): p. 3004-16.
137. Bahler, J., et al., *Heterologous modules for efficient and versatile PCR-based gene targeting in Schizosaccharomyces pombe.* Yeast, 1998. **14**(10): p. 943-51.
138. Liang, C. and B. Stillman, *Persistent initiation of DNA replication and chromatin-bound MCM proteins during the cell cycle in cdc6 mutants.* Genes Dev, 1997. **11**(24): p. 3375-86.
139. Cai, J., et al., *Reconstitution of human replication factor C from its five subunits in baculovirus-infected insect cells.* Proc Natl Acad Sci U S A, 1996. **93**(23): p. 12896-901.
140. Faleiro, L., et al., *Multiple species of CPP32 and Mch2 are the major active caspases present in apoptotic cells.* Embo J, 1997. **16**(9): p. 2271-81.
141. Hakes, D.J. and J.E. Dixon, *New vectors for high level expression of recombinant proteins in bacteria.* Anal Biochem, 1992. **202**(2): p. 293-8.
142. Uhlmann, F., F. Lottspeich, and K. Nasmyth, *Sister-chromatid separation at anaphase onset is promoted by cleavage of the cohesin subunit Scc1.* Nature, 1999. **400**: p. 37-42.
143. Sazer, S. and S.W. Sherwood, *Mitochondrial growth and DNA synthesis occur in the absence of nuclear DNA replication in fission yeast.* J Cell Sci, 1990. **97 (Pt 3)**: p. 509-16.

Appendix

Sequence alignment of separases from different species

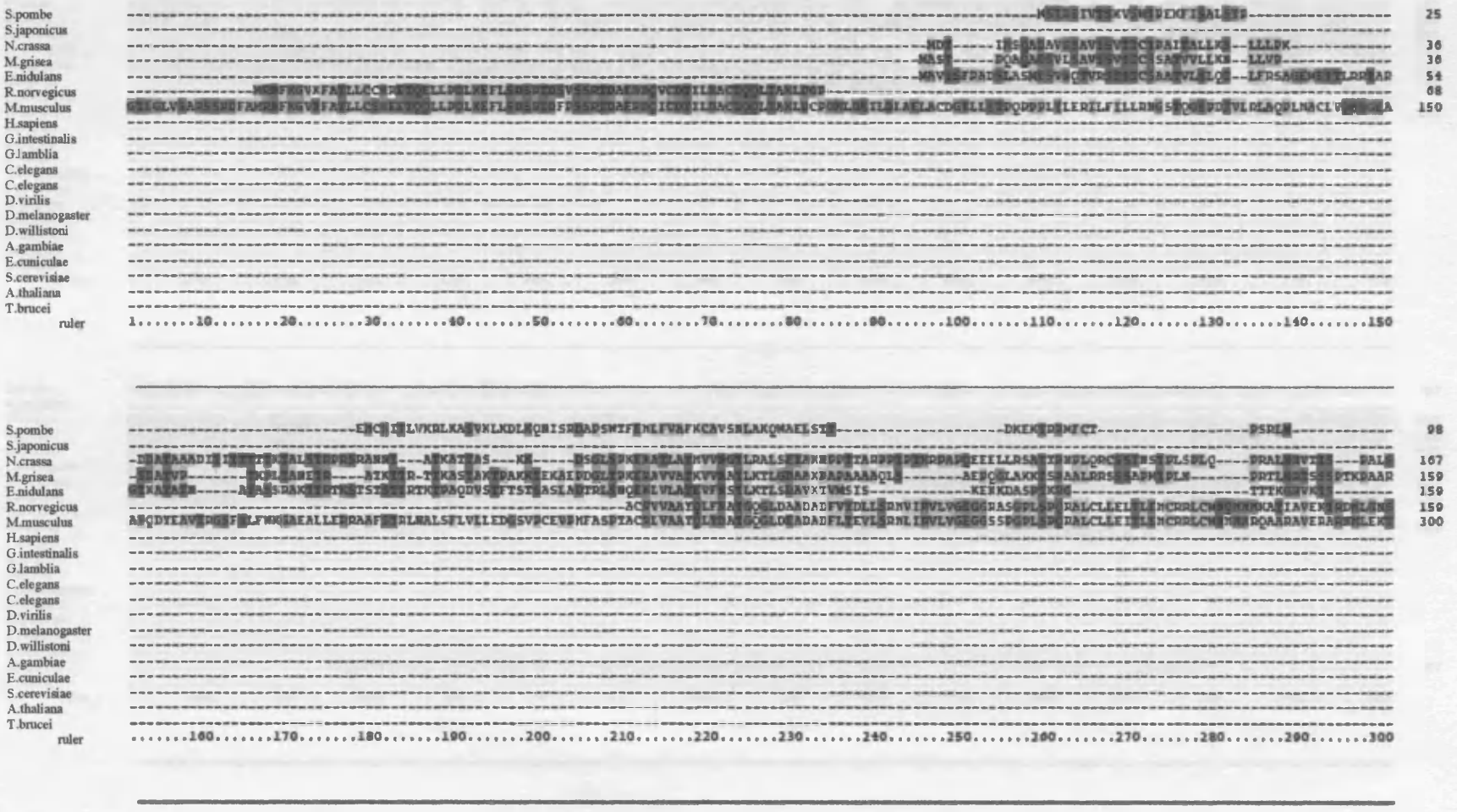

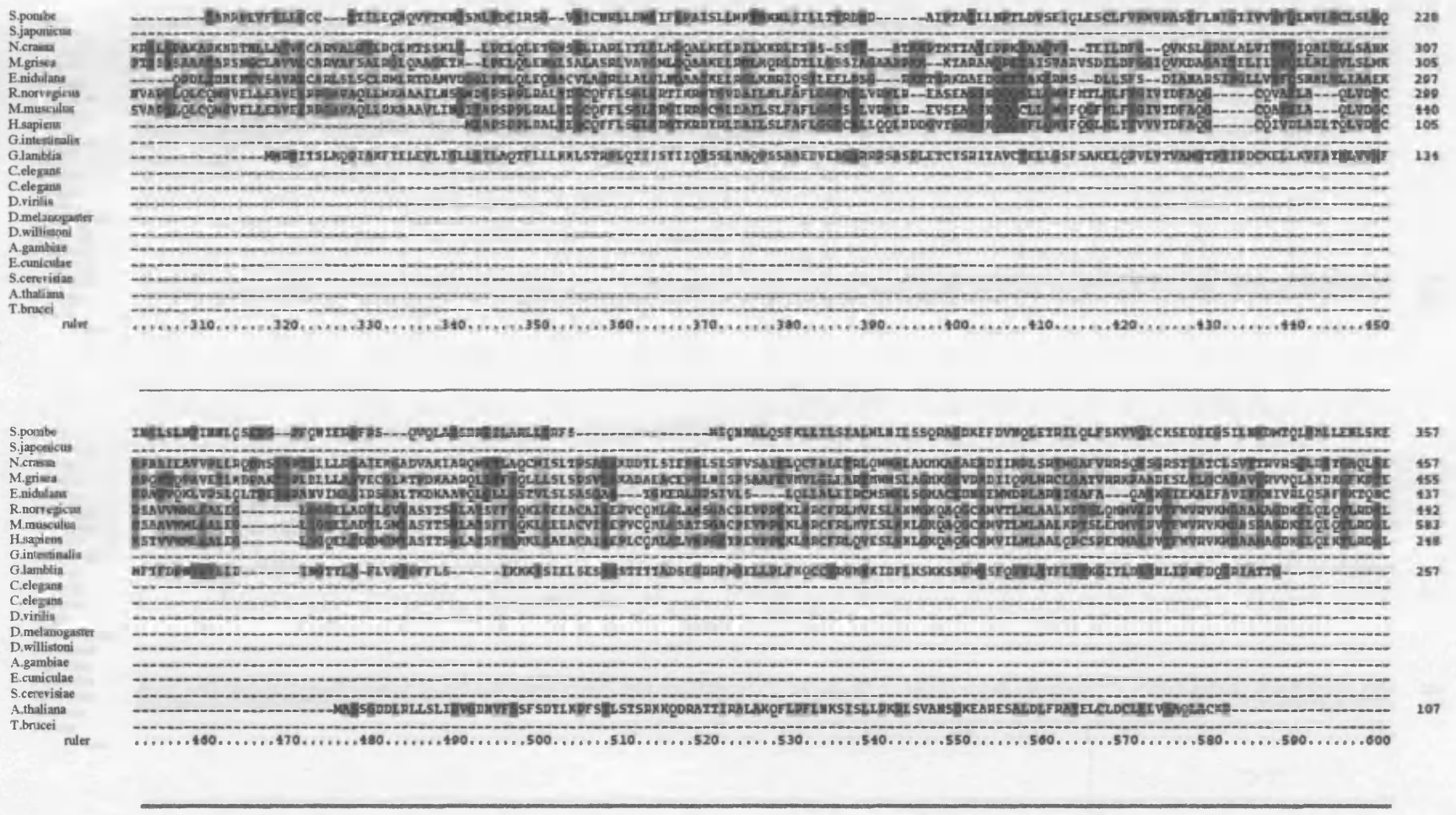
S.pombe
S.japonicus
N.crassa
M.grisea
E.nidulans
R.norvegicus
M.musculus
H.sapiens
G.intestinalis
G.lamblia
C.elegans
C.elegans
D.virilis
D.melanogaster
D.willistoni
A.gambiae
E.cuniculae
S.cerevisiae
A.thaliana
T.brucei
ruler
310
320
330
340
350
360
370
380
390
400
410
420
430
440
450
460
470
480
490
500
510
520
530
540
550
560
570
580
590
600

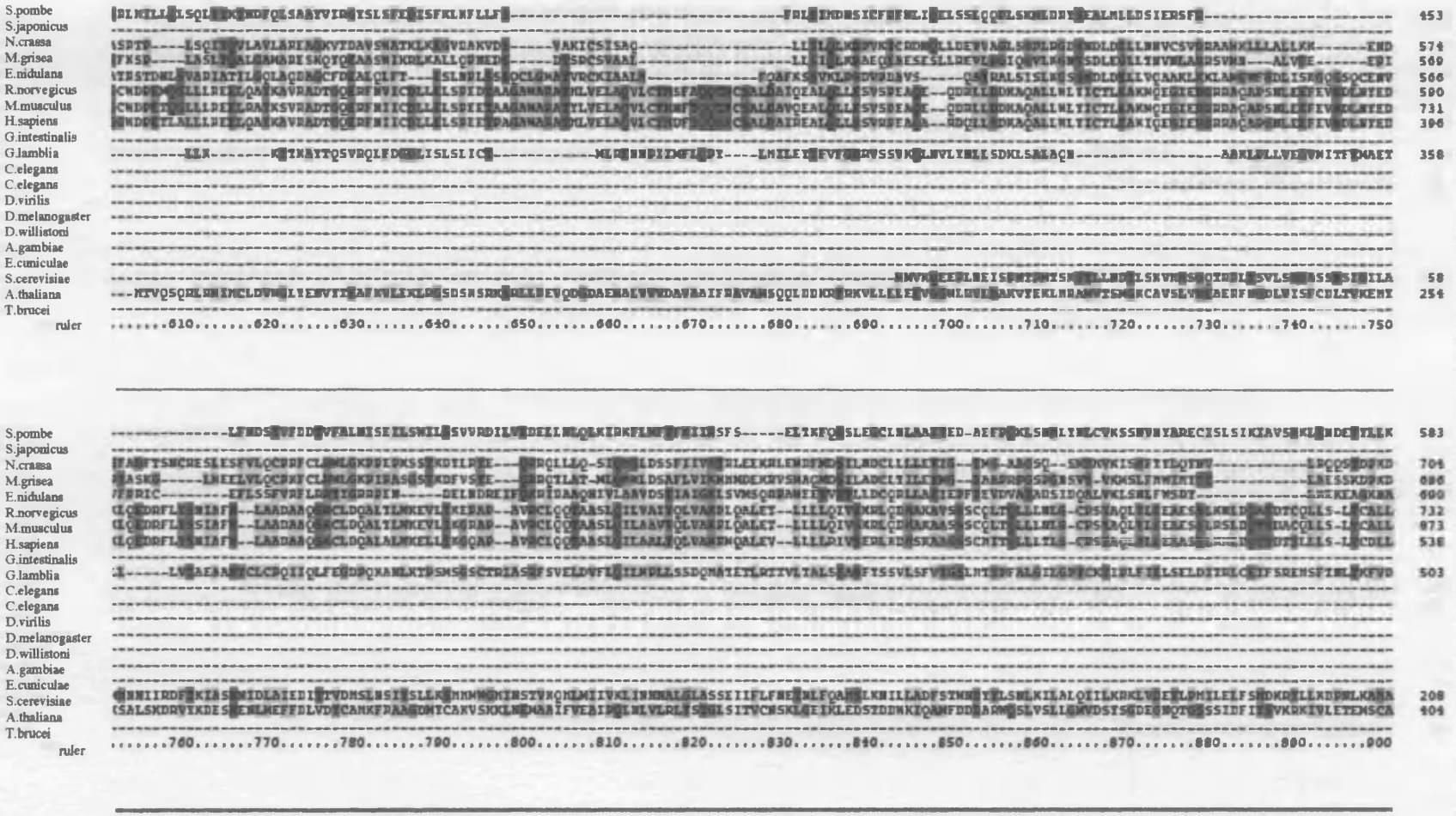
S.pombe
S.japonicus
N.crassa
M.grisea
E.nidulans
R.norvegicus
M.musculus
H.sapiens
G.intestinalis
G.lamblia
C.elegans
C.elegans
D.virilis
D.melanogaster
D.willistoni
A.gambiae
E.cuniculae
S.cerevisiae
A.thaliana
T.brucei
ruler
453
574
569
566
590
731
306
358
58
254
583
704
686
690
732
873
536
503
208
404
.....610.....620.....630.....640.....650.....660.....670.....680.....690.....700.....710.....720.....730.....740.....750
.....760.....770.....780.....790.....800.....810.....820.....830.....840.....850.....860.....870.....880.....890.....900

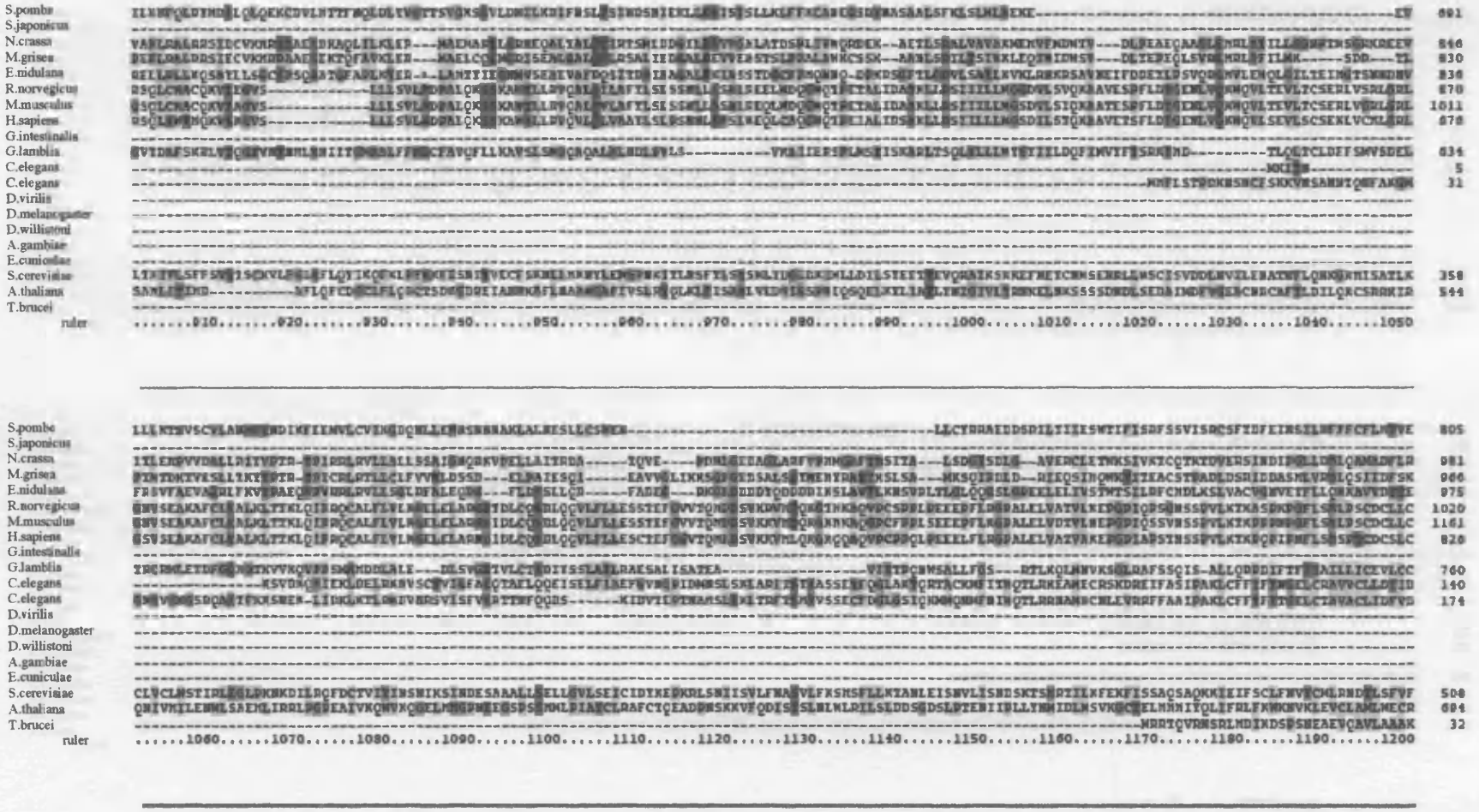
S.pombe
S.japonicus
N.crassa
M.grisea
E.midulana
R.norvegicus
M.musculus
H.sapiens
G.intestinalis
G.lamblia
C.elegans
C.elegans
D.virilis
D.melanogaster
D.willistoni
A.gambiae
E.cuniculae
S.cerevisiae
A.thaliana
T.brucei
ruler
.....910.....920.....930.....940.....950.....960.....970.....980.....990.....1000.....1010.....1020.....1030.....1040.....1050
S.pombe
S.japonicus
N.crassa
M.grisea
E.midulana
R.norvegicus
M.musculus
H.sapiens
G.intestinalis
G.lamblia
C.elegans
C.elegans
D.virilis
D.melanogaster
D.willistoni
A.gambiae
E.cuniculae
S.cerevisiae
A.thaliana
T.brucei
ruler
.....1060.....1070.....1080.....1090.....1100.....1110.....1120.....1130.....1140.....1150.....1160.....1170.....1180.....1190.....1200

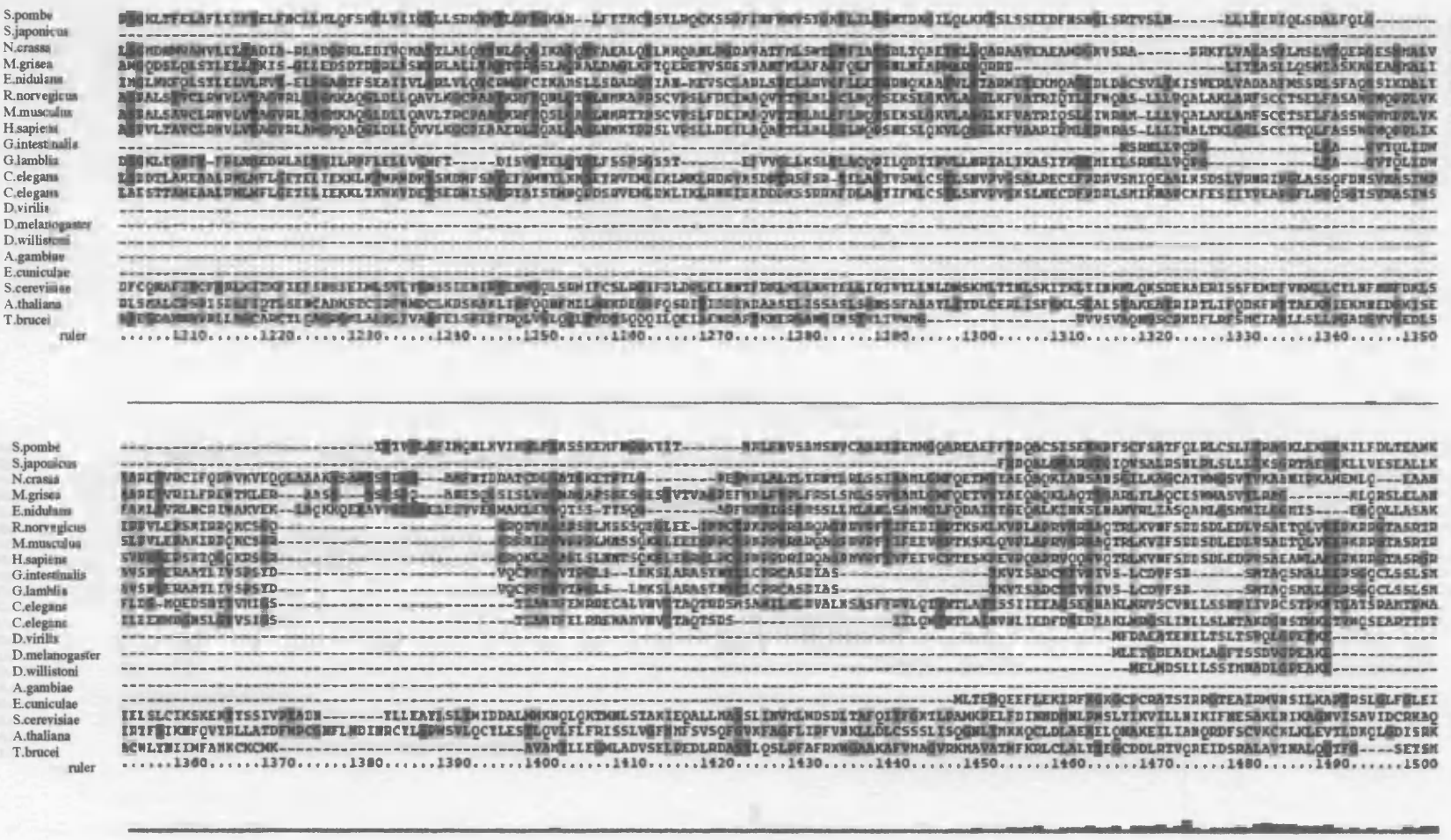
S.pombe
S.japonicus
N.crassa
M.grisea
E.nidulans
R.norvegicus
M.musculus
H.sapiens
G.intestinalis
G.lamblia
C.elegans
C.elegans
D.virilis
D.melanogaster
D.willistoni
A.gambiae
E.cuniculae
S.cerevisiae
A.thaliana
T.brucei
ruler

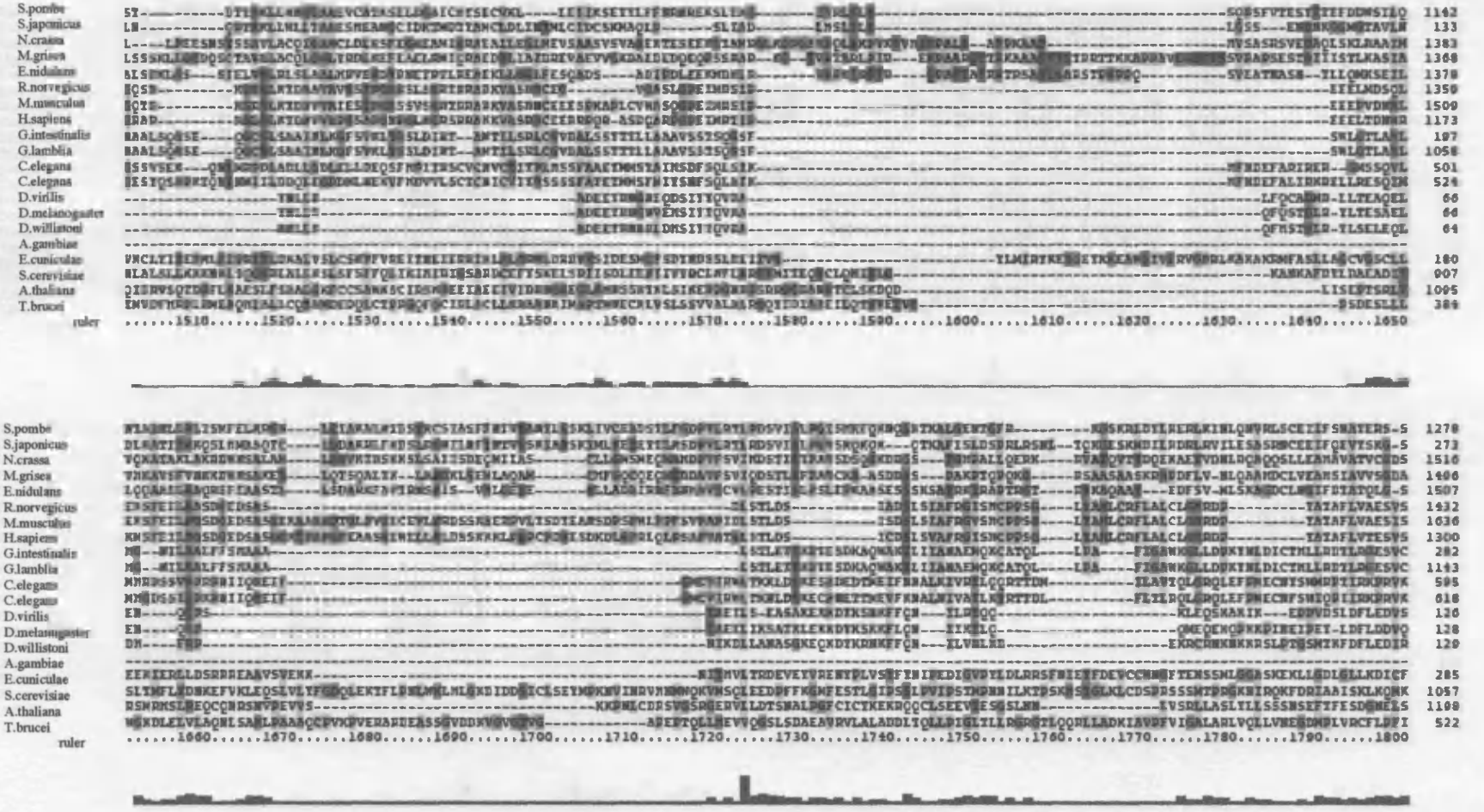
S.pombe
S.japonicus
N.crassa
M.grisea
E.nidulans
R.norvegicus
M.musculus
H.sapiens
G.intestinalis
G.lamblia
C.elegans
C.elegans
D.virilis
D.melanogaster
D.willistoni
A.gambiae
E.cuniculae
S.cerevisiae
A.thaliana
T.brucei
ruler

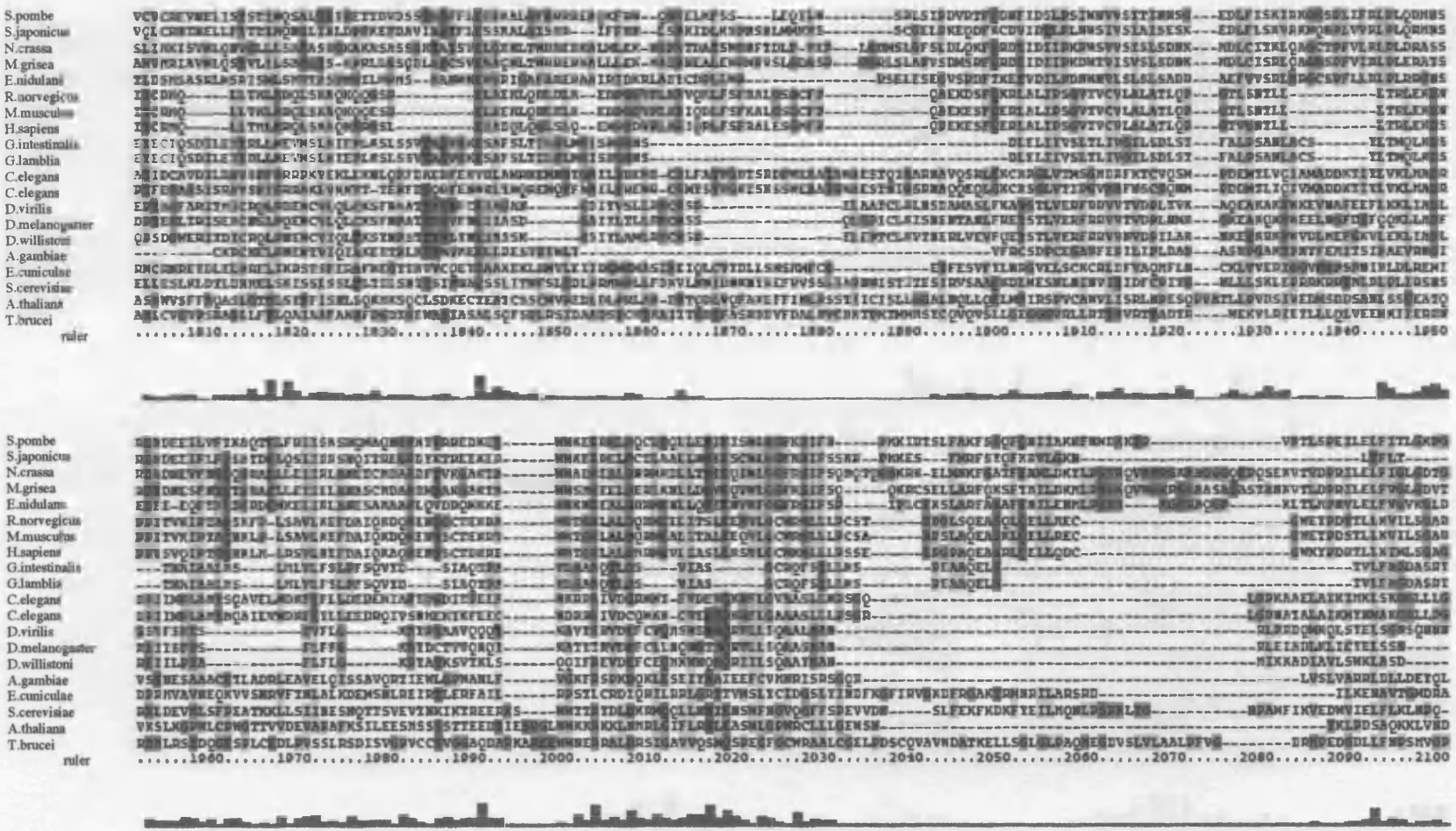
S.pombe
S.japonicus
N.crassa
M.grisea
E.nidulans
R.norvegicus
M.musculus
H.sapiens
G.intestinalis
G.lamblia
C.elegans
C.elegans
D.virilis
D.melanogaster
D.willistoni
A.gambiae
E.cuniculus
S.cerevisiae
A.thaliana
T.brucei
ruler
.....1810.....1820.....1830.....1840.....1850.....1860.....1870.....1880.....1890.....1900.....1910.....1920.....1930.....1940.....1950
.....1960.....1970.....1980.....1990.....2000.....2010.....2020.....2030.....2040.....2050.....2060.....2070.....2080.....2090.....2100

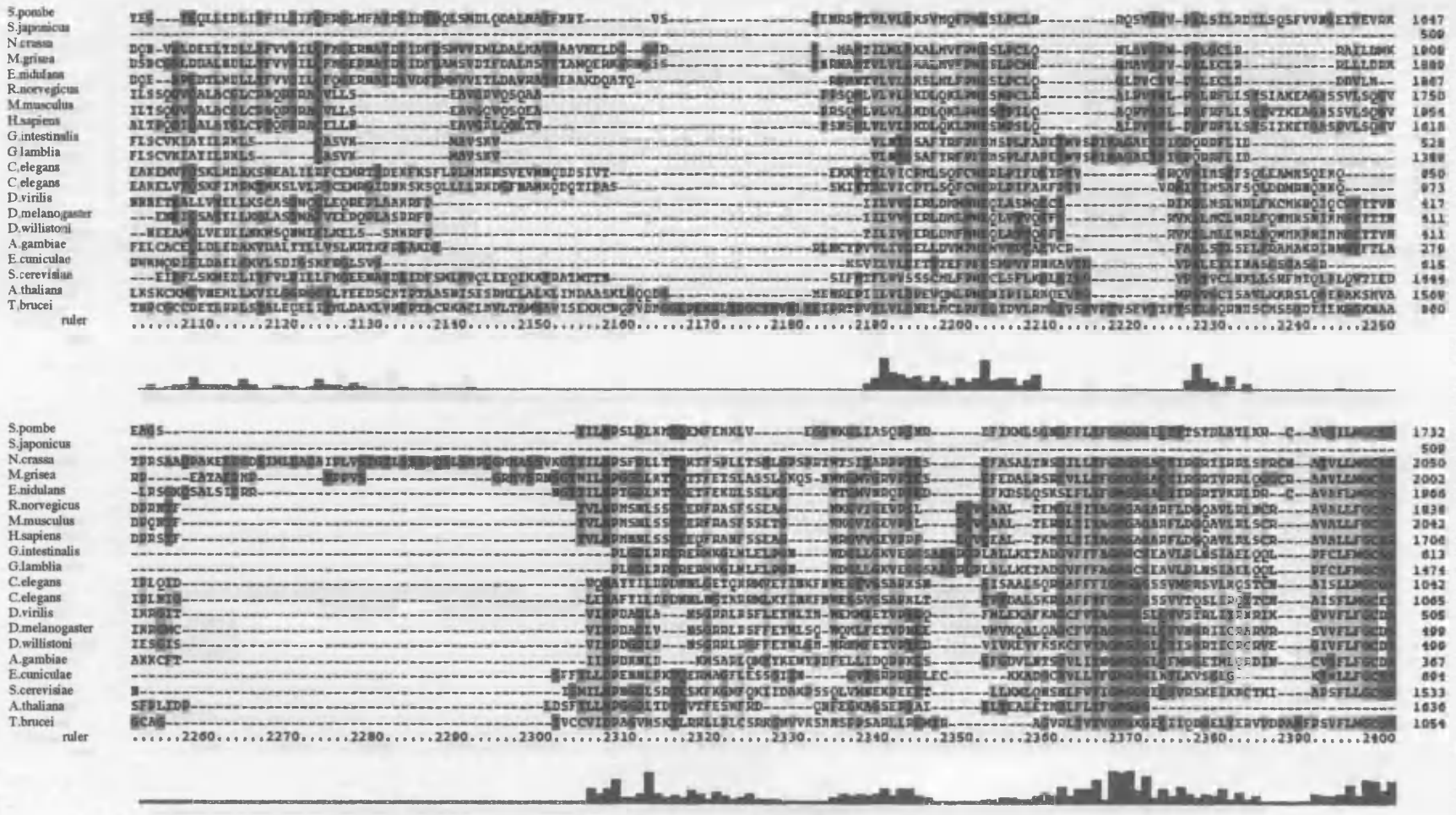
S.pombe
S.japonicus
N.crassa
M.grisea
E.nidulans
R.norvegicus
M.musculus
H.sapiens
G.intestinalis
G.lamblia
C.elegans
C.elegans
D.virilis
D.melanogaster
D.willistoni
A.gambiae
E.cuniculae
S.cerevisiae
A.thaliana
T.brucei
ruler
S.pombe
S.japonicus
N.crassa
M.grisea
E.nidulans
R.norvegicus
M.musculus
H.sapiens
G.intestinalis
G.lamblia
C.elegans
C.elegans
D.virilis
D.melanogaster
D.willistoni
A.gambiae
E.cuniculae
S.cerevisiae
A.thaliana
T.brucei
ruler

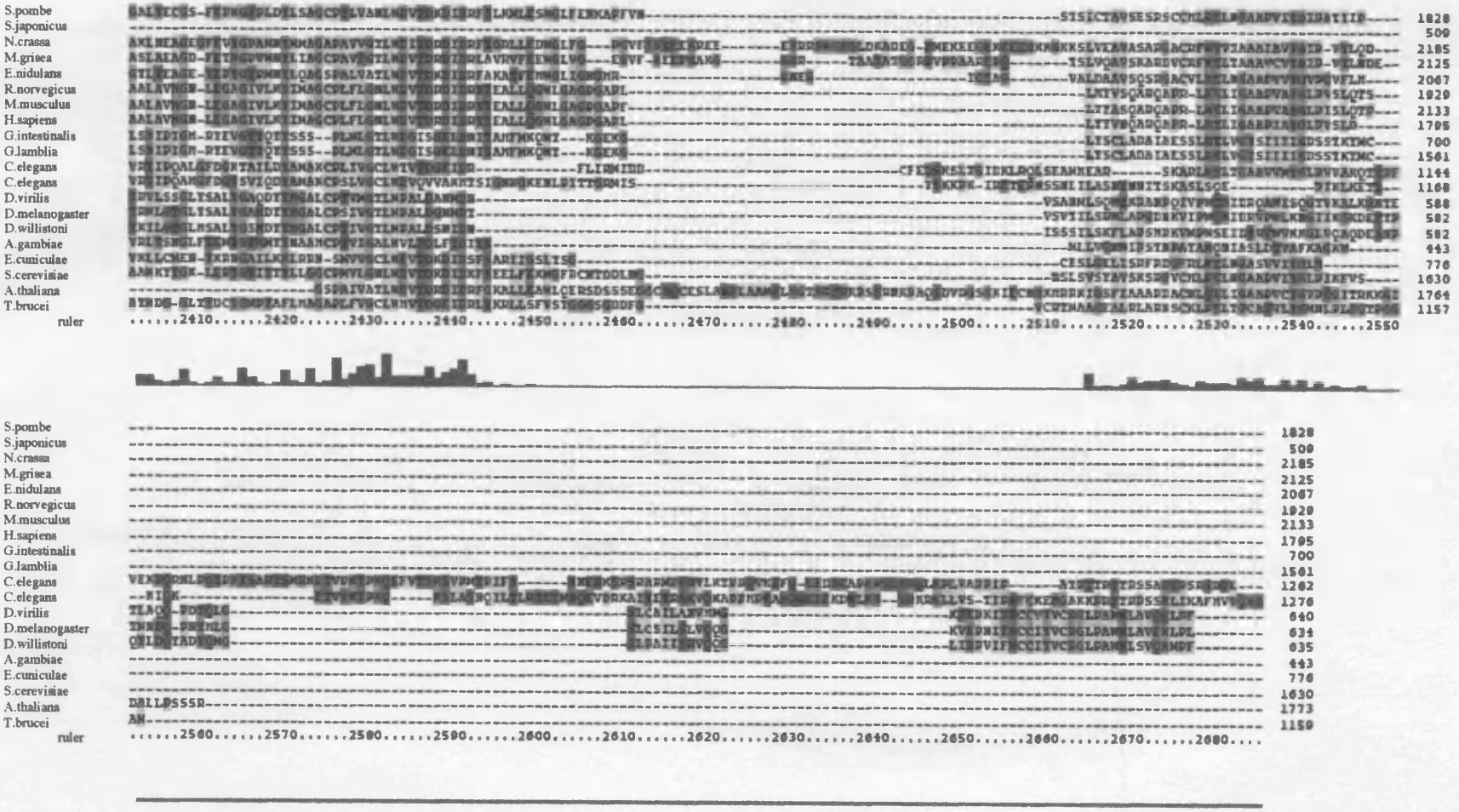
S.pombe
S.japonicus
N.crassa
M.grisea
E.nidulans
R.norvegicus
M.musculus
H.sapiens
G.intestinalis
G.lamblia
C.elegans
C.elegans
D.virilis
D.melanogaster
D.willistoni
A.gambiae
E.cuniculae
S.cerevisiae
A.thaliana
T.brucei
ruler
S.pombe
S.japonicus
N.crassa
M.grisea
E.nidulans
R.norvegicus
M.musculus
H.sapiens
G.intestinalis
G.lamblia
C.elegans
C.elegans
D.virilis
D.melanogaster
D.willistoni
A.gambiae
E.cuniculae
S.cerevisiae
A.thaliana
T.brucei
ruler